The role of CLE40 in shoot stem cell homeostasis

Inaugural- Dissertation

Zur Erlangung des Doktorgrades der
Mathematisch-Naturwissenschaftliche Fakultät der
Heinrich-Heine-Universität Düsseldorf

vorgelegt von

Jenia Sarah Schlegel

aus Wuppertal

Düsseldorf, Juni 2021

aus dem Institut für Entwicklungsgenetik der
Heinrich-Heine-Universität Düsseldorf

Gedruckt mit der Genehmigung der
Mathematisch-Naturwissenschaftlichen Fakultät der
Heinrich-Heine-Universität Düsseldorf

Referent: Professor Dr. Rüdiger Simon
Korreferent: Professor Dr. Matias Zurbriggen

Tag der mündlichen Prüfung: 11.10.2021

This study was funded by DFG through iGRAD-Plant (IRTG 2466), CRC 1208 and CEPLAS (EXC 2048).

iGRAD-Plant is a joint program with the Research Center Jülich and the Michigan State University, East Lansing, USA. Parts of this work were carried out in the laboratory of Prof. Federica Brandizzi at Michigan State University.

Parts of this thesis are published in the following article:

- **Control of Arabidopsis shoot stem cell homeostasis by two antagonistic CLE peptide signalling pathways**
  Jenia Schlegel, Grégoire Denay, Karine Gustavo Pinto, Yvonne Stahl, Julia Schmidt, Patrick Blümke, and Rüdiger Simon*
  bioRxiv, https://doi.org/10.1101/2021.06.14.448384

In addition, I was involved in the following research articles:

- **The Cell Fate Controlling CLE40 Peptide Requires CNGCs to Trigger Highly Localized Ca^{2+} Transients in *Arabidopsis Thaliana* Root Meristems**
  Maike Breiden, Vilde Olsson, Patrick Blümke, Jenia Schlegel, Karine Gustavo-Pinto, Petra Dietrich, Melinka A Butenko, Rüdiger Simon*
  Plant and Cell Physiology, https://doi.org/10.1093/pcp/pcab079
  Published: 01 June 2021
- **Receptor-like cytoplasmic kinase MAZZA mediates developmental processes with CLAVATA1 family receptors in Arabidopsis**
  Patrick Blümke, Jenia Schlegel, Carmen Gonzalez-Ferrer, Sabine Becher, Karine Gustavo Pinto, Jacqueline Monaghan, Rüdiger Simon*
  Journal of Experimental Botany, https://doi.org/10.1093/jxb/erab183
  Published: 28 April 2021
- **Optogenetic control of gene expression in plants in the presence of ambient white light**
  Rocio Ochoa-Fernandez, Nikolaj B. Abel, Franz-Georg Wieland, Jenia Schlegel, Leonie-Alexa Koch, J. Benjamin Miller, Raphael Engesser, Giovanni Giuriani, Simon M. Brandl, Jens Timmer, Wilfried Weber, Thomas Ott, Rüdiger Simon & Matias D. Zurbriggen*
  Nature Methods, https://doi.org/10.1038/s41592-020-0868-y
  Published: 29 June 2020

*corresponding author

Contents

1. Introduction

Plants are sessile life forms that, in contrast to animals, generate new organs throughout their entire lifetime. The generation of new organs requires a stable number of stem cells, which are undifferentiated cells that are able to undergo unlimited self-renewal. Plant stem cells are embedded in meristematic regions, such as the root apical meristem (RAM) and the shoot apical meristem (SAM), which give rise to all subterrestrial and above-ground plant tissues, respectively (Fletcher et al., 1999; Hall & Watt, 1989; Stahl & Simon, 2005).

1.1 The meristems of *Arabidopsis thaliana*

Shoot development in *A. thaliana* is governed by three different types of meristems: the shoot or vegetative meristem (SAM), the inflorescence meristem (IFM), and the floral meristem (FM). The SAM is a vegetative organ, which gives rise to the stem and forms leaves at its flanks. Upon flowering, the SAM undergoes a transition into the IFM. IFMs are indeterminately organs, which generate secondary inflorescences and flowers, whereas the development of FMs terminates after floral organ formation (Hempel & Feldman, 1994; Reddy et al., 2004).

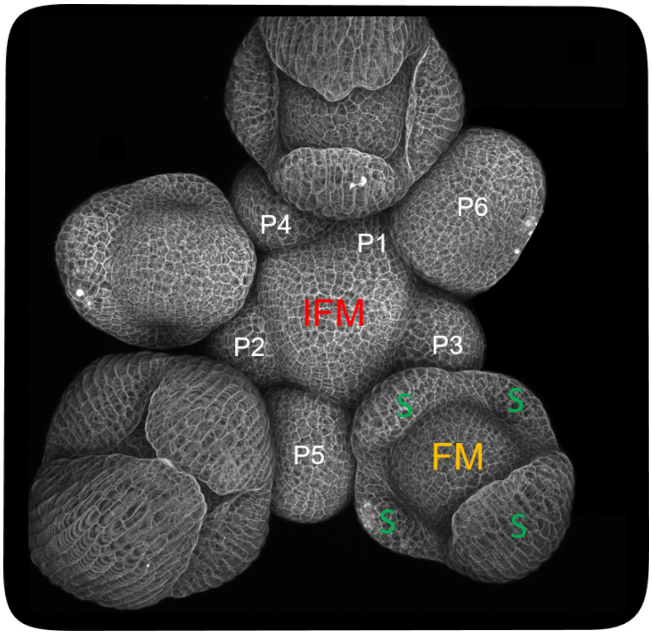

Fig. 1*: The IFM and FM of *Arabidopsis thaliana*

The inflorescence meristem (IFM) in the center of the shoot forms, in a radial pattern, new primordia (P1-P6), which carry in their center the floral meristem (FM). The primordia develop into flowers forming sepals (S) at their edge and petals, stamen, and carpels inside.

1.1.1 The flower meristem

The initiation of the flower meristems in Arabidopsis starts at the flanks of the IFM, where it forms new primordia (P0 - youngest) in a helicoidally pattern around the main axis due to an accumulation of the phytohormone auxin (Bowman et al., 1989, 1991; Pierre-Jerome et al., 2013; Reinhardt et al., 2000) (Fig. 1). Auxin is a small, mobile signaling molecule, which plays diverse roles in plant development and physiology (Davies, 1995; Sabatini et al., 1999). In the IFM auxin activates the AUXIN RESPONSE FACTOR5/MONOPTEROS (ARF5/MP), which controls different pathways of floral meristem identity (Pierre-Jerome et al., 2013). Active MP induces expression of *AINTEGUMENTA (ANT) and AINTEGUMENTALIKE6/PLETHORA3 (AIL6/PLT3),* which were both shown to promote flower growth (Krizek, 2009). Besides that, MP also activates *ARABIDOPSIS HISTIDINE PHOSPHOTRANSFER PROTEIN6 (AHP6)*, which plays an important role in the rhythmicity of organ initiation (Besnard et al., 2014). Additionally, MP activates the transcription factor (TF) *LEAFY (LFY*), which in turn activates the TF *APETALA1 (AP1)*. In a strong positive feedback loop, AP1 upregulates LYF and both activate various floral identity genes, such as *PISTILLATA, APETALA3*, and *AGAMOUS (AG)* (Kaufmann et al., 2010; Sundström et al., 2006; Winter et al., 2015; N. Yamaguchi et al., 2013). Thus, MP is a key regulator in flower meristem identity (Denay et al., 2017). Mature flowers consist of four whorls arranged in concentric rings (Davies, 1995). The cells of the outermost whorl give rise to the sepals; the second whorl forms the petals; the third one the male organs, the stamens; and the cells of the innermost whorl of the flower bud form the carpels, which are the female reproductive organs (Bowman et al., 1991; Coen & Meyerowitz, 1991). After the flower reaches its mature state, the FM identity is terminated by downregulation of WUSCHEL (WUS), since the main role of the TF WUS is to promote stem cell maintenance (Brand et al., 2002; Sun et al., 2009). AG binds and represses *WUS* and at the same time activates *KNUCKELS*, which also represses the transcription of *WUS* by recruiting polycomb group complexes to the *WUS* locus (Liu et al., 2011; Lohmann et al., 2001; Sun et al., 2014, 2019). Hence, a complex gene regulatory system is needed to keep the balance between stem cell maintenance and differentiation.

1.1.2 The inflorescence meristem

Unlike the FM, the IFM is an indeterminate organ, which generates secondary inflorescences and flowers throughout the entire life cycle of a plant. The IFM can be divided into three layers, the L1, L2, and L3. All cells of the outermost layers L1 and L2 divide anticlinally and have a clonal origin, thus, they form two separate layers consisting of one single cell layer respectively.

Beneath the L2, L3 cells divide in all directions and hence this zone comprises several cell layers. The outermost cell layer, L1, consists of epidermal progenitor cells while the second cell layer, L2, generates subepidermal tissue and gametes. The vasculature and most of the plant's above-ground tissue are derived from L3 cells (Jenik & Irish, 2000; Satina et al., 1940; Stahl & Simon, 2005) (Fig. 2).

Another way to classify the IFM into different zones is based on the function and gene expression patterns of the cells. The zone harboring the pluripotent stem cells is called the central zone (CZ), which is situated at the top of the meristem. Direct stem cell descendants, the transit amplifying (TA) cells, form a transitional zone between the CZ and the peripheral zone (PZ). Since stem cells divide slowly and infrequently, the main drivers to increase the meristem cell population are the TA cells. As such, the TA cells form an intermediate cell population with proliferative capacity and restricted differentiation potential. They receive differentiation signals and form new organ primordia on the flanks of the meristem. The cell group beneath the CZ is named the organization center (OC) since these cells are responsible for the "organization" or maintenance of the stem cell population. Finally, the zone beneath the OC is called the rib zone (RZ), where the cells give rise to the majority of the above-ground tissue in the plant (Fletcher et al., 1999; Hall & Watt, 1989; Reddy et al., 2004; Stahl & Simon, 2005) (Fig. 2).

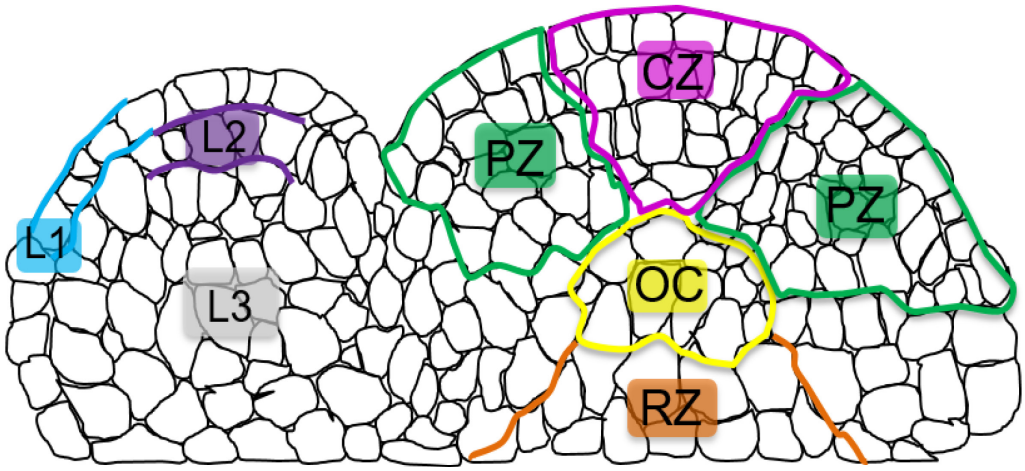

Fig. 2: Schematic cross-section through the IFM along its longitudinal axis

1.1.3 The root meristem

The root anchors the plant in the soil and thereby provides the plant with nutrients and water from its surrounding. The root can be divided into three different zones: the meristematic zone, the elongation zone, and the differentiation zone. In the elongation zone, cells elongate and afterwards differentiate into their final cell fate in the differentiation zone (Dolan et al., 1993). The meristematic zone consists of the distal root meristem, the stem cell niche, and the proximal meristem. In the center of the stem cell niche the quiescent center (QC) is located. The QC consists of four pluripotent stem cells that divide slowly and are surrounded by stem cells that divide more frequently and are often referred to as initial cells (Benfey & Scheres, 2000; Cruz-Ramírez et al., 2013; Dolan et al., 1993). Cells in lateral orientation to the QC are the cortex-endodermis initial cells and give rise to the tissues of the cortex and endodermis. The stem cells situated above the QC, the proximal stem cells, will develop into differentiated cells that form the stele and vasculature of the root. Cells beneath the QC, the distal stem cells, are divided into two groups. The lateral distal stem cells give rise to the lateral root cap or the endodermis, while the distal stem cells right below the QC are called the columella stem cells (CSCs) that differentiate to columella cells (CCs) (Fig. 3) (Drisch & Stahl, 2015). Thus, similar to the OC in the shoot, the QC is the computing center of the meristematic zone in the root.

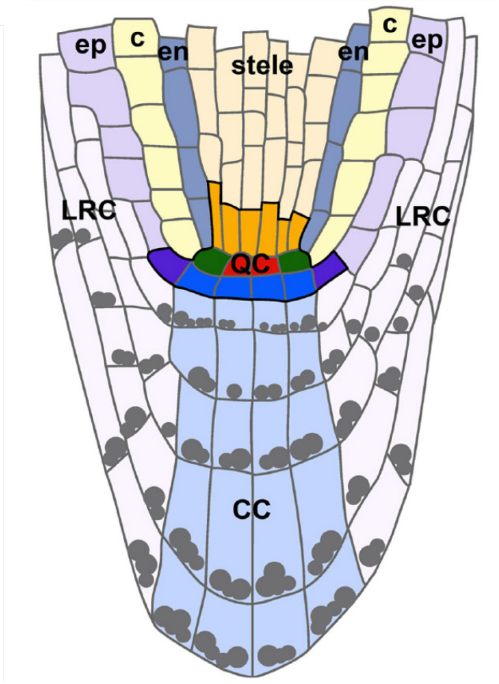

Fig. 3: The structure of the meristematic zone in the root of Arabidopsis

cap/epidermis initials (purple), and CSCs (blue). The black outline marks the stem cell niche of the root. ep, epidermis; c, cortex; en, endodermis; LRC, lateral root cap; CC, columella cells; gray dots indicate starch granules (Drisch & Stahl, 2015).

1. 2 The CLAVATA pathway in the IFM of *A. thaliana*

The CLAVATA (CLV) signaling pathway has been shown to play important roles in regulating the size and homeostasis of stem cells in SAMs, IFMs, and FMs of Arabidopsis. CLAVATA3 (CLV3) is a 13-amino acid arabinosylated glycopeptide and founding member of the CLV3/EMBRYO SURROUNDING REGION (ESR)-related (CLE) peptide family. *CLV3* is expressed and secreted from stem cells and can bind to the ectodomain of the leucine-rich-repeat (LRR) receptor-like kinase (RLK) CLAVATA1 (CLV1) (Ogawa et al., 2008; Ohyama et al., 2009; Shinohara & Matsubayashi, 2015; Yadav et al., 2011). After perception of CLV3, CLV1 activates a downstream signal transduction cascade involving autophosphorylation, interaction with membrane-associated cytoplasmic kinases, and with phosphatases (Blümke et al., 2021; Defalco et al., 2021). Furthermore, heterotrimeric G-proteins and mitogen-activated protein kinases (MAPKs) have been implicated in the signal transduction cascade in maize and Arabidopsis (Betsuyaku et al., 2011; Bommert et al., 2013; Ishida et al., 2014; Lee et al., 2019). This downstream signaling leads to the repression of *WUS* in the OC (Endrizzi et al., 1996; Fletcher et al., 1999). WUS, in turn, moves upwards through the plasmodesmata and activates the expression of *CLV3* in the stem cells, creating a negative feedback loop (Brand et al., 2000; Daum et al., 2014; Mayer et al., 1998; Schoof et al., 2000; Yadav et al., 2011). Besides CLV1, it was proposed that the receptor-like protein (RLP) CLV2 and the pseudokinase CORYNE (CRN) can form a heteromeric complex to operate as a potentially functional receptor kinase, which plays a critical role in stem cell control in the shoot meristems (Müller et al., 2008).

Loss-of-function mutations in the *CLV3* gene lead to additional organ formation as well as to strongly fasciated and enlarged meristems due to an over-proliferation of stem cells (Brand et al., 2000; Fletcher et al., 1999). Similarly, but less severely, the meristems of *clv1, clv2,* and *crn* mutants are fasciated. Interestingly, the double mutants of *clv1;clv2* and *clv1;crn* have a comparably increased meristem size as the *clv3* single mutant, suggesting that the CLV2-CRN complex acts in parallel to the CLV3-CLV1 pathway to repress *WUS* in the OC (Clark et al., 1993; Jeong et al., 1999; Kayes & Clark, 1998; Müller et al., 2008).

In contrast to the *clv* mutant phenotypes, the quadruple mutant *HAIRY MERISTEM1,2,3,4* (*ham1,2,3,4)* leads to termination of the meristem (Zhou et al., 2015). The *HAM* genes are

members of the GRAS family TFs and are also involved in the CLV3-WUS feedback loop. HAM1 strongly interacts with WUS and it was recently shown that WUS can only activate *CLV3* expression in the absence of *HAM* genes (Zhou et al., 2015, 2018). These results suggest that the main role of the HAMs in the IFM is to confine the expression of *WUS* and *CLV3* to the center of the meristem on its apical-basal axis (Zhou et al., 2018).

Besides the CLV receptors, LRR RLKs of the ERECTA family (ERf), comprising ER, ER-LIKE1 (ERL1), and ERL2, control cell fate in the SAM (Shpak, 2013; Shpak et al., 2004; Torii et al., 1996). ERf members were shown to control SAM size and shape by buffering cytokinin (CK) responses and directly regulating *WUS* expression (Mandel et al., 2014; Uchida & Tasaka, 2013). Recent data suggest that the ERf and their ligands, the EPIDERMAL PATTERNING FACTOR (EPF)-LIKE (EPFL) peptides, mainly restrict *WUS* and *CLV3* expression in the periphery of the SAM, thereby contributing to lateral inhibition of the stem cell domain (Han, Geng, et al., 2020).

1.2.1 Known receptor kinases of the CLV pathway

In contrast to the animal kingdom, where ligand perception is mediated by both receptor tyrosine and serine/threonine kinases, most of the RLKs in plants have a serine/threonine kinase specificity. RLKs consist of an extracellular domain that usually binds specific ligands, a transmembrane, and a kinase domain. There are over 600 RLKs predicted in the genome of Arabidopsis and the function of many of them is still unknown (Shiu & Bleecker, 2001). In general, RLKs regulate a wide range of processes such as the formation of new tissue, pathogen response, plant development, and growth (Butenko et al., 2009; Shiu & Bleecker, 2001). RLKs are often divided into subfamilies due to their different extracellular domain composition. One of the largest subfamilies in plants is the LRR class. Most of the RLKs which are involved in plant defense, like the FLAGELLIN-SENSITIVE 2 and elongation factor Tu (EFR) receptors, or in stem cell signaling, like CLV1 and BARELY ANY MERISTEM1 (BAM1), belong to the LRR subfamily (DeYoung et al., 2006; Gómez-Gómez & Boller, 2000; Zipfel et al., 2006).

1.2.1.1 CLAVATA1

The *clv1-4* mutant was the first identified CLV gene, which was published and named in 1962 by McKelvie (McKelvie, 1962). About 30 years later, the first studies linked the *CLV1* gene to the regulation of meristem and flower development in *A. thaliana* (Clark et al., 1993). Structural

analysis of the gene revealed an extracellular domain, consisting of 21 complete LRRs, a transmembrane domain, and an intercellular kinase domain (Clark et al., 1997; Williams et al., 1997). RNA-hybridization experiments showed that *CLV1* is expressed specifically in the center of shoot and floral meristems (Clark et al., 1997). The *clv1* mutant phenotype has fasciated meristems and additional floral organs due to the over-proliferation of stem cells (Clark et al., 1993; Kayes & Clark, 1998). In 2000, Brand and colleagues linked the expression of the TF WUS with the CLV3-CLV1 signaling pathway by showing a laterally expanded WUS domain in *clv* mutants (Brand et al., 2000; Schoof et al., 2000). Furthermore, ubiquitously expressed *CLV3* cannot rescue the fasciated *clv1* meristem phenotype. Thus, the pathway depends on functional CLV1 protein. It was also shown that continuous signaling through CLV3 causes down-regulation of *WUS* resulting in a complete loss of stem cells and meristem termination (Brand et al., 2000). However, Müller *et al.* showed that in an established stem cell niche a 10-fold higher induction of CLV3 does not lead to a change in the size of shoot or flower meristems, while reduced levels of *CLV3* expression (16% of wild type level) cannot fully rescue a *clv3-2* mutant, since increased SAM size and carpel numbers were still detected. These results indicate that *WUS*-expressing cells in the OC directly react to CLV3 signaling, but not in a proportional manner since wide ranges of *CLV3* expression do not affect the shoot meristem (Müller et al., 2006). In 2008 the direct binding of CLV3 to the ectodomain of CLV1 was shown by a radioactively labeled peptide assay (Ogawa et al., 2008).

Since CLV1 is an RLK with a transmembrane domain, it localizes at the plasma membrane (PM) and forms in *Nicotiana benthamiana* homomers as well as heteromers with the CLV2-CRN complex. Interestingly, the addition of CLV3 peptide (CLV3p) did not stimulate heteromeric complexes, as was shown for other peptide-receptor interactions (Bleckmann et al., 2010). Nevertheless, the addition of CLV3p on *A. thaliana* shoot meristems leads to an internalization of the CLV1 receptor, followed by VTI11/ZIG-dependent trafficking to the lytic vacuole (Nimchuk et al., 2011). Genetic interaction studies showed that CLV1 and the CLV2-CRN complex act independently from each other in two separate pathways, although they are able to form heteromers in *N. benthamiana* (Müller et al., 2008).

The closest homologue of CLV1 is BAM1 and recent studies showed that CLV1 represses the expression of *BAM1* in the shoot meristem of wild type plants, while BAM1 is able to partly substitute CLV1 function *clv1* mutants (Nimchuk, 2017; Nimchuk et al., 2015).

1.2.1.2 BARELY ANY MERISTEM

CLV1 plays an important role in stem cell homeostasis in the meristem. To find new candidates sharing a close common ancestry with CLV1, DeYoung and colleagues performed a phylogenetic analysis on CLV1. As a result, they found three other Arabidopsis genes, *BAM1*, *BAM2,* and *BAM3* in the same monophyletic group as CLV1, which all encode RLKs and show high sequence similarity to each other (DeYoung et al., 2006). Compared to *CLV1*, *BAM1* shows the highest overall sequence identity, 55%, and 81% sequence identity across the kinase domain (DeYoung et al., 2006).

Like CLV1, the BAMs were associated with key functions during shoot meristem development. However, in contrast to *clv1* mutants, higher ordered *bam* mutants display reduced meristem size (DeYoung et al., 2006). Secondly, CLV1 is highly specific in its role in stem cell homeostasis, whereas the *BAM* genes have a broad expression pattern and play important roles not only in meristem function, but also in the development of vascular strands within the leaf, leaf shape, and symmetry. Furthermore, the BAMs are required for the development of male gametophytes as well as in ovule specification and function (DeYoung et al., 2006). *BAM1* and *BAM2* were also shown to be important for early anther development, including aspects of cell division and differentiation (Hord et al., 2006). Since *CLV1* and *BAM* genes are such close homologues, the expression of *CLV1* under the control of the *ERECTA* promoter could fully rescue *bam1;bam2* double mutants (DeYoung et al., 2006). The ER RLKs are expressed in a broad pattern in the meristem as well as in young developing tissues and are thus very close to the native expression pattern of the *BAM1* and *BAM2* genes (Torii et al., 1996; Yokoyama et al., 1998). Thus, *BAM1/2* expression in the meristematic zone can partly rescue the *clv1* phenotype (DeYoung et al., 2006). Further genetic studies of different combinations of *bam* and *clv* mutants revealed different phenotypic results. *bam1;bam2;clv1* triple mutants showed the severest synergistic effect in defects in stem cell homeostasis compared to wild type and various other mutant combinations. The triple mutant plants were significantly smaller, had very small leaves, an increased number of rosette leaves, and thick stems. Double mutants of *bam1;clv1* and *bam2;clv1* enhanced the usual *clv1* phenotype strongly, showing an enlarged meristem, increased organ primordia, and increased carpel numbers (DeYoung & Clark, 2008). In a *clv3* mutant background, *bam* mutations suppressed the usual carpel phenotype and in combination with a *clv2* mutant, no effects were observed. In a speculative model, the authors suggest that *BAM* genes in the periphery of the meristem sequester CLE peptides and isolate the center of the meristematic zone from exogenous signals (DeYoung & Clark, 2008) (Fig. 4).

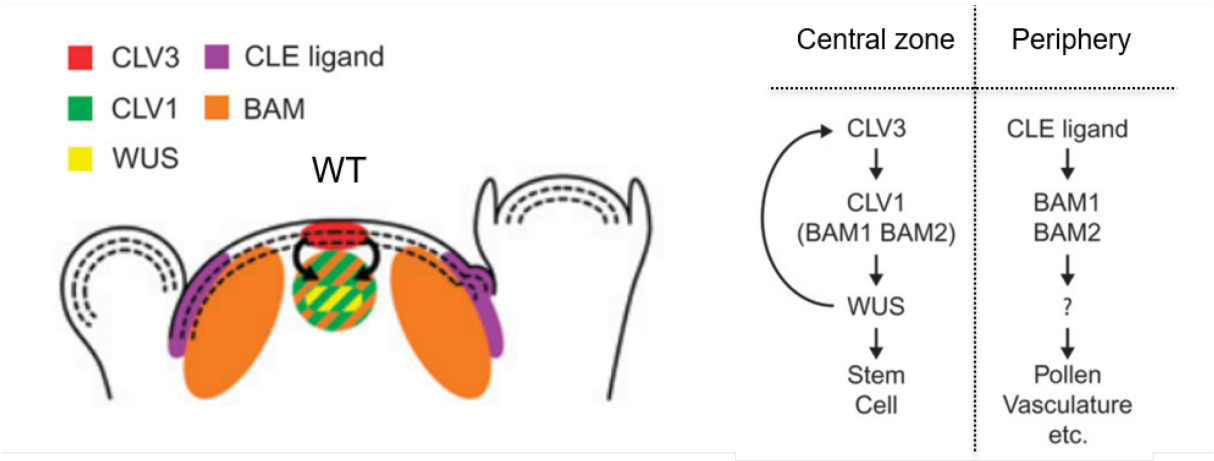

Fig. 4: A putative model for BAM function in the meristem

(left) Schematic model of the IFM showing possible expression patterns for the main players in the CLV pathway. In the CZ of the meristem *CLV3* (red) is activating the TF *WUS* (yellow), which is expressed in the OC where it overlaps with the expression of *BAMs* (orange) and *CLV1* (green). In the PZ, an unknown CLE peptide is expressed in the L1 and L2 layer (purple) while *BAM* genes are expressed in the L2 and L3 of the periphery. **(right)** In the CZ, the well-studied CLV pathway is outlined. CLV3 binds to CLV1, activating a downstream transduction cascade repressing *WUS,* which in turn activates CLV3 expression and promotes stem cell fate. BAM1 and BAM2 can substitute the absence of CLV1. In the periphery, an unknown CLE ligand of BAM1/BAM2 might activate an unknown protein, which eventually promotes pollen and vasculature development (Illustration adapted from DeYoung & Clark, 2008).

Although *clv1* and *bam* mutants show the opposite mutant phenotype in the SAM, ectopic expression experiments showed that CLV1 and BAM1 can perform similar functions in stem cell control and that CLV3 was found to interact with CLV1 and BAM1 in cell extracts (Shinohara & Matsubayashi, 2015). In line with that, Nimchuk and colleagues reported that in a wild-typic background *BAM1* transcripts are only present in the L1 of the meristem and that CLV1 represses *BAM* transcription in response to CLV3 signaling since they could detect *BAM1* expression also in the rib meristem in a *clv3* mutant. They also showed that *CLV1* expression under the control of the *WUS* promoter can rescue the carpel phenotype in a *bam1;bam2;bam3;clv1* quadruple mutant (Nimchuk et al., 2015). In addition, it was shown that ectopic receptor expression of *BAM1* can partly substitute for CLV1 signaling and that *BAM* expression is repressing itself in an additional negative feedback loop to buffer stem cell proliferation in the meristem (Nimchuk, 2017).

In the root, the receptor-peptide pair BAM1-CLE9/10 was shown to negatively regulate xylem file numbers, while Crook et al. linked *BAM1* expression in the root to formative root and hypocotyl ground tissue cell division (Crook et al., 2020; Qian et al., 2018). They could

demonstrate that BAM1 is able to bind the peptides CLE16 and CLE13 to regulate the correct expression of CyclinD6 and asymmetric cell division (Crook et al., 2020).

1.2.1.3 ARABIDOPSIS CRINKLY4

Becraft and colleagues first characterized the maize crinkley4 in 1996. They showed that mutation of CR4 affects the differentiation of leaf epidermis in terms of cell size, morphology, and surface structure of the leaves (Becraft et al., 1996; Jin et al., 2000). In Arabidopsis, five homologues of CR4 were found and the closest one was called ARABIDOPSIS CRINKLY4 (ACR4). The extracellular domain of ACR4 consists of seven copies of the 39-amino acid repeat, which is very similar to the tumor necrosis factor of mammalian cells (TNFR). Furthermore, the structure of ACR4 has a cysteine-rich region, a transmembrane domain, and a kinase domain.

ACR4 transcripts were detected in roots, young and old leaves, flower buds, siliques, and seedlings. *ACR4* expression stands out by being predominantly found at the outer layers of the cells or more precisely on the “internal” PM of outside cells (Gifford et al., 2003; Meyer et al., 2013; Tanaka, 2002). Knock-down plants of *acr4* showed defects in seed formation and the morphogenesis of the embryos (Tanaka, 2002).

Ovule integuments are entirely L1 derived and *ACR4* expression in shoot meristems and young organ primordia is exclusively found in the L1 layer. Thus, *ACR4* expression is required for normal cell organization during ovule integument development and the formation of sepal margins (Gifford et al., 2003; Jenik & Irish, 2000). Accordingly, it was shown that *acr4* mutants have fewer giant cells in the sepal endodermis than wild type plants. Moreover, *acr4* mutant sepals show increased proliferation in endoreduplication (Roeder et al., 2012).

ACR4, as a membrane-localized receptor kinase, is found on the lateral and basal surfaces of cells in the epidermis of leaf primordia where it supports the organization of the leave epidermis or seed coat. These results suggest a differentiating role of ACR4 in epidermal cells by perceiving and sending signals to neighboring cells (Tanaka, 2002; Watanabe et al., 2004). Gifford *et al.* proposed a unique RLK role for the kinase activity of ACR4 in 2005, as they discovered that ACR4 appears to undergo a rapid turnover, including ACR4 internalization from the PM via a Brefeldin A (BFA)-sensitive pathway. The extracellular domain is required for signaling and protein internalization (Gifford et al., 2005).

In the root of Arabidopsis, so far two main functions can be linked to ACR4: i) it is required to coordinate pericycle cell divisions during lateral root initiation by restricting formative cell divisions and ii) ACR4 controls cell fate in the columella lineage in the root apex where it

regulates the QC activity and position (Berckmans et al., 2019; De Smet et al., 2009; Stahl et al., 2009). In the root, ACR4 might be triggered by *CLE40* signaling, repressing the homeobox gene *WOX5*, as it also represses stem cell fate. In a negative feedback loop, WOX5, in turn, activates stem cell fate again (Stahl et al., 2009). In line with that, ACR4 can phosphorylate WOX5 *in vitro* and it was proposed that the KDSAF motif might be a possible conserved binding motif for an intracellular interaction domain (Czyzewicz et al., 2016; Meyer et al., 2015). However, *in vitro* binding assays revealed no direct interaction between CLE40 and ACR4. Additionally, the crystal structure of ACR4 suggests that ACR4 contributes indirectly to CLE40 perception (Satohiro Okuda, Ludwig A. Hothorn, 2020).

1.2.2 Known CLE peptides of the CLV pathway

Plant peptides are protein molecules smaller than 10 kDa and can be divided into two main classes: i) peptides with a biological function that are derived from larger precursor proteins, which must be first cleaved by peptidases, and ii) peptides that do not require post-translational processing for their function (Breiden & Simon, 2016; Farrokhi et al., 2008; Olsson et al., 2019). The first class can be further subdivided into three groups according to the characteristics of the mature peptide. The prepropeptide is usually non-functional and gets processed into a mature peptide, which results in either a peptide, rich in cysteine residues, a peptide that is post-translational modified (PTM), or a peptide containing specific amino acids required for its activity (Tavormina et al., 2015). The PTMs are usually tyrosine sulfation, proline hydroxylation, or hydroxyl arabinosylation (Matsubayashi, 2014). Most prepropeptides possess sorting sequences at their N-terminus to direct the peptides into the secretory pathway, where they are further processed by PTMs or proteolytic cleavage. In the first processing step, the N-terminal sorting sequence is removed by a peptidase located at the endoplasmic reticulum and the prepropeptide becomes a propeptide. The final processing step differs between different peptide families. The correct folding, length, and PTMs of a peptide are very important for the specific interaction with a receptor (Olsson et al., 2019).

1.2.2.1 CLAVATA3

The CLE peptide family was named after CLV3, which was the first CLE peptide that was analyzed and named after the Embryo Surrounding Region (ESR) from maize (Clark et al., 1995; Fletcher et al., 1999; Opsahl-Ferstad et al., 1997). There exist about 42 different CLE genes among various plant species and 24 of them were found in *A. thaliana* (Cock &

McCormick, 2001). CLE peptides belong to the first class of peptides, which form non-functional prepropeptides. These prepropeptides consist of three regions, the N-terminal hydrophobic sorting sequence (15 to 69 amino acids (aa)), the middle domain of 40 to 90 aa, and the C-terminal domain of 1 to 150 aa, which carries the CLE box motif (Strabala et al., 2014). In the case of CLV3, the N-terminal sorting sequence consists of one exon and one intron (56 aa), the middle region comprises 22 aa, and the C-terminal domain, containing the CLE-box motif, consists of 49 aa (Fig. 5). After the prepropeptide gets cut by a serine peptidase and the C-terminal domain gets processed by a carboxypeptidase, the PTMs of CLV3 include a proline hydroxylation and an arabinosylation, resulting in a mature peptide of 13 aa: RTV[Hyp]SG[(L-Ara)$_3$Hyp]D[Hyp]LHHH (Ito & Fukuda, 2006; Ni et al., 2011; Kondo et al., 2006) (Fig. 5). The mature CLV3 peptide is secreted to the extracellular space where it can activate signaling cascades by interacting with its corresponding LRR Receptor, such as CLV1 (Matsubayashi, 2014; Miyawaki et al., 2013).

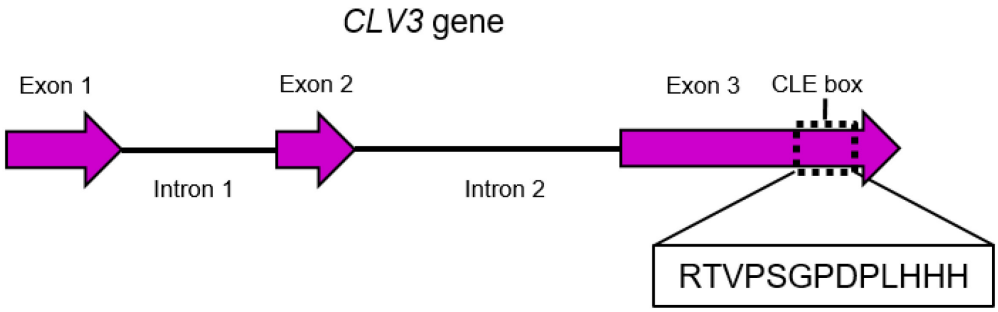

Fig. 5: Schematic representation of the genomic CLV3 gene

The genomic CLV3 region is about 600 bp long, comprising three exons (purple arrows) and two introns (black lines). The CLE-Box (dashed black line) in Exon3 carries the sequence for mature CLV3 signaling peptide consisting of the 13 aa: RTVPSGPDPLHHH.

CLV3 belongs to the CLE peptide family that is a major group of signaling peptides in plants. CLE peptides play, among others, important roles in plant immune response, growth, and development. In 1995, the first phenotypic observation of different *clv3* mutants revealed a similar phenotype to the *clv1* mutant described in 1993 (Clark et.al., 1993; Clark et al., 1995). As for *clv1* mutants, *clv3* mutants showed already at embryo stage an enlarged SAM. After passing vegetative and inflorescence state, the meristems of *clv3* mutants became up to 1000-fold bigger than meristems of wild type plants. Interestingly, no changes in root development of *clv3* mutants were detected, demonstrating that CLV3 is a specific regulator for shoot meristem development (Clark et al., 1995). Besides an enlarged and fasciated meristem, *clv3*

mutants show extra organs of all types, pronounced in stamens and carpels. Double mutants of *clv3;clv1* were found to be mutually epistatic, suggesting that *CLV1 and CLV3* genes act in the same pathway. RNA *in situ* experiments displayed *CLV3* expression in a very specific area at the tip of the meristem, indicating for the first time that CLV3 could be a ligand for the LRR receptor CLV1 (Fletcher et al., 1999). In 2000, Brand and colleagues showed that *clv* and *wus* mutants also act epistatic to each other, demonstrating that they are involved in the same pathway. It was proposed that CLV3 acts from the stem cell domain of the shoot meristem to repress WUS in the OC via CLV1 (Brand et al., 2000). Further studies confirmed this negative feedback loop, in which CLV3 activates two parallel signaling pathways via CLV1 and CLV2-CRN, both repressing the transcription factor *WUS*. In turn, WUS activates the expression of *CLV3* (Brand et al., 2000, 2002; Daum et al., 2014; Müller et al., 2008; Yadav et al., 2011). Finally, the direct interaction of CLV3 and CLV1 could be confirmed by a radio-active labeling technique (Ogawa et al., 2008). In addition, the CLV3-related peptide ZmFCP1 in maize was suggested to be expressed in primordia, and convey a repressive signal on the stem cell domain (Je et al., 2016).

Thus, it was shown that WUS function is required for *CLV3* expression (Brand et al., 2000; Brand et al., 2002). However, not only WUS but also the homeobox TF SHOOT MERISTEMLESS (STM) regulates *CLV3* expression. In contrast to *WUS, STM* is expressed throughout the entire SAM and inhibits cell differentiation to maintain stem cell fate (Endrizzi et al., 1996). Already in 2002, it was proposed that *WUS* and *STM* together repress cell differentiation in the stem cells and activate the expression of *CLV3* (Brand et al., 2002; Lenhard et al., 2002). Recently, it was confirmed that STM and WUS can physically interact, thereby enhancing the binding of WUS to the *CLV3* promoter. Furthermore, the authors showed that direct binding of WUS and STM is required for CLV3 expression in the meristem (Su et al., 2020).

1.2.2.2 CLE40

CLE40 is one of the 24 identified CLE peptides in Arabidopsis according to the Arabidopsis Information Resource Center (https://www.arabidopsis.org/). CLE40 is the closest homologue of CLV3, since their aa sequence only differs in 4 aa, and both prepropeptides consist of three exons and two introns, while all other CLE-peptides are intronless (Hobe et al., 2003; Schmid, 2015) (Fig. 6).

Fig. 6: CLE40 is the closest homologue of CLV3

The mature peptides of CLE40 and CLV3 show high similarity since they only differ in four (green and red) out of 13 aa. Three of the four aa are conservative substitutions (green), while only one aa is highly conserved (red).

However, in contrast to *CLV3,* which is only expressed in the tip of the meristem, *CLE40* transcripts showed ubiquitous weak expression in inflorescence apices, leaves, and roots. Overexpression of *CLE40* resulted in the termination of shoot and floral meristems, suggesting a downregulation of the transcription factor *WUS* similar to CLV3 function. However, *CLE40* expressed under the control of the *CLV3* promoter was able to fully rescue the *clv3* mutant phenotype. Even though *CLE40* expression under its endogenous promoter was also found in the inflorescences, no differences in shoot growth or floral organ number were detected in *cle40-2* mutants compared to *Col-0* plants (Hobe et al., 2003; Stahl et al., 2009). However, in 2015 it was shown that *cle40-2;clv1/2* double and triple mutants have a decreased number of carpels compared to *clv* single mutants, suggesting an indirect promoting effect on meristem size by CLE40 (Schmid, 2015).

CLE40 is also expressed in the root in the stele, the elongation zone, and in CCs in the distal root meristem (Stahl et al., 2009; Wink, 2013). Initial studies showed no changes in root meristem architecture in *cle40-2* mutants. However, these plants displayed shorter roots growing in a strongly waving pattern compared to *Col-0* roots (Hobe et al., 2003). Stahl and colleagues also demonstrated that CLE40 promotes differentiation in the distal root meristem in a dose-dependent manner. Investigation of root meristem morphology in *clv2*, *wox5,* and *acr4* mutants in response to CLE40 peptide (CLE40p) treatment revealed that *clv2* mutants act independently of CLE40 perception whereas ACR4 might be one of the receptors perceiving CLE40p (Stahl et al., 2009). WOX5 is the WUS homologue in the root meristem, promoting CSC fate (Sarkar et al., 2007). Stahl et al. could also show that CLE40 regulates *WOX5* expression, and thus proposed that CLE40 might be perceived by ACR4. ACR4 represses stem cell fate and *WOX5* expression, which acts in a negative feedback loop to promote stem cell fate (Stahl et al., 2009). 2013 Stahl et al. confirmed that *ACR4* expression was increased by exogenous CLE40p, but did not change *CLV1* expression levels. In *N. benthamiana* leaves ACR4 and CLV1 can form heteromeric complexes suggesting that a complex of ACR4 and CLV1 can perceive CLE40p in the distal root meristem (Stahl et al.,

2013). Furthermore, it was shown that one of the main functions of CLE40 in the root is the positioning of the QC. Thus, WOX5 represses cell differentiation in the QC while CLE40, probably via a heteromeric complex of CLV1 and ACR4, promotes CSC differentiation (Berckmans et al., 2019). However, Wang and colleagues suggested that similar to the shoot, *BAM* genes insulate the QC from CLE peptides, as they detected an obvious resistance to CLE40p, but not to CLV3p when using a truncated version of the *BAM1* gene (C. Wang et al., 2018). Confirming the hypothesis that CLV2 acts independently from CLE40, Pallakies and Simon could demonstrate that CLE40 and CLV2 control root meristem growth in antagonistic signaling pathways. They proposed that the receptor complex CLV2-CRN promotes cell differentiation in the transition zone of the proximal meristem, while CLE40 is inhibiting cell differentiation in the root meristem via phytohormones, like auxin and CK (Pallakies & Simon, 2014).

2. Aim of this thesis

The stem cell harboring shoot meristems give rise to all above-ground tissue and stay active throughout the entire life cycle of a plant. The perfect balance between stem cell proliferation and the replenishment of cells required for organ formation is pivotal for all plants. This homeostasis is coordinated by the CLV3-WUS signaling pathway. CLV3 is a dodecapeptide produced and secreted in stem cells at the tip of the shoot meristems and signals through the LRR receptor CLV1 to downregulate the activity of the homeodomain TF WUS. While *WUS* expression is confined to cells in the corpus of the meristem, WUS protein moves through plasmodesmata to the CZ at the tip and promotes stem cell identity together with *CLV3* expression. The mutual regulation of WUS and CLV3 provides a negative feedback loop controlling the size of the stem cell population.

How stem cell activity is coordinated with organ initiation and cell differentiation is so far not known. Thus, we need a better understanding of how other peptides and receptors are integrated into the maintenance of meristem size, the production of lateral organs, and overall plant growth.

We, therefore, analyzed the role of the closest homologues of CLV3 and CLV1 by e.g. measuring the meristem width, height, and area size in different mutant backgrounds and by generating transcriptional and translational reporter lines to perform detailed expression pattern analysis. Furthermore, the effect on WUS in various mutant backgrounds was evaluated.

The closest homologue of CLV3 is CLE40, since both genes consist of three exons and two introns, while all other *CLE*-genes in *A. thaliana* are intronless. The LRR receptor BAM1 shares, besides its structural similarity, a 55% sequence identity with CLV1. Thus, we here studied the function of CLE40 and BAM1 in the IFM to achieve a better understanding of how stem cell homeostasis is maintained. Additionally, we also analyzed the role of the RLK ACR4, as it was shown that ACR4 controls cell fate in the columella lineage of the root apex upon CLE40 signaling.

Considering that many genes are conserved throughout the plant lineage, new insights on the regulation mechanism determining meristem size, organ formation, and plant growth in Arabidopsis, could also improve crop breeding.

3. Material and Methods

Tab. 1: Chemicals used in this study.

Name	Producer	Product no.	CAS no.
BASTA® non-selective herbicide	Bayer CropScience	84442615	N/A
bacto™ agar	gibco	214010	9105960
bacto™ yeast extract	gibco	212750	9070604
Carbenicillin disodium salt	Carl Roth	6344.2	4800-94-6
DAPI (4,6-diamidino-2-phenylindole)	N/A	N/A	28718-90-3
DL-phosphinothricin (PPT)	Duchefa Biochemie bv	P0159	77182-82-2
D-Alanine	Sigma-Aldrich (Merck)	A7377	338-69-2
D(+)-Saccharose	Carl Roth	4661.1	N/A
Gentamicin sulfate	Sigma-Aldrich (Merck)	G1264	1405-41-0
Hygromycin B	Duchefa Biochemie bv	H0192	31282-04-9
Hypochloride acid (~37%)	Thermo Fischer Scientific	H/120/PB15	1884567
Kanamycin monosulfate	Duchefa Biochemie bv	K0126.0005	25389-94-0
Magnesium chloride x 6H2O	Grüssig GmbH	12087	205
MES hydrate	Sigma-Aldrich (Merck)	10240885	1266615-59-1
Murashige & Skoog (+ Gamborg B5 vitamins)	Duchefa Biochemie bv	M0231.0050	N/A
Phusion High-Fidelity PCR polymerase	Thermo Fischer Scientific	F530S	N/A
Plant agar	Duchefa Biochemie bv	P1001.1000	9002-18-0
Potassium hydroxide	Sigma-Aldrich (Merck)	9643807	N/A

Propidium iodide	Thermo Fischer Scientific	P1304MP	25535-16-4
Rifampicin	TCI	R0079	13292-46-1
Spectinomycin HCl pentahydrate	Duchefa Biochemie bv	S0188	22189-32-8
Sodium dodecyl sulfate (SDS)	Sigma-Aldrich (Merck)	L3771	151-21-3
Sodium chloride	Carl Roth	3957.1	N/A
Sodium hypochloride (13%)	Zentrale Chemikalienlager (ZCL)	2N370	N/A
Synthetic CLV3 (RCV[Hyp]SG[Hyp]DPLHHH)	Peptides & Elephants	costumized	N/A
Synthetic CLE40 (RQV[Hyp]TGSDPLHHK)	Peptides & Elephants	costumized	N/A
Synthetic CLV3-Tamra (R-(K-TAMRA)-V[Hyp]SG[Hyp]DPLHHH)	Centic Biotec	costumized	N/A
Synthetic CLV3-Atto488 (R (K-Atto488)-V[Hyp]SG[Hyp]DPLHHH)	N/A	costumized	N/A
Tetracycline	Sigma-Aldrich (Merck)	87128	60-54-8
Tryptone	gibco	N/A	57091
Tween	Sigma-Aldrich (Merck)	P9416	9005-64-5

3.1 Plant material and growth conditions

All wild type *Arabidopsis thaliana* (L.) Heynh. plants used in this study are ecotype Columbia-0 (*Col-0*). Details about the *Arabidopsis thaliana* plants carrying mutations in the following alleles: *acr4-2, acr4-8, bam1-3, bam1-4, cle40-2, cle40-cr1, cle40-cr2 cle40-cr3, clv1-20, clv1-101, clv3-9,* and *wus-7* are described in Tab. 2. All mutants are in the *Col-0* background, except for the *wus-7* mutants, which are in the Landsberg *erecta* background. *acr4-2* is a weak allele as it contains a T-DNA insertion at base 249 of the ACR4 ORF (Gifford et al., 2003). *acr4-8* mutant allele is considered as a null-mutation since it has a T-DNA insertion within the CDS of ACR4 (NASC ID: N543679). The four *cle40* peptide mutants (*cle40-2, cle40-cr1, cle40-cr2,* and *cle40-cr3*) have either a stop codon, a T-DNA insertion, or deletion in the crucial CLE box domain (Fig. 8). *clv3-9* mutants were generated in Ethyl methanesulfonate screen in 2003 by the lab of R. Simon and have a W62STOP before the critical CLE domain region and thus are considered as null mutations. The *bam1-3* and *clv1-101* mutants have been described as null mutations before (DeYoung et al., 2006; Kinoshita et al., 2010), while *clv1-20* is a weak allele, which contains an insertion within the 5'-UTR of CLV1 and results in a reduced mRNA level (Durbak & Tax, 2011). *bam1-4* mutant allele is considered as a null mutation since it has a T-DNA insertion within the CDS of the *BAM1* gene (NASC ID: N601542). *wus-7* is a weak allele and mutants were described in previous publications (Ma et al., 2019).

Double mutant combinations were obtained by crossing the single mutant plants until both mutations were proven to be homozygous for both alleles. Genotyping of the plants was performed either by PCR or dCAPS method with the primers and restriction enzymes listed in Tab. 3.

Before sowing, seeds were either sterilized for 10 min in an ethanol solution (80% v/v ethanol, 1,3% w/v sodium hypochloride, 0,02% w/v SDS) or for 1h in a desiccator in a chloric gas atmosphere (50ml of 13% w/v sodium hypochlorite with 1ml 37% HCL). Afterwards, seeds were stratified for 48h at 4°C in darkness. The seeds on soil were then cultivated in phytochambers under long day (LD) conditions (16h light/ 8h dark) at 21°C. For the selection of seeds or imaging of vegetative meristems seeds were sowed on ½ Murashige & Skoog (MS) media (1% w/v sucrose, 0.22% w/v MS salts + B5 vitamins, 0.05% w/v MES, 12g/l plant agar, adjusted to pH 5.7 with KOH) in squared petri dishes. Seeds in petri dishes were kept in phytocabinets under continuous light conditions at 21°C and 60% humidity.

3.2 Recombinant DNA work

CLV1 (*CLV1:CLV1-GFP*), BAM1 (*BAM1:BAM1-GFP*), ACR4 (*ACR4:ACR4-GFP*), CLV3 (*CLV3:NLS 3xmCherry*), *WUS:CLV1-mVenus*, *WUS:BAM1-GFP,* and *WUS:ACR4-GFP* reporter lines were cloned using the GreenGate method (Lampropoulos et al., 2013). Entry and destination plasmids are listed in Tab. 4 and Tab. 5. Promoter and coding sequences were PCR amplified from genomic *Col-0* DNA that was extracted out of rosette leaves. Primers used for amplification of promoters and coding sequences can be found in Tab. 6 with the specific overhangs used for the GreenGate cloning system. Coding sequences were amplified without the stop codon to allow transcription of fluorophores at the C-terminus. BsaI restriction sites were removed by site-directed mutagenesis using the "QuickChange II Kit" following the manufacturer's instructions (Agilent Technologies). Plasmid DNA amplification was performed by heat-shock transformation into Escherichia coli DH5α cells (10 min on ice, 1 min at 42°C, 1 min on ice, 1 h shaking at 37°C), which were subsequently plated on selective LB medium (1% w/v tryptone, 0.5% w/v yeast extract, 0.5% w/v NaCl) and cultivated overnight at 37°C. For DNA extraction from the liquid culture, the Miniprep kit from "PeqLab" was used. All entry and destination plasmids were validated by restriction digest and Sanger sequencing. All entry plasmids carry the bacterial resistance Ampicillin and all destination plasmids were cloned using the pGGZ000 backbone.

3.3 Generation of stable *A. thaliana* lines

Generation of stable *A. thaliana* lines was done by using the floral dip method (Clough & Bent, 1998). Beforehand, destination vectors were transformed into *A. tumefaciens GV3101 pMP90 pSoup* (rifampicin, gentamycin and tetracycline resistant) via heat-shock method (5 min in liquid nitrogen, 5 min at 37°C, 2 h shaking at 28°C) and cultivated on selective (50 µg/ml rifampicin (R), 50 µg/ml gentamycin (G), 2.5 µg/ml tetracycline (T), and 100 µg/ml spectinomycin (S)) double Yeast Tryptone (dYT, 1.6% w/v tryptone, 1% w/v yeast extract, 0.5% w/v NaCl) plates for 48 h at 28°C. After transformation, *A. tumefaciens* carrying the plasmid DNA were inoculated in 5 ml of liquid selective dYT (+RGTS) media overnight at 28°C. Subsequently, the preculture was mixed into 100ml of selective dYT (+RGTS) media and was again cultivated overnight at 28°C. Next, the main culture was centrifuged (10 min, 4000 x g, 4°C) and the pellet was resuspended in transformation medium (5% w/v sucrose, 10 nM $MgCl_2$, 0.01% Silwet). Afterwards, *A. thaliana* plants (siliques were removed beforehand) at about 5 weeks after germination (WAG) were dipped into the transformation solution for about 2 to 5 min. Plants were kept overnight under high humidity conditions and were then transferred back

into the phytochambers to grow under normal conditions (21°C, LD). After the plants' lifecycle, T1 seeds were harvested and selected for positive transformants.

The translational CLV1 (*CLV1:CLV1-GFP*), ACR4 (*ACR4:ACR4-GFP*), and the transcriptional CLV3 (*CLV3:NLS 3xmCherry*) reporter carry the BASTA plant resistance cassette. T1 seeds were sown on soil and sprayed with Basta ® (0.125% v/v Basta, 0.1% v/v Tween) after 5 and 10 DAG. Only positive plants survived and seeds of about 10 independent lines were harvested. Translational BAM1 (*BAM1:BAM1-GFP*) reporter line carries a D-Alanin resistance cassette and T1 seeds were sown on ½ MS media containing 3-4mM D-Alanin. The misexpression lines *WUS:ACR4-GFP, WUS:BAM1-GFP,* and *WUS:CLV1-mVenus* carry the hygromycin resistance cassette and T1 seeds were sown on ½ MS media containing 15 µg/ml hygromycin. Only viable plants were selected for the T2 generation.

T2 seeds were then selected on ½ MS media supplied with either 10 µg/ml of DL-phosphinothricin (PPT) as a BASTA alternative, 3-4 mM D Alanine or 15 µg/ml hygromycin. At ~10 DAG only plant lines showing about ~75% viability were kept, transferred to soil, and cultivated under normal plant conditions (21°C, LD).

Last, T3 seeds were plated on ½ MS media supplied with 10 µg/ml PPT, 3-4mM D-Alanin or 15 µg/ml hygromycin again and plant lines showing 100% viability were kept as homozygous lines.

CLV1:CLV1-GFP, ACR4:ACR4-GFP, and *CLV3:NLS-3xmCherry* were transformed into *Col-0* wild type plants and after a stable T3 line was achieved, plants carrying the *CLV1:CLV1-GFP,* and *ACR4:ACR4-GFP* construct were crossed into *acr4-8*, *bam1-3, cle40-2, clv3-9,* and *clv1-101* mutants until a homozygous mutant background was reached. *BAM1:BAM1-GFP* lines were floral dipped into *bam1-3* mutants and subsequently crossed into the *clv1-20* mutant background that rescued the extremely fasciated meristem phenotype of *bam1-3;clv1-20* double mutants. *BAM1:BAM1-GFP//bam1-3* plants were then also crossed into *acr4-8*, *cle40-2,* and *clv3-9* mutants until a homozygous mutant background was achieved.

Misexpression reporters *WUS:ACR4-GFP, WUS:BAM1-GFP* and *WUS:CLV1-mVenus* were transformed into homozygous *acr4-8*, *bam1-3* and *clv1-101* mutant backgrounds respectively und were cultivated until a stable T3 line was reached.

The *CLE40:Venus-H2B* reporter line was created and described in Wink, 2013 and the *WUS:NLS-GFP;CLV3:NLS-mCherry* reporter line was a gift from the Lohmann lab (Wink, 2013).

CLE40:Venus-H2B reporter line was crossed into homozygous *clv3-9* and heterozygous *wus-7* mutants. Homozygous *clv3-9* mutants were detected by their obvious phenotype and were brought into a stable F3 generation. Homozygous *wus-7* mutants were genotyped. Seeds were kept in the F2 generation since homozygous *wus-7* plants do not develop seeds. The *CLE40:Venus-H2B* reporter line was also crossed with the *CLV3:NLS-3xmCherry* reporter line and was brought into a stable F3 generation. To generate the *CLE40:Venus-H2B//CLV3:WUS* line, plants carrying the *CLE40:Venus-H2B* line were floral dipped with the *CLV3:WUS* construct. T1 seeds were sown on 10 µg/ml of DL-phosphinothricin (PPT) and the viable seedlings were imaged.

WUS:NLS-GFP;CLV3:NLS-mCherry//Col-0 reporter line was crossed into *clv3-9*, *cle40-2*, *clv1-101,* and *bam1-3* mutants until a stable homozygous F3 generation was reached respectively.

Auxin reporter lines, *PIN1:PIN1-GFP* and *DR5rev:GFP*, were a gift from J. Friml lab and were crossed into *cle40-2* mutants until a homozygous background was reached.

Detailed information of all used Arabidopsis thaliana lines can be found in Tab. 7.

3.4 Confocal imaging of vegetative, inflorescence, and root meristems

To image IFMs *in vivo*, plants were grown under long-day (16h light/ 8h dark) conditions and inflorescences were cut off at 5 or 6 WAG. Inflorescences were stuck on double-sided adhesive tape on an objective slide and dissected until only the meristem and primordia from P0 to maximum P10 were visible. Next, inflorescences were stained with either propidium iodide (PI 5 mM) or 4′,6-Diamidin-2-phenylindol (DAPI 1 µg/ml) for 2 to 5 min. Inflorescences were then washed three times with water and subsequently covered with water and a cover slide and placed under the microscope. All imaging was performed with a Zeiss LSM780 or LSM880 using a W Plan Apochromat 40x/1.2 objective. Laser excitation, emission detection range and detector information for fluorophores and staining can be found in Tab. 8. All IFMs were imaged from the top taking XY images along the Z-axis, resulting in a Z-stack through the inflorescence. The vegetative meristems were imaged as described for IFMs.

Live imaging of fluorescent reporter lines in *A. thaliana* plants was performed by dissecting primary inflorescences (except for *clv3-9* mutants) at 5 WAG under LD conditions. For imaging of reporter lines in the mutant backgrounds of *clv3-9* secondary IFMs were dissected, since

the primary meristems are highly fasciated. For each reporter line in every mutant background, at least 8 IFMs were imaged.

Vegetative meristems were cultivated in continuous light conditions at 21°C on ½ MS media plates and were imaged at 10 DAG.

Roots were cultivated in continuous light conditions at 21°C on ½ MS media plates and were imaged at 7 DAG. Roots were carefully placed on the objective slide and stained with 10 µM PI. After covering the roots with a cover slide they were imaged with a Zeiss LSM880 using the W Plan Apochromat 40x/1.2 objective.

3.5 Phenotyping of plant size, leaf length, and meristem sizes

For phenotyping, photos of the whole plant, inflorescence, and carpels were taken at 6 WAG under normal LD conditions with a Canon EOS 700D camera.

Leaf measurements were performed at 4 WAG. Photos of plants were taken and afterwards four leaves of each plant were measured in ImageJ and plotted with Prism. Data were obtained from 3 independent experiments.

For meristem measurements (area size, width and height) primary and secondary IFMs of wild type (*Col-0*) and mutant plants (*acr4-2*, *acr4-8, bam1-3, bam1-4, cle40-2, cle40-cr1-3, clv1-20, clv1-101, clv1-101;cle40-2, cle40-2;bam1-3, acr4-8;cle40-2, acr4-8;clv1-101, acr4-8;clv1-101;cle40-2*) were dissected at 6 WAG under LD conditions. For *clv3-9* and *clv1-101;bam1-3* only secondary IFMs were imaged and analyzed, due to the highly fasciated primary meristems. Optical sections of the Z-stacks were performed through the middle of the meristem starting in the center of primordia P5 and ending in the center of primordia P4. Based on the optical sections (XZ), meristem height, width, and area size were measured.

The same procedure was used to count the cells expressing *WUS* in different mutant backgrounds (Fig. 11, Fig. 18, Fig. 23, Fig. 28). Optical sections of IFMs at 5 WAG were performed from P4 to P5 and only nuclei within the meristem area were counted.

3.6 Peptide treatment on inflorescence and root meristems

Peptide treatment was performed on IFMs at 5 WAG carrying either the *ACR4:ACR4-GFP* or *CLV1:CLV1-GFP* marker.

IFMs of the *CLV1:CLV1-GFP* reporter line were dipped for 1 to 5 min into a peptide solution (10 µM CLV3hyp13 or CLE40hyp13, 0.002% Silwet) 48 h, 24 h and 10 min before imaging. As a negative control, IFMs were dipped for 1 to 5 min into ½ liquid MS media supplied with 0.002% Silwet. As a positive control, IFMs at 5 WAG were dipped into a Brefeldin A solution (50 µM BFA, 0.002% Silwet) 15 min before imaging (Fig. 33).

To visualize the effect of peptide treatment over a short period of time, IFMs carrying the *ACR4:ACR4-GFP* reporter were dissected at 5 WAG, stained with PI (1 mM), and imaged before treatment. After imaging, the cover slide was removed carefully and the IFM was treated with either ½ liquid MS media supplied with 0.002% Silwet or with a peptide solution containing 10 µM CLE40hyp13 and 0.002% Silwet. After 1 min of treatment, the IFM was covered with the cover slide again and imaged. After imaging, the same procedure was repeated but now the IFM was treated for 30 min with either ½ liquid MS media or the peptide solution (Fig. 34).

In a second experiment, only a few cells in the L1 of IFMs at 5 WAG carrying the *ACR4:ACR4-GFP* reporter were imaged without treatment, after 5 min, 10 min, and 20 min of treatment with either ½ liquid MS media supplied with 0.002% Silwet or with a peptide solution containing 10 µM CLE40hyp13 and 0.002% Silwet. All IFMs were stained with 1 mM PI solution for cell wall detection. For each time point and treatment, at least 3 IFMs were imaged (Fig. 35).

To test if the CLV3hyp13-Tamra and the CLV3hyp13-Atto488 peptides are functional, *Col-0* and *clv2-101* mutants were grown on ½ MS media containing 100 nM, 200 nM, or 1 µM of the peptide. Root lengths were measured after 7, 10, or 14 DAG as indicated in each figure.

3.7 Data analysis

For visualization of images the open-source software ImageJ v 1.53c (Schneider et al., 2012) was used. All images were adjusted in “Brightness and Contrast”. MIPs were created by using the “Z-Projection“ function and optical sections were performed with the “Reslice…” function resulting in the XZ view of the image. Meristem width, height, and area size were measured with the “Straight line” for width and height and the “Polygon selection” for area size.

For L1 visualization the open-source software MorphoGraphX (https://www.mpipz.mpg.de/MorphoGraphX/) was used that was developed by Richard Smith. 2½ D images were created by following the steps in the MorphoGraphX manual (de Reuille et al., 2015). After both channels (PI and fluorophore signal) were projected to the created mesh, both images were merged using ImageJ v 1.53c.

Analysis of IFMs treated with CLE40hyp13p for 5, 10, or 20 min, was performed with ImageJ v 1.53c and plotted in GraphPad Prism v8.0.0.224. For each meristem, randomly three lines were drawn with the cell wall in its center and an intensity plot profile (grey values) was created for the green channel (ACR4). The mean of all nine measurements (3 meristems á 3 lines) for each condition was plotted (Fig. 35).

For all statistical analyses, GraphPad Prism v8.0.0.224 was used. Statistical groups were assigned after calculating p-values by ANOVA and Turkey's or Dunnett's multiple comparison test (differential grouping from $p \leq 0.001$) as indicated under each figure. Same letters indicate no statistical differences. All plasmid maps and cloning strategies were created and planned using the software VectorNTI®.

3.8 Authors contribution

Cloning of entry plasmids was performed by Patrick Blümke, Grégoire Denay, Rebecca Burkhart, and me, as indicated in Tab. 4. Generation of stable Arabidopsis lines (*ACR4:ACR4-GFP*, *CLV1:CLV1-GFP* and *BAM1:BAM1-GFP)* was performed by Grégoire Denay as shown in Tab. 7. Reporter lines for *CLE40:Venus-H2B*, *CLV3:NLS-mCherry;WUS:NLS-GFP* and *PIN1:PIN1-GFP* were gifts from Rene Wink (Simon lab), Anne Pfeiffer (Lohmann lab) and J. Friml, respectively (Tab. 7). Karine G. Pinto, Grégoire Denay, and me, performed crossings of stable Arabidopsis lines into mutant backgrounds. All imaging and other experiments were performed by me.

Tab. 2: Mutants used in this study.

Alelle	Gene	Mutation	Reference
acr4-2	AT3G59420	T-DNA	Gifford et al., 2003; SAIL_240_B04
acr4-8	AT3G59420	T-DNA	SALK_043679.1
bam1-3	AT5G65700	T-DNA	Alonso et al., 2003; SALK_015302
bam1-4	AT5G65700	T-DNA	SALK_101542
cle40-2	AT5G12990	Transposon mutation	Stahl et al., 2009
cle40-cr1 *cle40-cr2* *cle40-cr3*	AT5G12990	CRISPR	Yamaguchi et al., 2017
clv3-9	AT2G27250	EMS	Rüdiger Simon, 2003
clv1-20	AT1G75820	T-DNA	SALK_008670
clv1-101	AT1G75820	T-DNA	Kinoshita et al., 2010; CS858348
wus-7	AT2G17950	EMS	Graf et al., 2010

Tab. 3: Primers and methods used for genotyping.

Allele	Method	Primer	PCR product
acr4-2	PCR	acr4-2_F: GTGAGAACTCCGCAAGTGAAG acr4-2_R: TTGTGAACTTCGTGTGACTCG LBb3sail: TAGCATCTGAATTTCATAACCAATCTCGATACAC	WT amp. : ~1000 bp mutant amp. : ~750 bp
acr4-8	PCR	acr4-8_F: AGAAGCAGCAGTTTTGGTCG acr4-8_R: CAAGAATGCCACAAACATGG LBb1.3: ATTTTGCCGATTTCGGAAC	WT amp. : ~1112 bp mutant amp. : ~650 bp
bam1-3	PCR	bam1-3_F: CTAACGACTCTCCGGGAGCT bam1-3_R: TAAGGACCACAGAGATCAGGATTAC LbaI_R: TGGTTCACGTAGTGGGCCATCG	WT amp. : 1208 bp mutant amp. : 998 bp
bam1-4	PCR	bam1-4_F: AACAATGTCTTCAACGGTTCG bam1-4_R: ATCAATCTTCGAGAGCTGCTG Lbb1.3_R: ATTTTGCCGATTTCGGAAC	WT amp. : 1152 bp mutant amp. : ~660 bp
cle40-2	dCAPS	cle40-2_F: GGAGAAACACAAGATACGAAAGCCATG cle40-2_R: ATTGTGATTTGATACCAACTTAAAA	Restriction enzyme: AseI WT amp. : 460 + 200 bp mutant amp. : 410 + 200 + 60 bp
cle40-cr1 *cle40-cr2* *cle40-cr3*	dCAPS	cle40-cr_F: ATGGCGGCGATGAAATACAA cle40-cr_R: GTTACGCTTTGGCATCTTTCC	Restriction enzyme: BamHI WT amplification: 750 bp mutant amp. : 491 + 259 bp
clv1-20	PCR	clv1-20_F: TTTGAATAGTGTGTGACCAAATTTGA clv1-20_R: TCCAATGGTAATTCACCGGTG LBa.1: TGGTTCACGTAGTGGGCCATCG	WT amp.: 860bp mutant amp: 1200bp
clv1-101	PCR	clv1-101_F: TTCTCCAAATTCACCAACAGG clv1-101_R: CAACGGAGAAATCCCTAAAGG WiscLox_LT6_R: AATAGCCTTTACTTGAGTTGGCGTAAAAG	WT amp. : 1158 bp mutant amp. : 896 bp
wus-7	dCAPS	wus-7_F: CCGACCAAGAAAGCGGCAACA wus-7_R: AGACGTTCTTGCCCTGAATCTTT	Restriction enzyme: XmnI WT amplification: 216 bp mutant amp. : 193 bp + 23 bp

Tab. 4: Entry plasmids used in this study.

Name	Description	Backbone	Reference/ Origin
proACR4	ACR4 promoter 1942 bp upstream from transcription start	pGGA000	Jenia Schlegel
proBAM1 (pGD288)	BAM1 promoter 3522 bp upstream from transcription start	pGGA000	Grégoire Denay
proCLV3	CLV3 promoter 1480 bp upstream from transcription start	pGGA000	Jenia Schlegel
proCLV1	CLV1 promoter 5759 bp upstream from transcription start	pGGA000	Patrick Blümke
proWUS (pGGA004)	WUS (WUSCHEL; 4.4 kb) promoter	pGGA000	Lampropoulos et al., 2013
omega-element (pGGB002)	Omega- element	pGGB000	Lampropoulos et al., 2013
SV40 NLS (pGGB005)	SV40 NLS (SIMIAN VIRUS 40 NUCLEAR LOCALIZATION SIGNAL)	pGGB000	Lampropoulos et al., 2013
ACR4_CDS (pGD351)	ACR4 coding region genomic region of ACR4 START to one codon before STOP, including introns, internal BsaI sites removed	pGGC000	Jenia Schlegel
BAM1_CDS (pGD351)	BAM1 coding region genomic region of BAM1 START to one codon before STOP, including introns, internal BsaI sites removed	pGGC000	Grégoire Denay
CLV1_CDS	CLV1 coding region 2946 bp coding region amplified from genomic Col-0 DNA without STOP codon and internal BsaI site removed	pGGC000	Jenia Schlegel
3x-mCherry (pGGC026)	3x mCherry	pGGC000	Lampropoulos et al., 2013
linker-GFP (pGD165)	linker(10aa)-eGFP	pGGD000	Grégoire Denay
linker-GFP (pGGD001)	linker-GFP	pGGD000	Lampropoulos et al., 2013
mVenus (pRD43)	mVenus	pGGD000	Rebecca Burkhart
d-dummy (pGGD002)	d-dummy	pGGD000	Lampropoulos et al., 2013

tCLV3	CLV3 terminator 1257 bp downstream of transcription stop	pGGE000	Jenia Schlegel
tUBQ10 (pGGE009)	UBQ10 terminator	pGGE000	Lampropoulos et al., 2013
BastaR (pGGF008)	pNOS:BastaR (chi sequence removed):tNOS	pGGF000	Lampropoulos et al., 2013
D-AlaR (pGGF003)	pMAS:D-AlaR:tMAS	pGGF000	Lampropoulos et al., 2013
HygromycinR (pGGF005)	pUBQ10:HygrRi:tOCSj	pGGF000	Lampropoulos et al., 2013

Tab. 5: Destination plasmids used in this work.

Name	Promoter	N-tag	CDS	C-tag	Terminator	Resistance
ACR4:ACR4-GFP	proACR	Ω- element (pGGB002)	ACR4-CDS	linker(10aa)- eGFP (pGD165)	tUBQ10 (pGGE009)	BastaR (pGGF008)
BAM1:BAM1-GFP	proBAM1	Ω- element (pGGB002)	BAM1-CDS	linker(10aa)- eGFP (pGD165)	tUBQ10 (pGGE009)	D-Alanin (pGGF003)
CLV1:CLV1-GFP	proCLV1	Ω- element (pGGB002)	CLV1-CDS	linker(10aa)- eGFP (pGD165)	tUBQ10 (pGGE009)	BastaR (pGGF008)
CLV3:NLS-3xmCherry	proCLV3	SV40 NLS (pGGB005)	3x-mCherry (pGGC026)	d-dummy (pGGD002)	tCLV3	BastaR (pGGF008)
WUS:ACR4-GFP	proWUS (pGGA004)	Ω- element (pGGB002)	ACR4-CDS	linker-GFP (pGGD001)	tUBQ10 (pGGE009)	HygroR (pGGF005)
WUS:BAM1-GFP	proWUS (pGGA004)	Ω- element (pGGB002)	BAM1-CDS	linker-GFP (pGGD001)	tUBQ10 (pGGE009)	HygroR (pGGF005)
WUS:CLV1-mVenus	proWUS (pGGA004)	Ω- element (pGGB002)	CLV1-CDS	mVenus (pRD43)	tUBQ10 (pGGE009)	HygroR (pGGF005)

Tab. 6: Primers used for cloning.

Name	Primer
proACR4	F: AAAGGTCTCAACCTCTTGTTTGAAGGG R: AAAGGTCTCATGTTTCTTTTCAAAGTCAAC BsaI-site_#1_F: CTTAGAATCAGTAATGGACTCAAGTCAACTTTAAAGACG BsaI-site_#1_R: CGTCTTTAAAGTTGACTTGAGTCCATTACTGATTCTAAG BsaI-site_#2_F: GAATCAGTAATGGTATCAAGTCAAC BsaI-site_#2_R: GTTGACTTGATACCATTACTGATTC
ACR4_CDS	F: TTTGGTCTCAGGCTCGATGAGAATGTT R: TTTGGTCTCACTGAGAAATTATGATGCAA BsaI-site_#1_F: TCTGATGGCTCTCATCTTGTGG BsaI-site_#1_R: CCACAAGATGAGAGCCATCAGA BsaI-site_#2_F: GCTGATTTTGGACTCTCCTTACTTG BsaI-site_#2_R: CAAGTAAGGAGAGTCCAAAATCAGC
proBAM1 (pGD288)	F: AAAGGTCTCAACCTATGATCCGATCCTCAAAAGTATGTA R: AAAGGTCTCATGTTTCTCTCTATCTCTCTTGTGTG
BAM1_CDS (pGD351)	F: TTTGGTCTCAGGCTCTATGAAACTTTTTCTTCTCCTTC R:TTTGGTCTCACTGATAGATTGAGTAGATCCGGC BsaI-site_#1_F: CTTGATCTCTCCGGACTCAACCTCTCCGG BsaI-site_#1_R: CCGGAGAGGTTGAGTCCGGAGAGATCAAG BsaI-site_#2_F: CTCATGTTGCTGACTTTGGACTCGCTAAATTCCTTCAAG BsaI-site_#2_R: CTTGAAGGAATTTAGCGAGTCCAAAGTCAGCAACATGAG
proCLV1	F: AAAGGTCTCAACCTGACTATTGTTTATACTTAGTTG R: TTTGGTCTCATGTTCATTTTTTTAGTGTCCTC
CLV1_CDS	F: AAAGGTCTCAGGCTTAATGGCGATGAGAC R: TTTGGTCTCACTGAACGCGATCAAGTTC BasI-site_#1_F: CTAAAGGACACGGACTGCACGACTG BasI-site_#1_R: CAGTCGTGCAGTCCGTGTCCTTTAG BasI-site_#2_F: CTTAGAGTATCTTGGACTGAACGGAGCTGG BasI-site_#2_R: CCAGCTCCGTTCAGTCCAAGATACTCTAAG
proCLV3	F: AAAGGTCTCAACCTCGGATTATCCATAATAAAAAC R:AAAGGTCTCATGTTTTTTAGAGAGAAAGTGACTGAG
tCLV3	F: TTTGGTCTCTCTGCCGCCCTAATCTCTTGTT R: TTTGGTCTCGTGATATGTGTGTTTTTTCTAAACAATC
mVenus (RD43)	F: AAAGGTCTCATCAGCAATGGTGAGCAAGG R: AAAGGTCTCAGCAGTTACTTGTACAGCTC

Tab. 7: Arabidopsis lines used in this work.

Name/Construct	Background	Plant resistance	Generation	Reference
ACR4:ACR4-GFP (GD166)	*Col-0*	Basta	T4	Grégoire Denay
ACR4:ACR4-GFP	*bam1-3*	Basta	F3	Jenia Schlegel
ACR4:ACR4-GFP	*clv3-9*	Basta	F3	Jenia Schlegel
ACR4:ACR4-GFP	*cle40-2*	Basta	F3	Jenia Schlegel
ACR4:ACR4-GFP	*clv1-101*	Basta	F3	Jenia Schlegel
BAM1:BAM1-GFP (GD409)	*bam1-3*	D-Ala	T4	Grégoire Denay
BAM1:BAM1-GFP	*bam1-3;acr4-8*	D-Ala	F3	Jenia Schlegel
BAM1:BAM1-GFP	*bam1-3;clv1-20*	D-Ala	F3	Grégoire Denay
BAM1:BAM1-GFP	*bam1-3;clv3-9*	D-Ala	F3	Jenia Schlegel
BAM1:BAM1-GFP	*bam1-3;cle40-2*	D-Ala	F3	Jenia Schlegel
CLE40:Venus-H2B	*Col-0*	Hygromycin	T5	Rene Wink
CLE40:Venus-H2B	*clv3-9*	Hygromycin	F3	Jenia Schlegel
CLE40:Venus-H2B	*wus-7*	Hygromycin	F2	Jenia Schlegel
CLE40:Venus-H2B	*CLV3:WUS//Col-0*	Hygromycin/Basta	T1*	Grégoire Denay
CLV1:CLV1-GFP (GD167)	*Col-0*	Basta	T4	Grégoire Denay
CLV1:CLV1-GFP	*acr4-8*	Basta	T4	Jenia Schlegel
CLV1:CLV1-GFP	*bam1-3*	Basta	F3	Jenia Schlegel
CLV1:CLV1-GFP	*clv3-9*	Basta	F3	Jenia Schlegel
CLV1:CLV1-GFP	*cle40-2*	Basta	F3	Jenia Schlegel
WUS:ACR4-GFP	*acr4-8*	Hygromycin	T3	Jenia Schlegel

WUS:BAM1-GFP	*bam1-3*	Hygromycin	T3	Jenia Schlegel
WUS:CLV1-mVenus	*clv1-101*	Hygromycin	T3	Jenia Schlegel
CLV3:NLS-3xmCherry	*CLE40:Venus-H2B //Col-0*	Basta/ Hygromycin	F3	Jenia Schlegel
CLV3:NLS-mCherry WUS:NLS-GFP	*Col-0*	Kanamycin	N/A	Anne Pfeiffer
CLV3:NLS-mCherry WUS:NLS-GFP	*cle40-2*	Kanamycin	F3	Jenia Schlegel
CLV3:NLS-mCherry WUS:NLS-GFP	*bam1-3*	Kanamycin	F3	Jenia Schlegel
CLV3:NLS-mCherry WUS:NLS-GFP	*clv1-101*	Kanamycin	F3	Jenia Schlegel
CLV3:NLS-mCherry WUS:NLS-GFP	*clv3-9*	Kanamycin	F3	Jenia Schlegel
PIN1:PIN1-GFP	*Col-0*	Kanamycin	N/A	J. Friml lab
PIN1:PIN1-GFP	*cle40-2*	Kanamycin	F3	Jenia Schlegel
DR5rev:GFP	*Col-0*	Sulfonamide	N/A	J. Friml lab
DR5rev:GFP	*cle40-2*	Sulfonamide	F3	Jenia Schlegel

Tab. 8: Microscopy settings.

Flurophore/ Staining	Excitation	Emisson	MBS	Detector	Light source
DAPI	405 nm	410 - 490 nm	405	PMT*	Diode
GFP	488 nm	500 - 545 nm	488/461	GaAsP	Argon laser
Atto488	488 nm	500 - 545 nm	488/461	PMT*	Argon laser
mCherry	561 nm	570 - 640 nm	458/561	PMT*	DPSS laser**
PI	561 nm	595 - 650 nm	488/461	PMT*	DPSS laser**
Tamra	561 nm	570 - 650 nm	488/461	PMT*	DPSS laser**
Venus	514 nm	518 - 540 nm	458/514	GaAsP	Argon laser

* Photomultiplier tubes
** Diode-pumped solid state

4. Results

The maintenance of stem cells is one of the most important regulatory processes in a plant. Stem cells are essential to create new plant tissues and organs (Hall & Watt, 1989). In plants, stem cells reside in the meristems and the well-studied CLV pathway regulates the homeostasis of the stem cells in the shoot meristems (see page 5). While the key elements of CLV signaling are described, little is known about how other peptides and receptors are integrated into the maintenance of the SAM. The following results demonstrate a new antagonistic pathway playing an important role in stem cell signaling. Furthermore, a detailed analysis of the expression pattern of the involved receptors in various mutant backgrounds provides a comprehensive view of the interdependencies of receptors and ligands in stem cell maintenance.

4.1 The role of CLE40 in the IFM

Of the 24 described CLE peptides in *A. thaliana*, CLV3 is the best characterized. It is exclusively expressed in the stem cells of the SAMs, IFMs, and FMs, and therefore often serves as a stem cell marker. However, very little is known about CLE40, the closest homologue of CLV3. Both peptides share a highly similar sequence structure since they are the only CLE peptides that consist of two introns and three exons (Fig. 7, A).

4.1.1 *cle40* mutants have smaller meristems than wild type plants

CLE40 was previously shown to fully rescue *clv3-2* mutants if expressed from a CLV3 promoter (Hobe et al., 2003). Loss-of-function mutations in *CLV3* cause a cumulative increase in stem cells and floral organs, and often fasciation of the mutant SAM and IFMs (Fig. 7, C, C'), demonstrating a restricting effect of the functional *CLV3* gene on meristem size. In contrast, *cle40-2* IFMs are smaller compared to wild type (*Col-0*) plants (Fig. 7, D, D', E), resulting in a promoting effect on meristem size. We observed that *cle40-2* mutants have 1.5 times smaller meristems than *Col-0* and around 6 times smaller meristems than *clv3-9* mutants (Fig. 7, E).

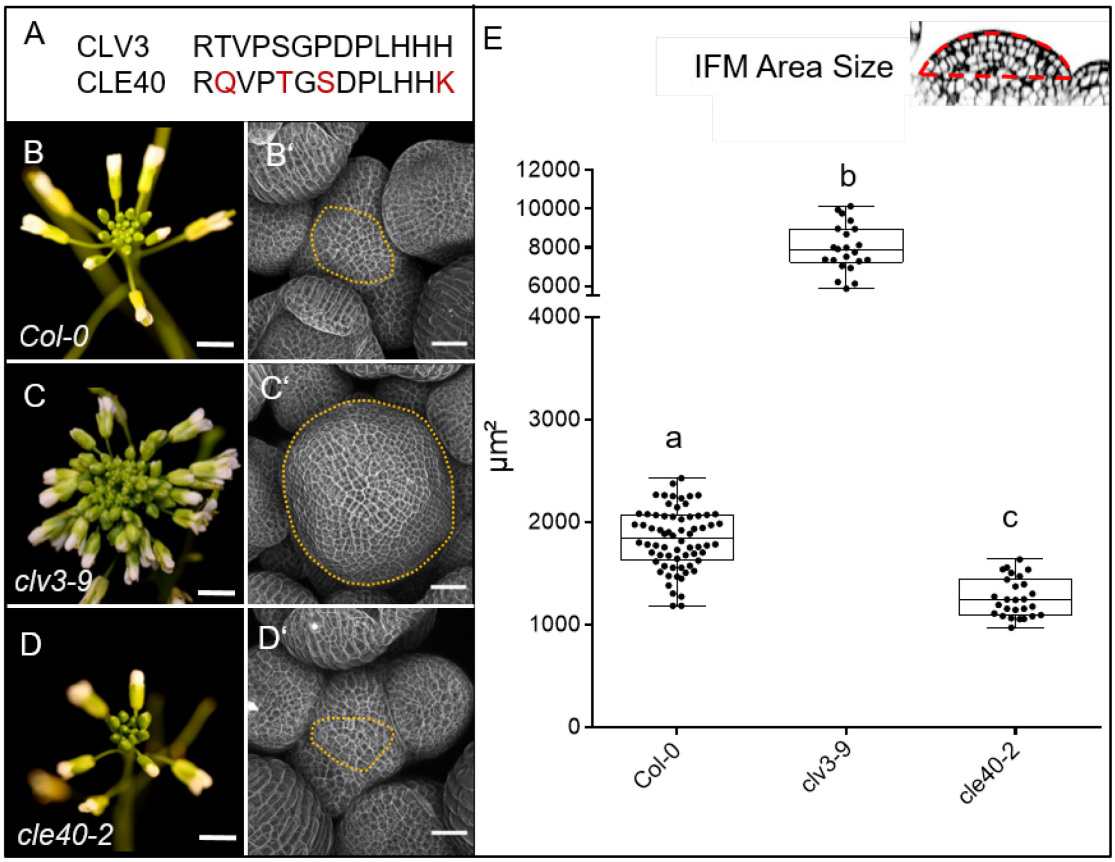

Fig. 7: CLV3 and CLE40 exert opposite effects on meristem size

(A) The aa sequences of the mature CLV3p and CLE40p differ in four aa (differences marked in red). **(B)** A 6 WAG *Col-0* inflorescence with flowers. **(B´)** IFM at 6 WAG, maximum intensity projection (MIP) of a z-stack taken by confocal microscopy. **(C)** *clv3-9* inflorescence at 6 WAG **(C´)** The MIP of a *clv3-9* IFM shows a fasciated, dome-shaped meristem with an increased meristem size. **(D)** The inflorescence of *cle40-2* is decreased in its size and develops fewer flowers compared to *clv3-9* or *Col-0*. **(D´)** MIP of a *cle40-2* IFM. **(E)** The IFM area size of *clv3-9* (N=22) mutants is approximately 4.5 times larger than that of wild type plants (*Col-0* N=59), while *cle40-2* (N=27) mutants have 1.5 times smaller meristems than wild type and ~6.5 times smaller IFMs than *clv3-9* mutants.

Scale bars: 50 µm (B, C, D), 10 mm (B', C', D'), Statistical groups were assigned after calculating p-values by ANOVA and Turkey's multiple comparison test (differential grouping from $p \leq 0.01$). Same letters indicate no statistical differences. Yellow dotted lines in B´ to D´ enclose the IFM, red line in the inset meristem in E indicates the area that was used for the quantifications in E.

To explore allele-specific effects, we studied, besides *cle40-2* mutants, the *cle40* CRISPR mutants *cle40-cr1, cle40-cr2,* and *cle40-cr3* (Y. L. Yamaguchi et al., 2017) (Fig. 8, A). While the *cle40-2* mutant depicts a transposon insertion mutation leading to a stop codon at position

463bp (after transcription start), the CRISPR mutant *cle40-cr1* carries an 11bp insertion, and the *cle40-cr2* and *cle40-cr3* both have a deletion of 34bp and 28bp, respectively. All mutations are within the conserved CLE-box domain in Exon 3 of the *CLE40* gene (Fig. 8, B'). *cle40-cr2* and *cle40-cr3* mutants were shown to exhibit the same delayed columella differentiation phenotype in the root as it was reported for *cle40-2* (Stahl et al., 2009; Y. L. Yamaguchi et al., 2017). Like *cle40-2*, the *cle40-cr1/2/3* mutants do not show a plant growth phenotype, as they all have a similar height compared to *Col-0* (Fig. 8, A). However, all three *cle40* CRISPR mutations showed a smaller IFM at 6 WAG (Fig. 8, C).

We measured the area of secondary and primary IFMs by taking z-stacks with a confocal microscope and performed longitudinal sections from P4 to P5. Since primary IFMs from *clv3-9* mutants are highly fasciated we only measured secondary IFMs.

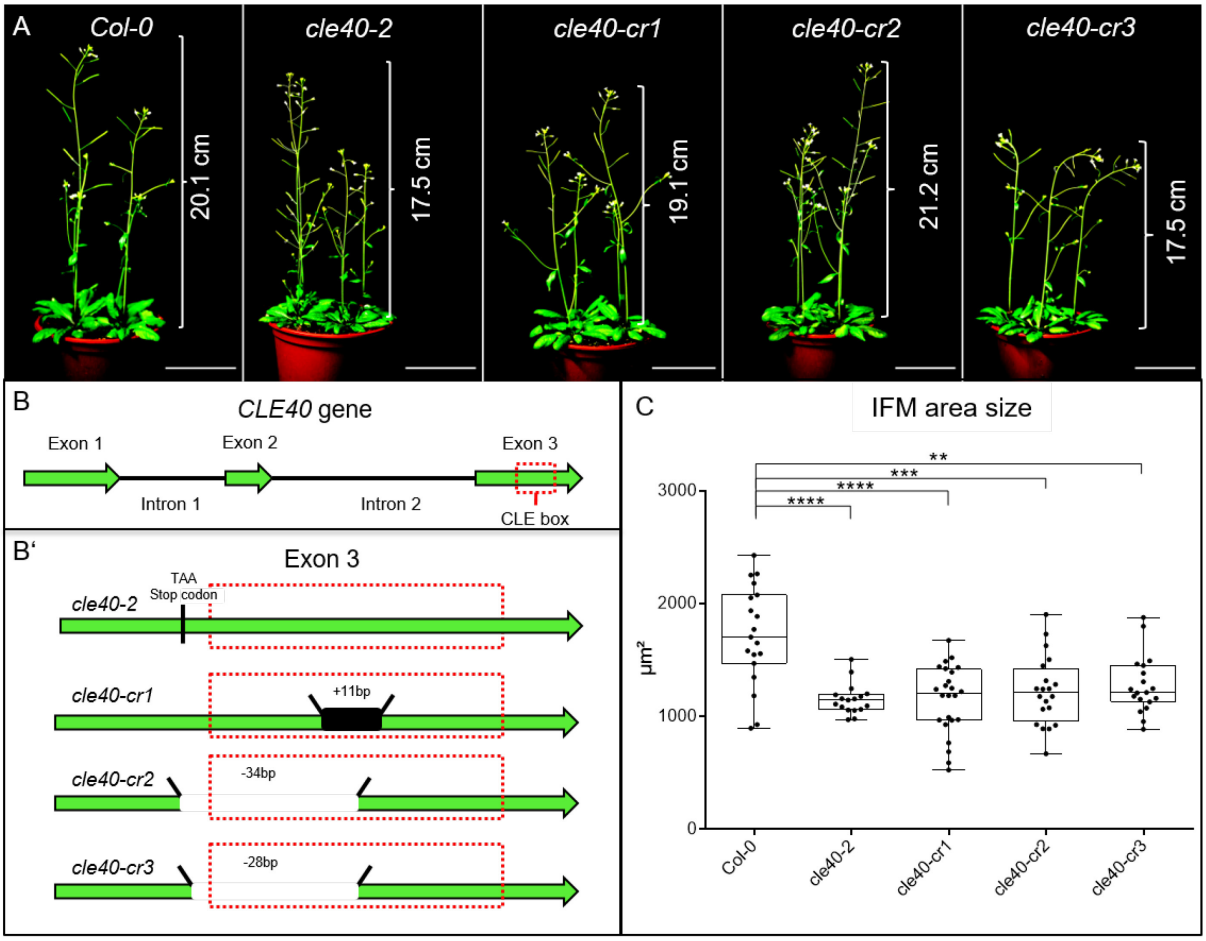

Fig. 8: *cle40* mutants have smaller IFMs

(A) Wild type *Arabidopsis thaliana* plants (*Col-0*) and *cle40* mutants (*cle40-2*, *cle40-cr1*, *cle40-cr2*, *cle40-cr3*) were grown for 6 weeks under long-day conditions. All plants show a similar height ranging from 17.5cm to 21.2cm. **(B)** Schematic representation of the *CLE40* gene, consisting of three exons and two introns. Exon 3 carries the crucial CLE box. **(B')**

Schematic representation of all four *CLE40* mutations. All four lines have mutations in the CLE box domain in Exon 3. *cle40-2* mutants were created by transposon mutagenesis resulting in a stop codon inside the CLE box (Stahl et al., 2009). *cle40-cr1*, *cle40-cr2,* and *cle40-cr3* mutants were created using the CRISPR-Cas9 method (Y. L. Yamaguchi et al., 2017). *cle40-cr1* has an 11bp insertion inside the CLE box domain while *cle40-cr2* and *cle40-cr3* have a deletion of -34bp and -28bp within the CLE box. **(C)** At 6 WAG, inflorescence meristems of wild type (*Col-0* N=16) and *cle40* mutant plants were dissected and the area of each meristem was imaged and measured. All four *cle40* mutants show significantly reduced meristem areas compared to *Col-0* plants (*cle40-2* N=17, *cle40-cr1* N=24, *cle40-cr2* N=20, *cle40-cr3* N=19). Asterisks were assigned after calculating p-values by ANOVA and Dunnett's multiple comparison test (differential grouping from $p \leq 0.05$)

4.1.2 The expression pattern of *CLE40* is complementary to that of *CLV3* in the IFM

The expression of *CLE40* was characterized in 5 WAG Arabidopsis plants carrying the transcriptional reporter line *CLE40:Venus-H2B* (Wink, 2013). *CLE40* expression was detected in the IFM as well as in the entire primordium of older flowers (P5 and P6), and in young sepals (Fig. 9, A). In the L1, *CLE40* is expressed in the PZ of the IFM but is excluded from the CZ (Fig. 9, B). In L2 and L3, high *CLE40* expression is found at the flanks of the meristem (Fig. 9, C, P1-P6). Expression of *CLE40* changed dynamically during development: expression was concentrated in the IFM but downregulated at sites of primordia initiation (Fig. 9, C). In older primordia from P5/6 onwards, *CLE40* expression is detectable from the center of the young FM and expands towards the FM periphery. In the FMs, CLE40 is lacking in young sepal primordia at P6 but starts to be expressed on the adaxial sides of petals at P7 (Fig. 9, P1-P6).

We next introduced a CLV3 transcriptional reporter into the CLE40 reporter background (*CLV3:NLS-3xmCherry//CLE40:Venus-H2B*) to analyze their spatial distribution in direct comparison. *CLV3* is specifically expressed in the CZ, i.e. the stem cells of the meristem (Fig. 9, D-F). In the L1, *CLV3* is exclusively found in the center of the meristem while *CLE40* is detected in the PZ (Fig. 9, E-E'''). The longitudinal section of the IFM reveals that *CLV3* expression in the L2 and L3 is distributed in a cone-shaped pattern in the center of the meristem surrounded by *CLE40* expression in the flanks (Fig. 9, F-F''). Thus, the expression patterns of *CLE40* and *CLV3* are precisely complementary to each other (Fig. 9, E, F).

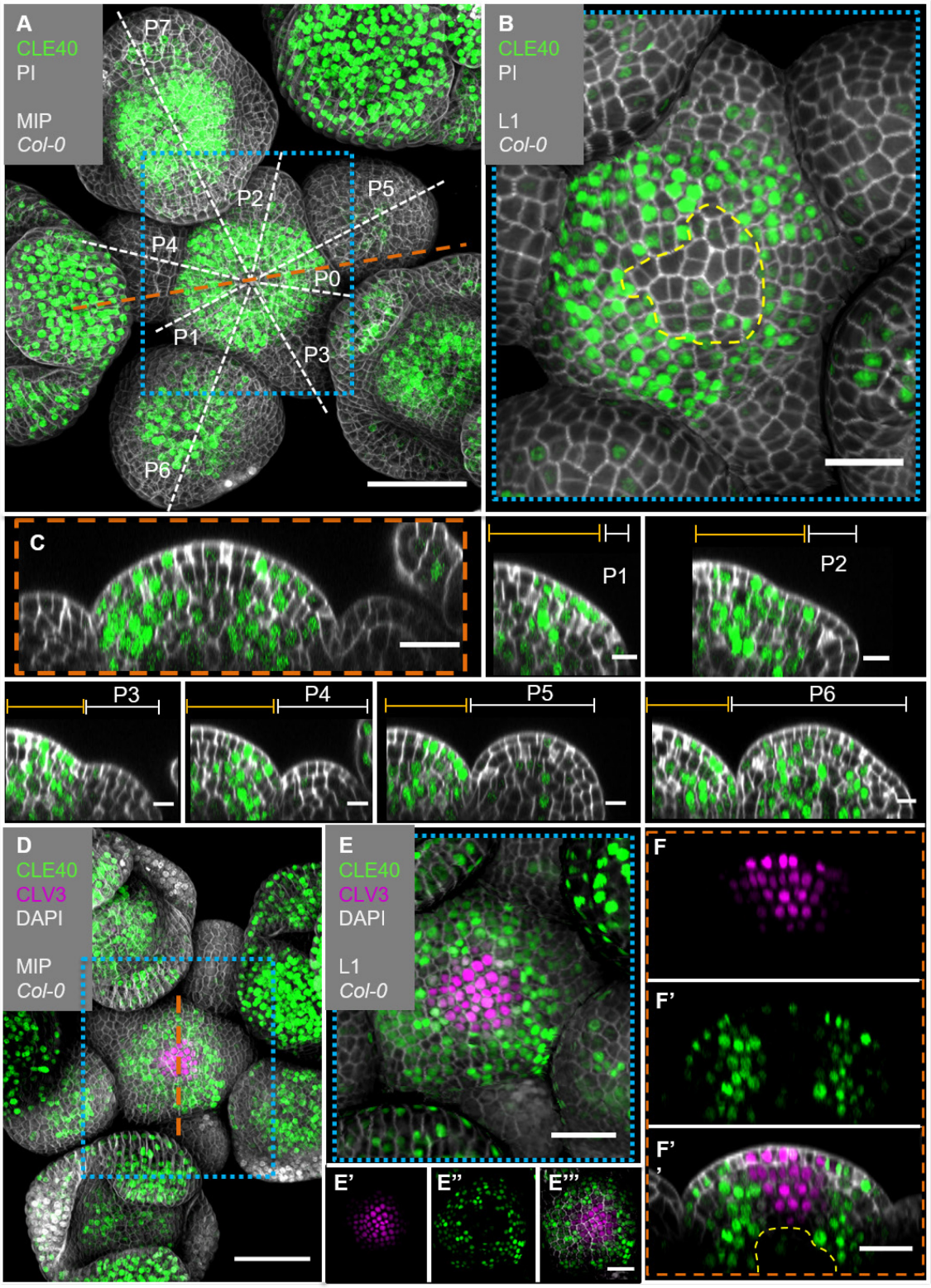

Fig. 9: *CLE40* and *CLV3* show complementary expression patterns in the IFM.

(A) MIP of an inflorescence at 5 WAG expressing the transcriptional reporter *CLE40:Venus-H2B//Col-0* showing *CLE40* expression in the IFM, older primordia, and sepals (N=25). **(B)** The L1 projection shows high expression in the epidermis of the periphery of the

IFM and only weak expression in the CZ. **(C)** Longitudinal section through the IFM shows the expression of *CLE40* in the periphery, but lack of expression in the CZ. **(P1 –P4)** In young primordia, no *CLE40* expression is detected, while cells close to emerging primordia in the IFM show high *CLE40* expression. **(P5, P6)** Older primordia show *CLE40* expression at first only in a few cells in the center of the floral meristem (P5), and in later stages *CLE40* expression expands through the entire primordium (P6). **(D)** The MIP of the double reporter line of *CLE40* and *CLV3* (*CLE40:Venus-H2B;CLV3:NLS-3xmCherry//Col-0*) shows *CLV3* expression in the CZ surrounded by *CLE40* expression in the periphery (N=12). **(E-E''')** The L1 projection shows that *CLV3* **(E')** and *CLE40* **(E'')** are expressed in a distinct complementary pattern in the epidermis of the IFM. *CLV3* is present in the center of the L1 layer while *CLE40* is expressed in the PZ of the IFM in the L1. **(F)** The longitudinal section through the center of the IFM shows *CLV3* expression in the CZ while *CLE40* **(F')** is mostly expressed in the surrounding cells. **(F'')** *CLE40* and *CLV3* are expressed in complementary patterns.

Dashed blue lines indicate magnified areas, dashed white and orange lines indicate planes of optical sections, dashed yellow line in B marks CZ and in F'' the OC. Scale bars: 50 µm (A, D), 20 µm (B, C, E, E''', F''), 10 µm (P0 to P6), MIP = Maximum intensity projection, PI = Propidium iodide, L1 = visualization of layer 1 only, P1 to P7 = primordia at consecutive stages

4.1.3 *CLE40* is repressed by WUS activity

To further analyze the regulation of *CLE40* expression, we introduced the CLE40 transcriptional reporter into the *clv3-9* mutant background. In *clv3-9* mutants, WUS is no longer repressed by the CLV signaling pathway, and the CZ of the meristem increases in size as described previously (Clark et al., 1995). The *WUS* expression domain is extended (SupplFig. 1) and not restricted to the OC, since it can now also be found in the L2 layer of the meristem (Brand et al. 2000). In wild type plants, *CLE40* is not expressed in the CZ and the OC of the meristem, but in the periphery surrounding the CZ (Fig. 10, A, A'). In *clv3-9* mutants with an increased stem cell domain, *CLV3* and *WUS* expression are detected within the tip and the center of the meristem, where no *CLE40* expression is found (Fig. 10, B, B'; SupplFig. 1). Whereas, at the flanks of the meristem and in sepals, where WUS is absent, *CLE40* expression can be detected (Fig. 10, B, B'; SupplFig. 1). These results suggest a repressing effect of WUS on *CLE40* activity.

In vegetative meristems (10 DAG) (Fig. 10, C), expression of *CLE40* can be detected in the periphery of the meristem and in leaf primordia, while no expression is found in the CZ and in young leaf primordia (Fig. 10, E, LP1-3). Comparable to the expression in an IFM, *CLE40* expression is neither present in the stem cell zone of a vegetative meristem, but elevated expression can be found in the flanks of the meristem (Fig. 10, E'). To explore if *WUS* expression is negatively correlated with *CLE40* expression, we expressed *WUS* in an

expanded domain. We, therefore, brought *WUS* expression under the control of the *CLV3* promoter (*CLV3:WUS//Col-0*), which results in the formation of enlarged meristem with an expanded central domain expressing both, *CLV3* and *WUS* (Fig. 10, D, D'). Consistent with our previous results, we did not detect any *CLE40* expression in the meristem area. *CLE40* expression was only visible in the cotyledons of the seedling (Fig. 10, F, F'). These data indicate that *CLE40* expression is negatively regulated by WUS.

In an additional experiment, we crossed the *CLE40* reporter line into *wus-7* mutants (*CLE40:Venus-H2B//wus-7*). Since *wus-7* is a weak allele, plants are still able to form a functional meristem for some time but are not able to develop siliques (Graf et al., 2010; Ma et al., 2019). In all *wus-7* meristems (N=12) *CLE40* expression could be detected within the entire IFM and in the center of FMs (Fig. 10, H; SupplFig. 2). In contrast to wild type IFMs (Fig. 10, G, G'), *CLE40* is also expressed in the CZ and OC in *wus-7* mutant meristems (Fig. 10, H, H'). These findings show that WUS is repressing *CLE40* expression, either in an indirect or direct manner.

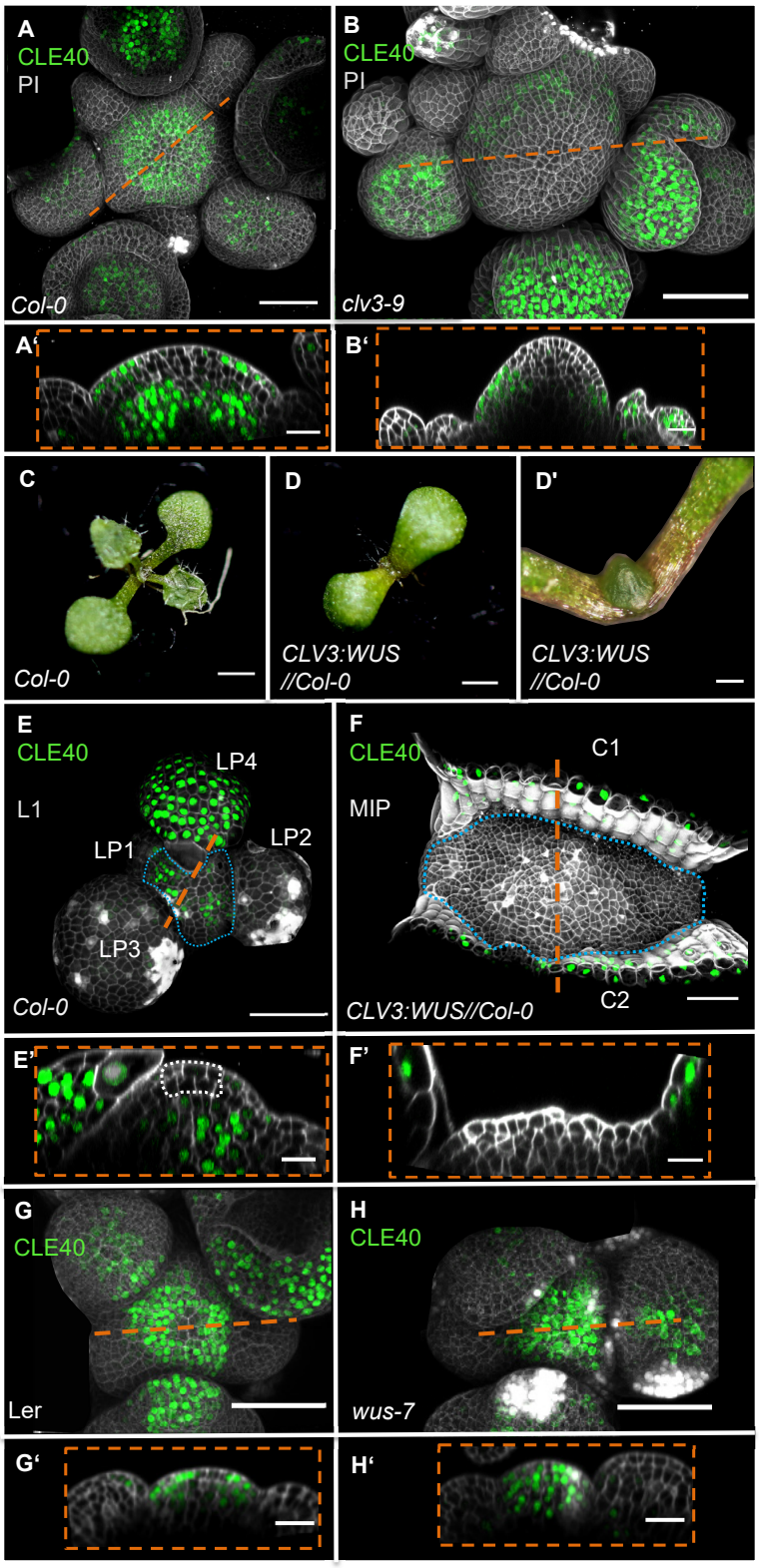

Fig. 10: WUS-dependent repression of *CLE40* expression in the shoot meristem

(A) *CLE40* promoter expression is shown via a z-stack of a transcriptional reporter line (*CLE40:Venus-H2B//Col-0*). The MIP shows *CLE40* expression in the periphery of the IFM and

in flower primordia (N=25). **(A')** The XZ-view shows no *CLE40* expression in the stem cell domain and in the center of the meristem. Cells in the L2 layer also show less *CLE40* expression. High *CLE40* expression is found in the L1 and L3 in the flanks. **(B)** *CLE40* promoter expression in a *clv3-9* mutant background is shown via a MIP of a z-stack of a transcriptional reporter line (*CLE40:Venus-H2B//clv3-9*) and shows expression only in the periphery of the meristem, in older flower meristems and sepals (N=6). **(B')** A longitudinal section through the meristem depicts no *CLE40* expression at the tip and the center of the meristem. *CLE40* expression can only be detected in cells at the flanks of the IFM and in sepals. **(C)** 10 days old wild-typic Arabidopsis seedling carrying the *CLE40:Venus-H2B* reporter line. **(D)** 10 days old Arabidopsis seedling expressing *WUS* under the control of the CLV3 promoter carrying the *CLE40:Venus-H2B* reporter is shown. **(D')** The 10 DAG old Arabidopsis seedling expressing *CLV3* under the WUS promoter (*CLV3:WUS//Col-0*) has a fasciated, dome-shaped meristem that does not develop flowers. **(E)** The L1 projection and the XZ view **(E')** of a vegetative meristem expressing *CLE40:Venus-H2B* shows expression in the PZ and young leaves (LP4) but no expression in the CZ and young leaf primordia (LP1-LP3**)** (N=5). **(F)** The MIP of a fasciated meristem expressing *WUS* and *CLV3* in the entire meristem (*CLE40:Venus-H2B*//pCLV3:WUS), does not show any *CLE40* signal. *CLE40* expression can only be found in the cotyledons (C1 and C2) next to the meristem (N=5). **(F')** The longitudinal section reveals also no *CLE40* expression in the layer L1, L2, and L3 of the meristem. *CLE40* expression is only detected in the epidermis of the cotyledons. **(G and G')** The MIP **(G)** and the longitudinal section **(G')** of *CLE40* expression (*CLE40:Venus-H2B*//*Ler*) in a wild type (*Ler*) background shows no signal in the CZ and the OC. *CLE40* expression can be detected in the PZ, as well as in the center of older flower primordia and sepals (N=8). **(H and H')** The MIP of *CLE40* expression (*CLE40:Venus-H2B*//*wus-7*) in a *wus-7* mutant background shows expression through the entire IFM and in the center of flower primordia. The longitudinal section (H') reveals that *CLE40* is also expressed in the CZ as well as in the OC of the IFM (N=12).

Dashed orange lines indicate longitudinal sections, dashed blue lines indicate the meristem, dashed white line shows the stem cell domain. Scale bars: 50 µm (A, B), 20 µm (A', B', E, E', F, F'), 1 mm (C, D), 500 µm (D'), MIP = Maximum intensity projection, PI = Propidium iodide, L1 = layer 1 projection, C = Cotyledon, LP = Leaf Primordium

4.1.4 CLE40 promotes *WUS* expression

In wild type plants, the *WUS* promoter is active in the center of the meristem (Fig. 11, A-H). From the OC, WUS protein moves through plasmodesmata to the tip of the meristem to activate *CLV3* expression. In *cle40-2* mutants, *WUS* is also expressed in the OC but showed a reduction in the number of *WUS* expressing cells down to approx. 50% wild type levels (Fig. 11, I-P; SupplFig. 3). Importantly, *WUS* remained expressed in the center of the meristem but was there found in a narrow domain (Fig. 11, I-P). While in wild type plants approximately 19 cells show WUS promoter activity, only approximately 10 cells express WUS in *cle40-2*

mutants, demonstrating a promoting effect of CLE40 on *WUS* expression (Fig. 11; SupplFig. 3).

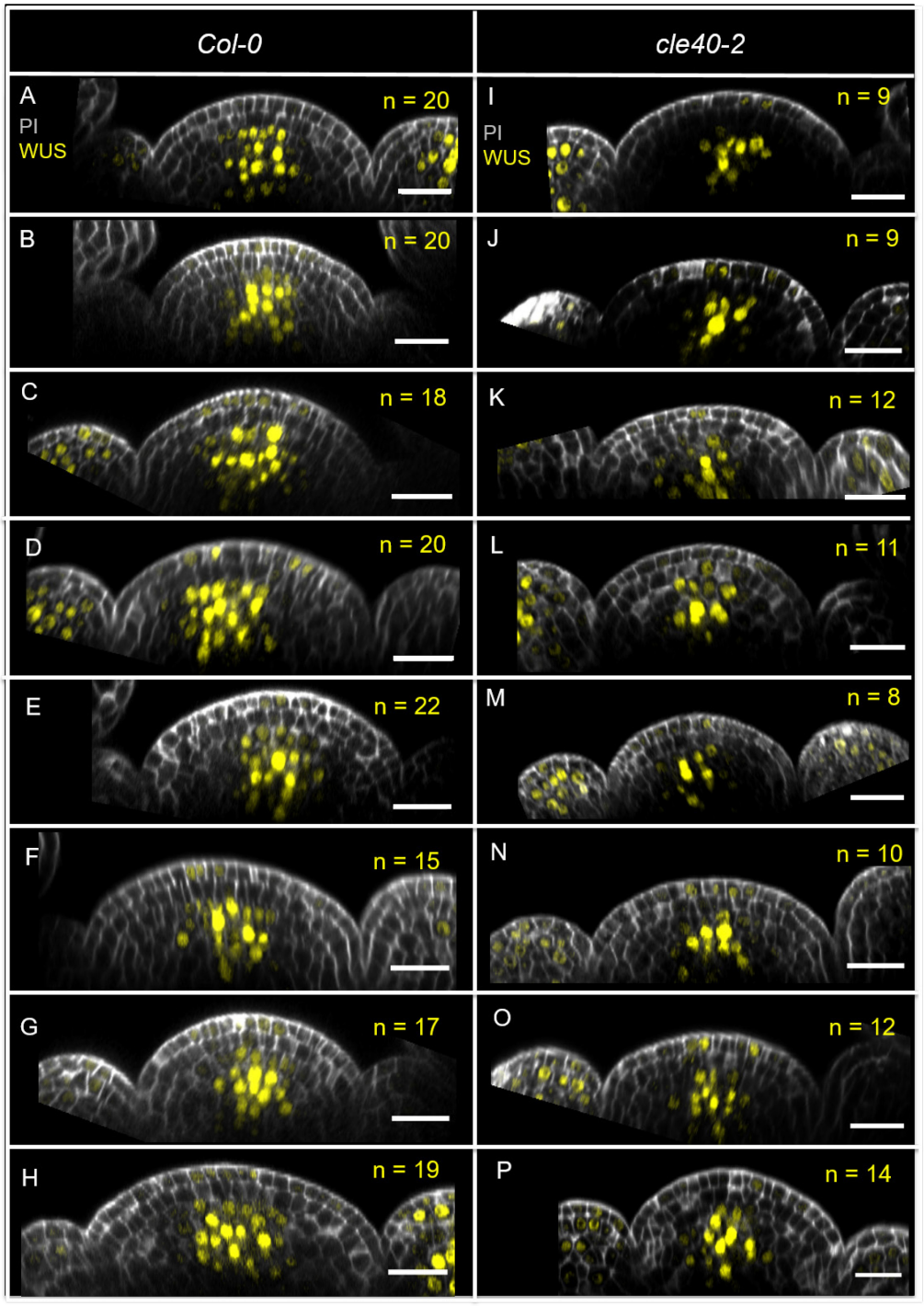

Fig. 11: CLE40 promotes *WUS* expression in the IFM

Longitudinal sections of wild type (N=8) **(A-H)** and *cle40-2* mutant (N=8) **(I-P)** plants expressing the reporter *WUS:NLS-GFP.* Longitudinal sections were performed through the middle of the meristem from P4 to P5 and *WUS* expressing cells were counted. On average, wild type plants

express *WUS* in about 19 cells in the center of the meristem, whereas *cle40-2* mutants show an average WUS activity in approximately 10 cells in the meristem center. The reduced *WUS* expression in *cle40-2* mutants demonstrates a promoting effect of *CLE40* on WUS activity. Scale bars: 50 µm (A-P), PI = Propidium iodide

4.1.5 Receptor kinases in the IFM are candidates for CLE40 peptide perception

The signaling pathway of CLV3 is well-studied. The peptide CLV3 is perceived by the LRR receptor CLV1 or by the CLV2/CRN complex; both activating a downstream signaling cascade to repress the transcription factor *WUS* (Brand et al., 2000; Daum et al., 2014; Yadav et al., 2011). In terms of CLE40, little is known about the binding with receptors. It was proposed that CLE40 might act through the RLK receptor ACR4 in the root of Arabidopsis (Stahl et al., 2009). However, it was recently shown that the direct interaction of this peptide-receptor pair is highly unlikely, as indicated by *in vitro* binding assays and analysis of the crystal structure of ACR4 (Satohiro Okuda et al., 2020). Nevertheless, ACR4 still might indirectly contribute to CLE40 perception in the root or the shoot *of A. thaliana* (Berckmans et al., 2020).

Since CLV3 signals through the receptor CLV1 and in its absence through the LRR receptor BAM1, detailed expression pattern analysis of the LRR receptors CLV1 and BAM1, as well as the RLK receptor ACR4 were performed. Overlapping areas of expression could indicate a possible peptide-receptor interaction.

The longitudinal section of a meristem expressing the *CLE40* reporter line reveals *CLE40* expression in the PZ of the meristem with elevated expression in the flanks, while no expression is detected in the CZ and the OC (Fig. 12, A). A similar expression pattern is found for *BAM1*. BAM1 is an LRR receptor and is localized to the PM. *BAM1* expression is found in most cells of the IFM with elevated expression in the flanks but no expression in the OC of the meristem (Fig. 12, B). In contrast to *BAM1* and *CLE40*, *CLV1* is not expressed at the flanks of the meristem, but highly in the center of the L3 in the IFM and FMs (Fig. 12, C). Besides the L3, *CLV1* expression is detected in cells of the L1 and L2 in incipient organ primordia (Fig. 12, C).

The RLK ACR4 is exclusively present in the L1 of the meristem at the PM (Fig. 12, D). ACR4 is expressed throughout the entire L1 of the shoot meristem and its primordia.

In summary, the longitudinal sections through the IFMs reveal that *BAM1* and *CLE40* overlap in the PZ of the meristem, that *CLV1* and *BAM1* show a complementary pattern, and that the

ACR4 receptor is exclusively located in the L1. Thus, expression patterns of all four proteins only overlap in a few cells in the L1 in incipient organ primordia (Fig. 12).

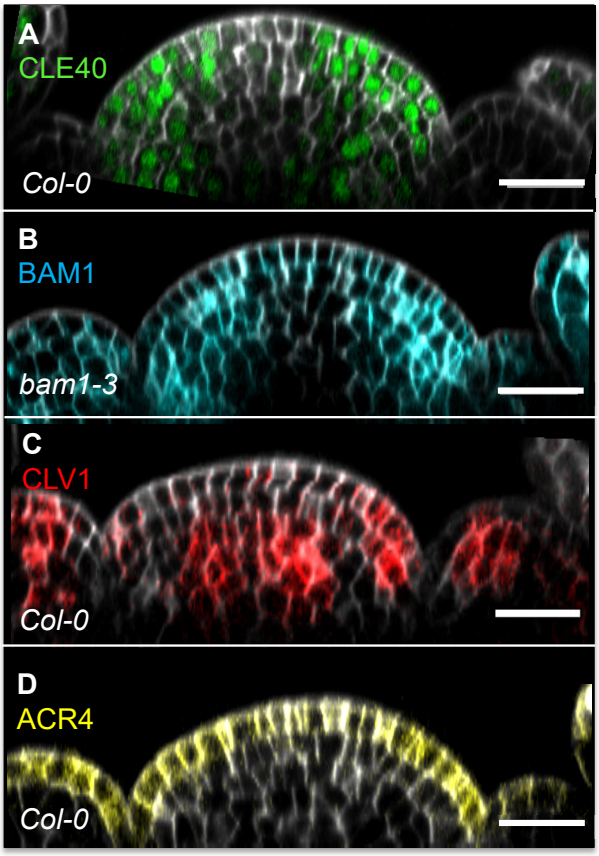

Fig. 12: Expression pattern of the peptide CLE40 and its putative receptors, BAM1, CLV1, and ACR4 in the IFM

(A) The longitudinal section of an IFM expressing *CLE40:Venus-H2B* is shown. A lack of *CLE40* expression is detected in the CZ and OC. *CLE40* is expressed in the PZ and at the flanks of the meristem (N=25). **(B)** Longitudinal section of an IFM expressing *BAM1* under its endogenous promoter (*BAM1:BAM1-GFP//bam1-3*) shows *BAM1* expression in the PZ, the CZ, and in young primordia. No expression of *BAM1* is detected in the OC (N=15). **(C)** Native expression of *CLV1* (*CLV1:CLV1-GFP//Col-0*) in an IFM longitudinal section can be depicted in the center of the meristem, as well as in cells of the L1 and L2 layer close to emerging primordia. *CLV1* expression can also be found in the center of young primordia (N=15). **(D)** The longitudinal section through an IFM carrying the translational ACR4 construct (*ACR4:ACR4-GFP//Col-0*) reveals expression of ACR4 exclusively in the L1 of the meristem (N=12). Scale bars: 20µm (A-D)

4.2 The role of BAM1 in the IFM

The LRR receptor BAM1 was already described in 2006 by DeYoung et al. as the closest homologue of CLV1 (DeYoung et al., 2006). However, its function in the inflorescence, the shoot, and root meristem remains mostly unclear. To date, neither a specific function nor a specific peptide interaction in the IFM could be demonstrated for BAM1. While Shinohara et al. reported that BAM1 is able to bind the CLV3p, recent *in vitro* binding studies showed no binding affinity between BAM1 and CLV3 (Crook et al., 2020; Shinohara & Matsubayashi, 2015).

However, DeYoung et al. suggested a promoting function of *BAM1* on meristem size, as it is located in the PZ of the meristem, where it is proposed to sequester CLE peptides and insulate exogenous signals from the center of the meristematic zone (DeYoung et al., 2006; DeYoung & Clark, 2008). Previous studies also showed that *CLV1* represses *BAM1* transcription in response to CLV3 signaling and that in a negative feedback loop *BAM* expression is self-repressing to buffer stem cell proliferation. *BAM1* is also able to partly substitute for *CLV1* in its absence (Nimchuk, 2017; Nimchuk et al., 2015).

Here, we propose that CLE40 signals via BAM1 in the PZ of the meristem to promote meristem size in an antagonistic pathway to CLV3 and its receptor CLV1. Evidence from the root already showed that CLE40 is able to act via BAM1 (unpublished data Rene Wink).

4.2.1 *bam1* mutants have smaller meristems than wild type plants

In section 4.1.1 it was shown that *CLE40* mutants have 1.5-fold smaller meristems compared to wild type plants at 6 WAG. Similar results were obtained for *bam1* mutants. At 6 WAG a wild type IFM depicts an area of ~1800 µm², whereas the average size of a *bam1-3* IFM only showed an average size of 1186 µm² (Fig. 13). To exclude allele-specific effects, the meristem area of a second BAM1 allele, *bam1-4*, was analyzed. The knockout mutant *bam1-4* showed smaller meristems with an average meristem size of 1283 µm² (Fig. 13). Thus, both, *bam1* and *cle40* mutants display a 1.5-fold reduction in meristem size compared to wild type plants, demonstrating a promoting effect on meristem size.

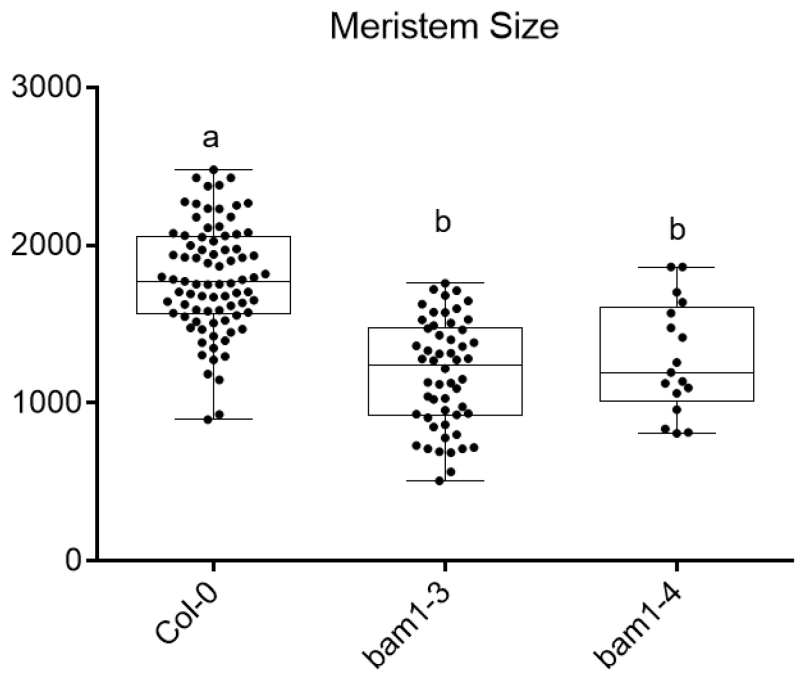

Fig. 13: The meristem area of *bam1* mutants is smaller compared to *Col-0* plants

At 6 WAG the meristem size of *Col-0* (N=82), *bam1-3* (N=54), and *bam1-4* (N=17) mutants were measured by taking a z-stack of each meristem. *bam1-3* and *bam1-4* show significantly smaller meristems compared to *Col-0* plants. *bam1-3* and *bam1-4* have no significant change in meristem size compared to each other.

Statistical groups were assigned after calculating p-values by ANOVA and Turkey's multiple comparison test (differential grouping from $p \leq 0.01$).

4.2.2 *BAM1* is expressed in the periphery of the IFM

The expression of endogenous *BAM1* (*BAM1*:*BAM1*-GFP//*bam1-3*) was detected in the entire inflorescence, showing expression in the meristem, the flower primordia, and the sepals (Fig. 14, A). In the L1, *BAM1* expression was detected in all organs (Fig. 14, B). However, longitudinal sections through the IFM and developing flower primordia reveal *BAM1* expression in all cells besides cells in the OC (Fig. 14, C). Expression of *BAM1* is detected in all layers of primordia (P1- P6). Higher expression of *BAM1* can be found at the flanks of the meristem and especially at the borders to new emerging primordia (Fig. 14, P4). In older primordia, *BAM1* expression is elevated in the entire organ (Fig. 14, P6).

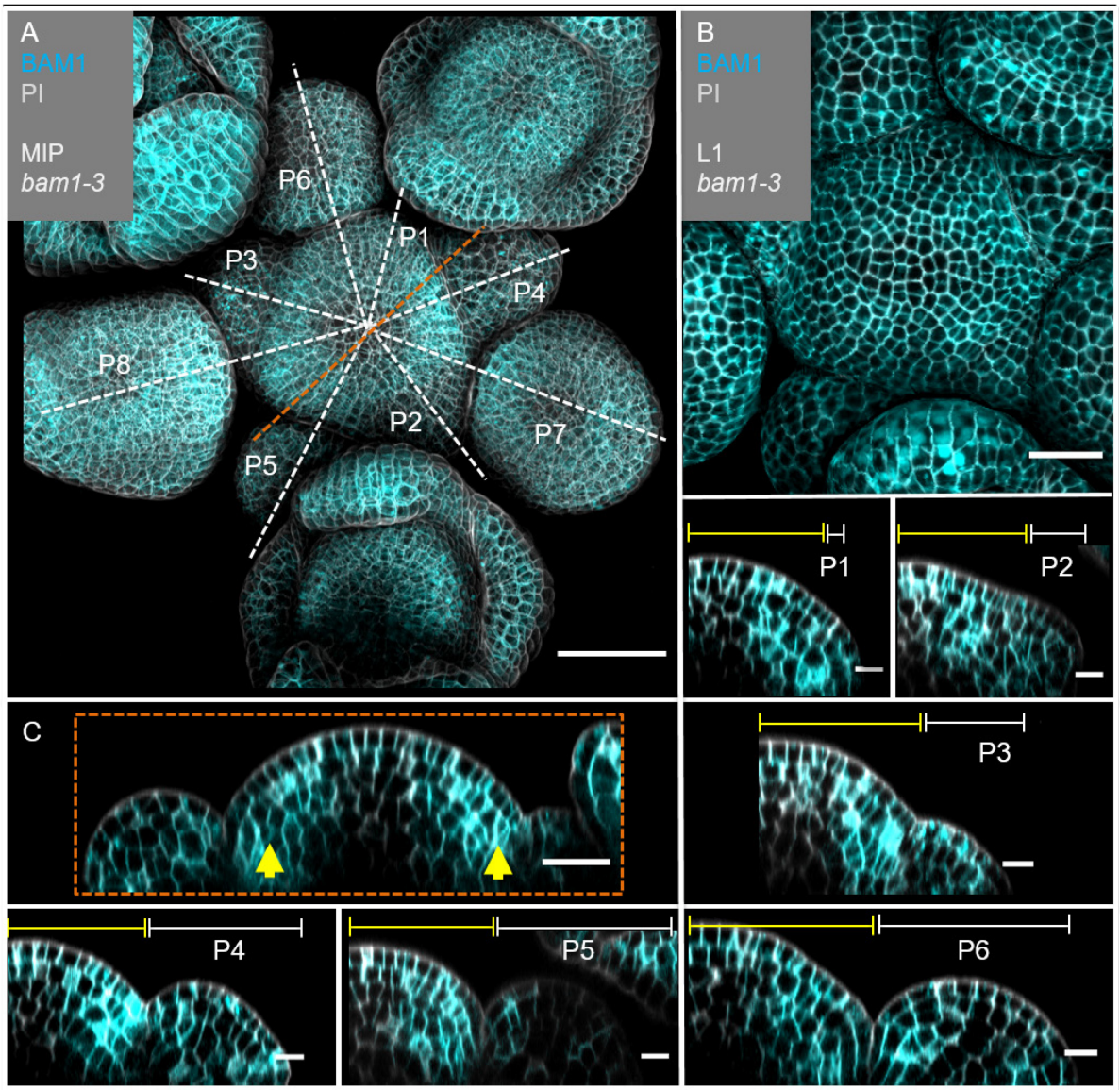

Fig. 14: *BAM1* expression is elevated in the flanks of the IFM and not detectable in the OC

(A) The MIP shows inflorescence at 5 WAG expressing *BAM1* under its endogenous promoter (*BAM1*:*BAM1*-GFP//*bam1-3*). *BAM1* expression is detected in most parts of the inflorescence. Less expression can be found in the CZ of IFM and FMs (N=15). **(B)** In the L1 projection of the meristem, *BAM1* is ubiquitously expressed with less expression in the CZ. **(C)** The longitudinal section through the meristem shows elevated *BAM1* expression in the flanks (yellow arrow), but no expression in the OC. **(P1 - P6)** In all primordia from stage P1 to P6 *BAM1* expression is detected in all cells.

Dashed white and orange lines indicate longitudinal sections; yellow lines (P1 to P6) indicate the IFM region, white lines (P1 to P6) mark the primordium, yellow arrows indicate high *BAM1* expression in the PZ. Scale bars: 50 µm (A), 20 µm (B, C), 10 µm (P1 to P6), MIP = maximum intensity projection, PI = propidium iodide, L1 = layer 1, P = primordium

4.2.3 Expression pattern of *CLE40* and *BAM1* overlap in the periphery of the IFM

In section 4.1.5, longitudinal sections through IFMs showed an overlapping expression pattern of *BAM1* and *CLE40*. Comparing the expression of both proteins in the meristem and emerging primordia in detail, demonstrated that both genes show a broad expression in the IFM with elevated expression at the flanks and cells close to emerging primordia, whereas neither of the genes are expressed in the OC (Fig. 15). In young primordia, no *CLE40* expression can be detected from P1 to P3 (Fig. 15, A). In primordia P4, a few cells in the center express *CLE40,* and nearly all cells in older primordia P5 and P6 express *CLE40*. *BAM1* is ubiquitously expressed in all primordia and thus *CLE40* and *BAM1* expression overlap in older primordia (Fig. 15). The highly overlapping expression patterns of *CLE40* and *BAM1* indicate a high possibility for them to act as a peptide-receptor pair.

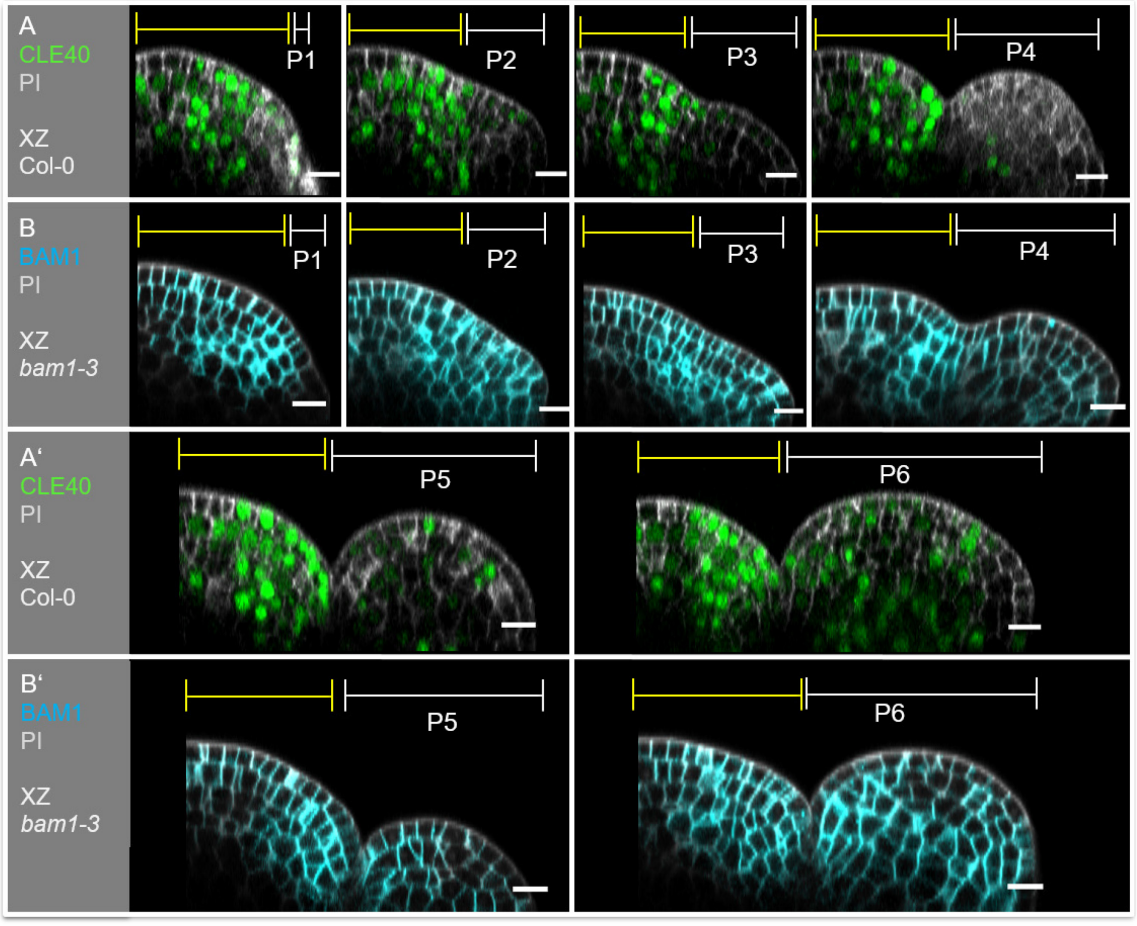

Fig. 15: The expression pattern of *CLE40* and *BAM1* overlap in the IFM

Longitudinal optical sections through an IFM and its developing primordia P1 to P6 are shown expressing either **(A)** *CLE40* (*CLE40:Venus-H2B*) (N=25) or **(B)** *BAM1* (*BAM1*:*BAM1*-GFP)

(N=15). No *CLE40* expression is detected in young primordia P1 to P3. From P4 on a few cells in the center of the primordia express *CLE40*. Its expression expands in P5 and can be found in nearly all cells of P6. *BAM1* is expressed ubiquitously in all primordia from P2 to P6. In the meristem, *CLE40* and *BAM1* show elevated expression at the flanks and in cells close to emerging primordia. Neither *BAM1* nor *CLE40* expression can be depicted in the center of the meristem. Scale bar: 10 µm, white lines indicate meristem and grey lines primordia, P = Primordia

4.2.4 Expression pattern of *BAM1* alters in mutant backgrounds

The expression of the translational *BAM1:BAM1-GFP* reporter line is able to rescue the *bam1-3;clv1-101* double mutant phenotype regarding the number of carpels and the highly fasciated meristem phenotype (Fig. 14, D-F and unpublished data Grégoire Denay). Thus, the expression of *BAM1:BAM1-GFP* in a *bam1-3* mutant background shows a wild-typic background.

In a wild type background, *BAM1* is expressed in the entire inflorescence (meristem and primordia) besides in cells of the OC. Elevated expression of *BAM1* is detected in the flanks of the meristem (Fig. 14, C; Fig. 16, A). In contrast to that, the expression pattern of *BAM1* alters in a *clv1-20* mutant background. *BAM1* transcription was reported to be upregulated in the meristem center in the absence of CLV3 or CLV1 signaling (Nimchuk, 2017). Indeed, we could also detect a shift of *BAM1* expression towards the center of the meristem in *clv1-20* mutants (Fig. 16, B). *BAM1* expression in *clv1-20* mutants shows a similar expression pattern as the *CLV1* expression in a wild type background. The longitudinal section through the IFM depicts *BAM1* expression now in the L1 and in the center of the IFM and FM (Fig. 16, B). Importantly, in a *clv1-20* background BAM1 is absent in the peripheral region of the IFM and the L2 (Fig. 16, B).

In a *clv3-9* mutant, the IFM drastically expands along the apical-basal axis, since *WUS* is no longer repressed by the CLV pathway, which leads to an over-proliferation of stem cells (Brand et al., 2002; Clark et al., 1995). *BAM1* expression in a *clv3-9* mutant is still detected at the flanks of the meristem but its expression is shifted to the inner layers. Comparable to the wild type expression of *BAM1*, it is not detected in the CZ of the meristem in *clv3-9* mutants (Fig. 16, C). In contrast to the expression in *bam1-3* mutants, expression of *BAM1* is not detected in the L1 and L2 of the IFM and thus not at the tip of the meristem (Fig. 16, C). *CLE40* shows a similar expression pattern in *clv3-9* mutants (Fig. 10, B'), since no *CLE40* expression was found in the CZ and OC in *clv3-9* mutants. *CLE40* expression was also only detectable at the

flanks of the meristem. These results support the hypothesis of *BAM1* being the main receptor for *CLE40*.

In line with that, the spatial distribution of the *BAM1* receptor in *cle40-2* mutants appears to be broader compared to wild type plants, since *BAM1* expression is also found in the center of the meristem (Fig. 16, D). The enlarged expression domain of *BAM1* in *cle40-2* mutants suggests that *BAM1* expression expands to the center of the meristem to perceive signals from CLV3p since no CLE40p is available in the periphery of the meristem. Nevertheless, more experiments need to be performed to confirm these results. In *acr4-8* mutants, no difference in the expression pattern compared to wild type plants can be seen (Fig. 16, A, E). No *BAM1* expression is detected in the OC, while elevated expression can be found in the flanks of the IFM (Fig. 16, E).

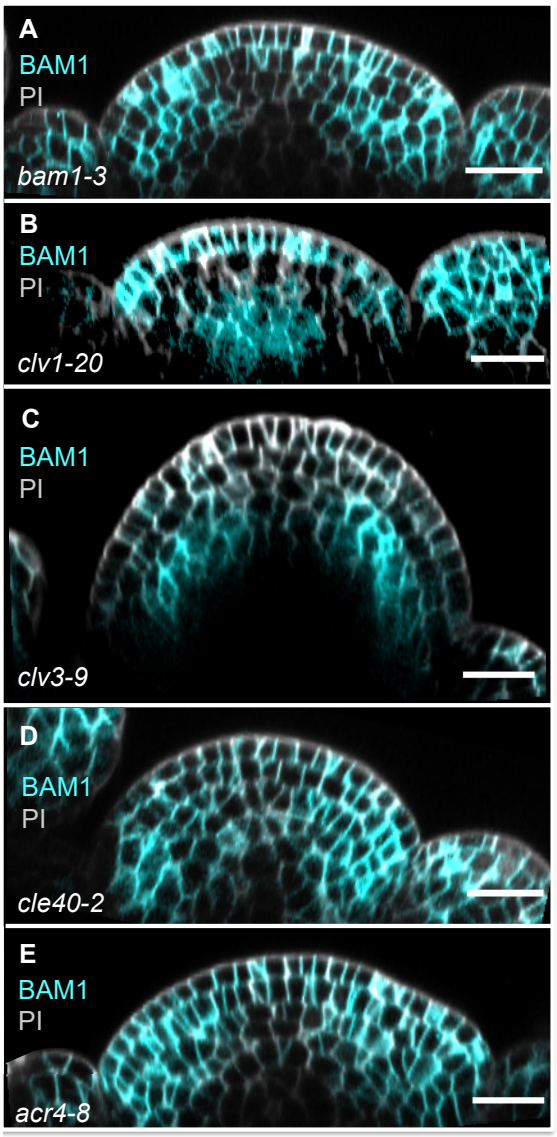

Fig. 16: The expression pattern of *BAM1* in various mutant backgrounds

Longitudinal optical sections through IFMs carrying the translational *BAM1:BAM1-GFP* construct in different mutant backgrounds are shown. **(A)** The translational reporter line *BAM1:BAM1-GFP* is expressed in the PZ, the CZ, and in all cells of developing primordia. Only in the OC of the meristem *BAM1* expression is not detected (N=15). **(B)** In *clv1-20* mutants, *BAM1* expression is shifted to the center of the meristem and can be found in the entire L1, but not in the L2 and the periphery of the meristem (N=9). **(C)** *clv3-9* mutants show expression of *BAM1* at the inner flanks of the meristem in the L2 and L3, while no *BAM1* expression is detected in the L1 or the tip of the meristem (N=5). **(D)** The spatial distribution of BAM1 in *cle40-2* (N=9) mutants seems to be extended compared to wild type meristems. *BAM1* is ubiquitously expressed in the meristem of *cle40-2* mutants, besides a few cells in the center. **(E)** In *acr4-8* mutants, no change in the expression pattern of *BAM1* compared to *Col-0* plants is detected. *BAM1* is expressed in the PZ, the CZ and is not detected in the center of the meristem (N=5). Scale bars: 20µm (A-E)

4.2.5 Ectopic expression of *BAM1* in the OC can rescue its meristem phenotype

As mentioned in section 4.2.4, expression of *BAM1* in a *clv1-20* mutant is shifted to the center of the meristem and can rescue the highly fasciated meristem phenotype of *clv1;bam1* double mutants (Fig. 16, B). Mutants of *bam1* had smaller meristems compared to *Col-0* plants (section 4.2.1). Thus, the question arises as to whether the expression of *BAM1* in the center of the meristem can rescue the small meristem phenotype of *bam1* mutants. Hence, we expressed the *BAM1* gene under the control of the WUS promoter, introduced the construct into *bam1-3* mutants (*WUS:BAM1-GFP//bam1-3*), and measured the meristem size of plants at 6 WAG. To confirm that the *BAM1* receptor was only expressed in the center of the meristem, GFP was tagged to the C-terminal of the *BAM1* gene. The GFP signal shows *BAM1* localization at the PM only in *WUS* expressing cells in the center of the IFM and FMs (Fig. 17, A, A'). Analysis of the meristems could demonstrate that expression of *BAM1* in the OC can rescue the small meristem phenotype of *bam1-3* mutants (Fig. 16, B). Thus, these results suggest, that the broad expression of *BAM1* in the OC is sufficient to signal via CLE40 or CLV3 to promote meristem size.

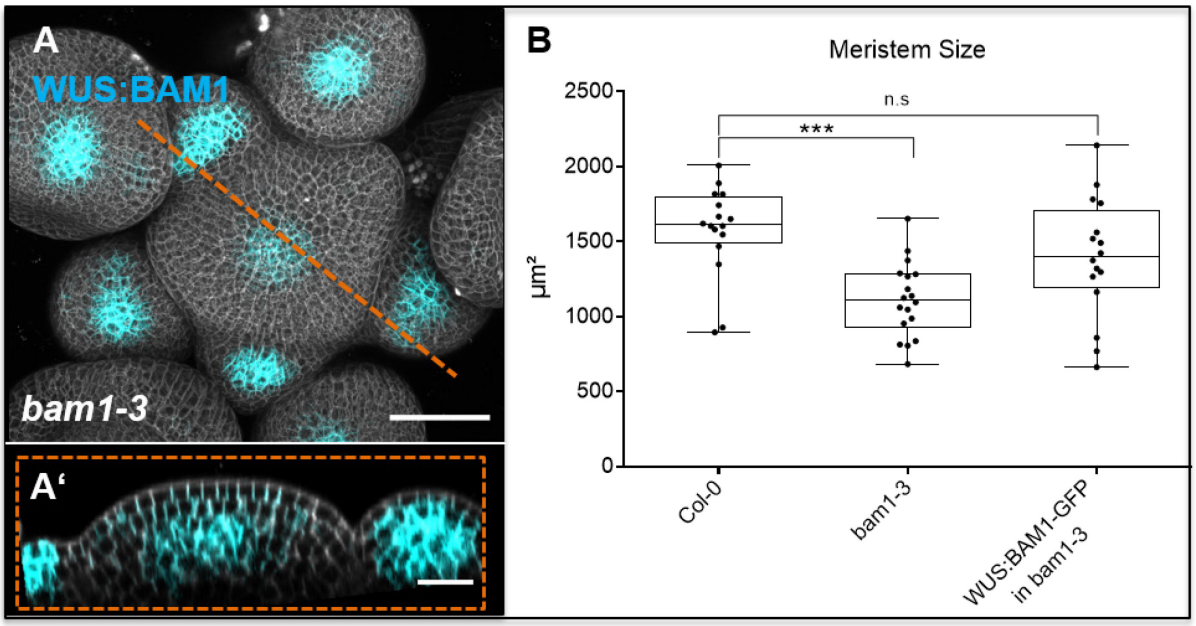

Fig. 17: *BAM1* expression in the center of the IFM meristem can rescue the *bam1-3* meristem phenotype

(A) MIP of an IFM expressing the *BAM1* gene under the control of the WUS promoter in a *bam1-3* mutant background (*WUS:BAM1-GFP//bam1-3*) shows expression in the center of the IFM and FMs. **(A')** The longitudinal section through the center of the meristem shows that

BAM1 localization at the PM of OC cells. **(B)** At 6 WAG, IFMs of *Col-0* (N=16), *bam1-3* (N=18), and *bam1-3* plants carrying the *WUS:BAM1-GFP* (N=16) construct were imaged and the meristem area was measured and plotted. *bam1-3* mutants show significantly decreased meristems compared to *Col-0*, while *bam1-3* plants carrying the *WUS:BAM1-GFP* construct showed no significant change in their meristem area size compared to wild type plants.

Scale bars: 50 µm (A), 20 µm (B), Asterisks were assigned after calculating p-values by ANOVA and Dunnett's multiple comparison test (differential grouping from $p \leq 0.01$)

4.2.6 BAM1 promotes *WUS* expression

As shown in section 4.1.4 *WUS* is expressed in the center of the meristem in wild type plants (Fig. 11 and Fig. 18). In *bam1-3* mutants, *WUS* is also expressed in the center of the meristem, but in fewer cells than in *Col-0* plants, and less expression is found in the periphery of the L3 layer (Fig. 18, G-L). While in wild type plants approximately 19 cells show WUS promoter activity, only approximately 12 cells express *WUS* in *bam1-3* mutants, demonstrating, like *cle40-2* mutants, a promoting effect of BAM1 on *WUS* expression (SupplFig. 3). IFMs of *WUS*-expressing cells in wild type plants are the same as presented in section 4.1.4 (Fig. 11).

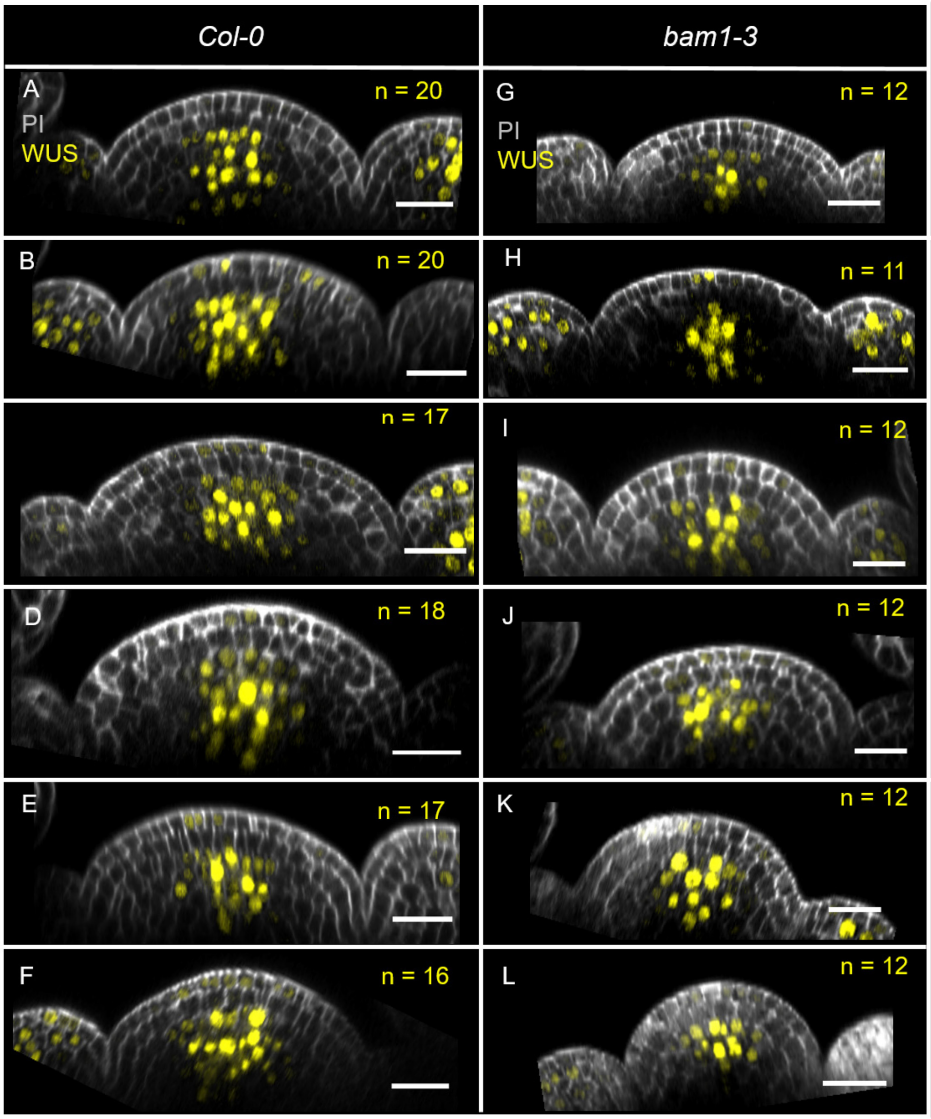

Fig. 18: BAM1 promotes *WUS* expression in the IFM

(A-F) Longitudinal sections of wild type (N=8) and **(G-L)** *bam1-3* mutant (N=6) plants expressing the reporter *WUS:NLS-GFP*. Longitudinal sections were performed through the middle of the meristem from P4 to P5 and WUS expressing cells were counted. On average wild type plants express *WUS* in about 19 cells in the center of the meristem, whereas *bam1-3* mutants show an average of *WUS* activity in approximately 12 cells in the meristem center. Scale bars: 20 µm (A-L), PI = Propidium iodide

4.3 The role of CLV1 in the IFM

The role of CLV1 in the shoot meristem is well studied. It was shown that the LRR receptor CLV1 can bind CLV3p and that this interaction leads to a downstream signaling cascade restricting the TF WUS (Brand et al., 2000; Ogawa et al., 2008; Schoof et al., 2000). Thus, CLV1 is an important player in regulating stem cell maintenance in the shoot and hence *clv1* mutants have defects in meristem size and organ formation. Mutants of *clv1* alleles have an enlarged meristem, as well as an increased number of carpels and floral organs (Clark et al., 1993; Kayes & Clark, 1998). Until now, the expression of *CLV1* was described to be only found in the center of the meristem (Nimchuk et al., 2015).

4.3.1 *clv1* mutants have enlarged meristems compared to wild type plants

Previous publications already showed that defects in the *CLV1* gene lead to increased meristems. To confirm these data, IFMs at 6 WAG of two different *CLV1* alleles were measured. The *clv1-20* mutant was before characterized as a knock-down mutation (Durbak & Tax, 2011), whereas *clv1-101* is a knock-out mutation (Kinoshita et al., 2010). However, both *clv1* mutations have larger meristems with an average area of 2713 µm² and 2457 µm² respectively (Fig. 19). Compared to the *Col-0* meristem size of about 1800 µm² both *clv1* mutants have significantly enlarged meristems (Fig. 19).

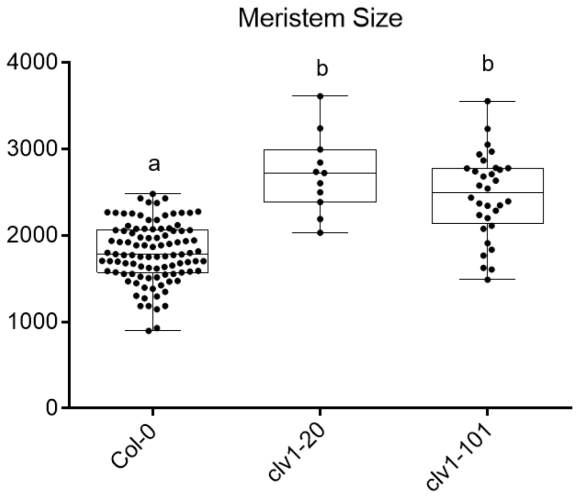

Fig. 19: The meristem area of *clv1* mutants is increased compared to *Col-0* plants

At 6 WAG the meristem sizes of *Col-0* (N=82), *clv1-20* (N=11), and c*lv1-101* (N=32) mutants were measured by taking a z-stack of each meristem. *clv1-20* and *clv1-101* show significantly

enlarged meristems compared to *Col-0* plants whereas *clv1-20* and *clv1-101* have no significant change in meristem size compared to each other.

Statistical groups were assigned after calculating p-values by ANOVA and Turkey's multiple comparison test (differential grouping from $p \leq 0.01$)

4.3.2 *CLV1* is dynamically expressed in the inflorescence

CLV1 is a LRR receptor, which has an extracellular domain, a kinase domain, and a transmembrane domain, and thus, is predominately localized at the PM of cells. Nevertheless, expression is also detected within the cytosol, as CLV1 is known to internalize upon CLV3 activation (Nimchuk et al., 2011). The expression pattern of *CLV1* (*CLV1*:*CLV1*-GFP//*Col-0*) in the inflorescence was detected in the center of the meristems (IFM and FMs), but also in organ boundary domains and in the L1 and L2 layers of incipient organ primordia at P-1 to P1 (Fig. 20, A). The L1 projection shows *CLV1* expression only in incipient organ primordia (Fig. 20, B), while the longitudinal section of the IFM reveals expression of *CLV1* in the center of the meristems (IFM and FM) and in incipient organ primordia (Fig. 20, C, P0). *CLV1* expression in the center of the FMs starts at P4, increases in its spatial distribution until P9, and then decreases again (Fig. 20, A, P4 – P11). In older primordia, P7 to P9, *CLV1* is also expressed in cells of developing sepals (Fig. 20, A). Higher *CLV1* expression in the L1 and L2 is detected in cells where new primordia will develop (Fig. 20, P1 and P5).

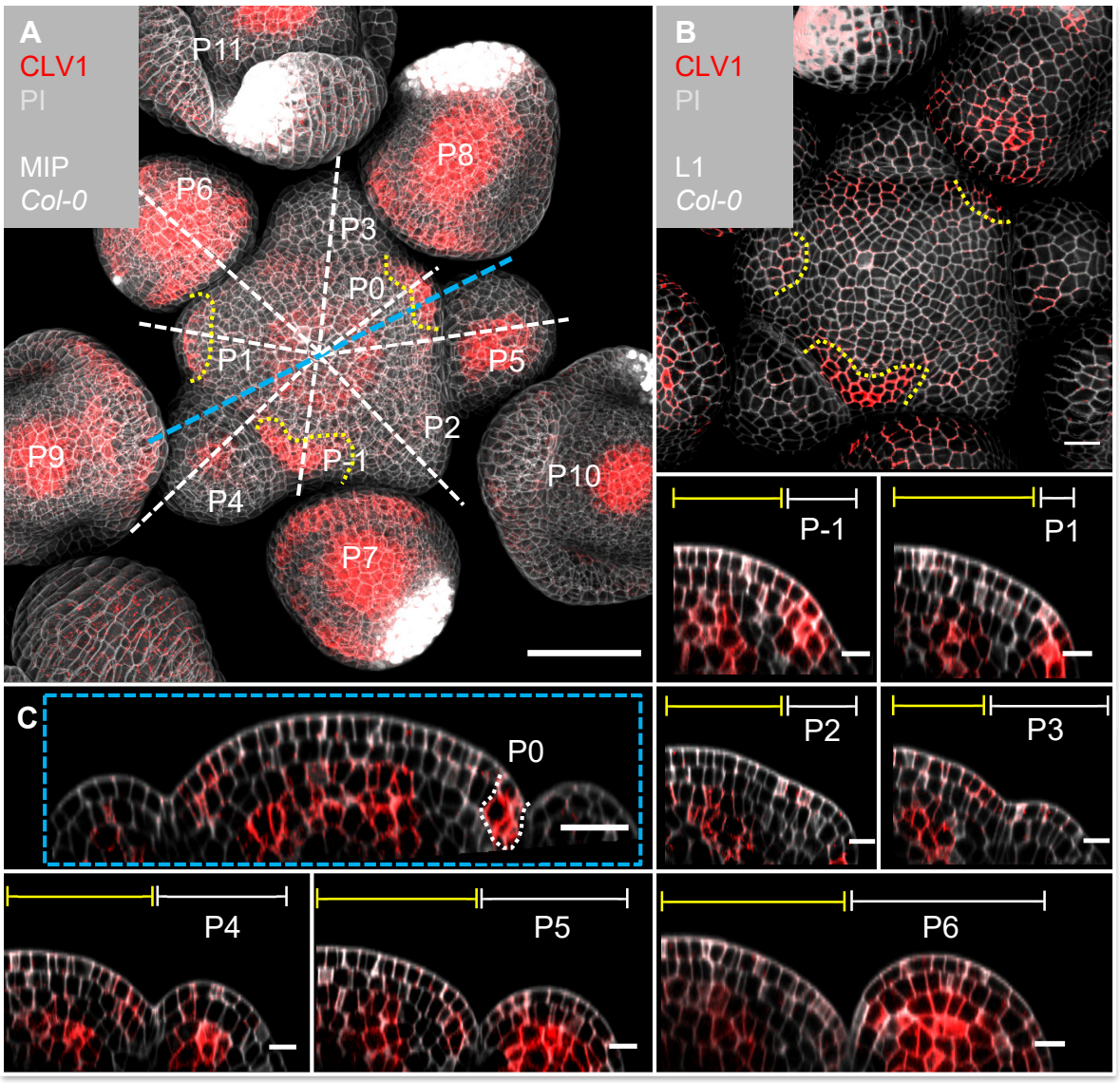

Fig. 20: *CLV1* is expressed in the L3 and in a dynamic pattern in the primordia

(A) MIP of *CLV1* under its endogenous promoter (p*CLV1:CLV1-GFP//Col-0*) at 5 WAG shows *CLV1* expression in the OC of the meristems, IFM, and FMs, in incipient organ primordia (P-1 to P1) and in sepals (N=15). **(B)** In the L1 projection *CLV1* expression is detected in cells of incipient organs. **(C)** Optical section through the IFM shows *CLV1* expression in the OC and in P0. **(P-1-P6)** *CLV1* expression is detected in incipient organ primordia in L1 and L2 (-P1, P0), in the L2 of P1, and in the OC of the IFM and FMs from P4 to P6.

Dashed white and blue lines indicate longitudinal sections. Scale bars: 50 µm (A), 20 µm (B, C), 10 µm (P1 to P6), MIP = Maximum intensity projection, PI = Propidium iodide, L1 = layer 1 projection, P = Primordium

4.3.3 *CLV1* expression alters in mutant backgrounds

In order to analyze how CLV1 function is influenced by the lack of other proteins involved in the CLV pathway, the translational reporter line *CLV1:CLV1-GFP* was imaged in different mutant backgrounds. As described in section 4.3.2, *CLV1* expression is detected in the center of the IFM and FMs, as well as in a few cells in the L1 and L2 in incipient organ primordia (Fig. 20; Fig. 21, A). The same expression pattern can be observed in single mutants of *bam1-3, cle40-2,* and *acr4-8*. In all three single mutant backgrounds *CLV1* is expressed in a few cells right next to the primordia (P4 right and P5 left) and in the center of the L3 (Fig. 21, B, D, E). No differences in the spatial distribution of *CLV1* expression patterns are detected in the different mutant backgrounds of *bam1-3, cle40-2,* and *acr4-8* compared to *Col-0* (Fig. 21, A, B, D, E). Nevertheless, the expression of *CLV1* in *bam1-3* mutants seems elevated compared to wild type plants, whereas it is decreased in *cle40-2* mutants (Fig. 21, B, D). Even though these results need to be quantified in a precise way, they suggest that CLE40 and CLV3 can bind to *BAM1* and *CLV1* in a promiscuous manner. *In bam1-3* mutants, the main receptor for CLE40 signaling is missing and thus *CLV1* substitutes, and its expression is increased. While in *cle40-2* mutants only the peptide CLV3 is available and is perceived by both LRR-receptors, *BAM1* and *CLV1*, resulting in a decreased expression level of *CLV1* in *cle40-2* mutants.

The only change in the spatial distribution of *CLV1* expression was detected in a *clv3-9* mutant background. *CLV1* expression is shifted to the tip of the meristem and is visible in in all three layers (Fig. 21, C). Since no CLV3p is produced, *CLV1* signaling is not activated and thus the *CLV1* receptor is not limited to the CZ of the meristem, but instead is “waiting” for the CLV3 signal at the periphery (Fig. 21, C).

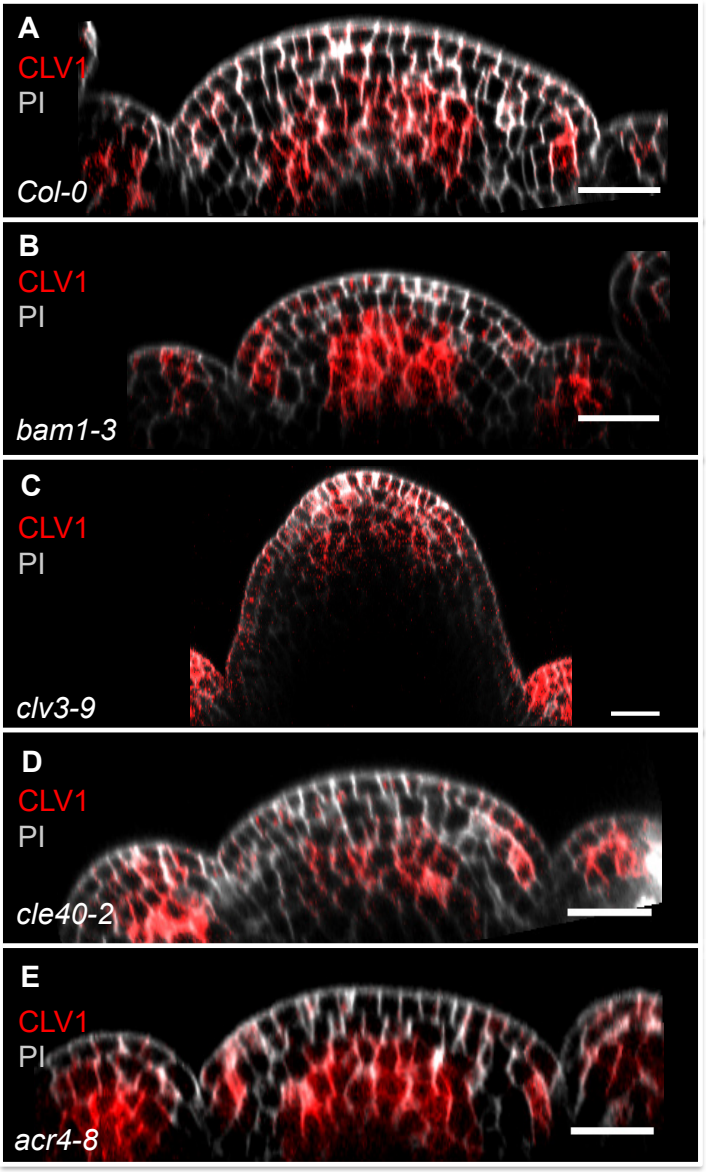

Fig. 21: The spatial distribution of *CLV1* expression in different mutant backgrounds does not change, except in *clv3-9* mutants

The translational reporter *CLV1:CLV1-GFP* was expressed in **(A)** wild type plants and in **(B)** *bam1-3* (N=7), **(C)** *clv3-9* (N=5), **(D)** *cle40-2* (N=9), and **(E)** *acr4-8* (N=9) mutant backgrounds. **(A, B, D, E)** In wild type and in *bam1-3, cle40-2,* and *acr4-8* mutants, *CLV1* expression is found in the center of the IFM and FMs, and in incipient organ primordia in the L1 and L2. **(C)** In *clv3-9* mutants, the expression pattern of *CLV1* is shifted from the center of the meristem to the tip.

Scale bars: 20 µm (A-E), PI = Propidium iodide

4.3.4 Ectopic expression of *CLV1* in the OC can rescue its meristem phenotype

CLV1 is highly expressed in the center of the meristem (section 4.3.2). Thus, the expression of *CLV1* under the control of the WUS promoter can rescue the meristem and carpel (data not shown) phenotype of *clv1-101* mutants (*WUS:CLV1-mVenus//clv1-101*). Plants expressing *CLV1* under the WUS promoter show a similar meristem size compared to *Col-0* plants and have a decreased meristem compared to *clv1-101* mutants (Fig. 22, B). Even though the *CLV1* receptor is not localized to the PM (Fig. 21, A, A'), the presence of the protein in the L3 is sufficient to rescue the enlarged phenotype of *clv1* mutants (Fig. 21, B). To confirm these results, more measurements have to be performed.

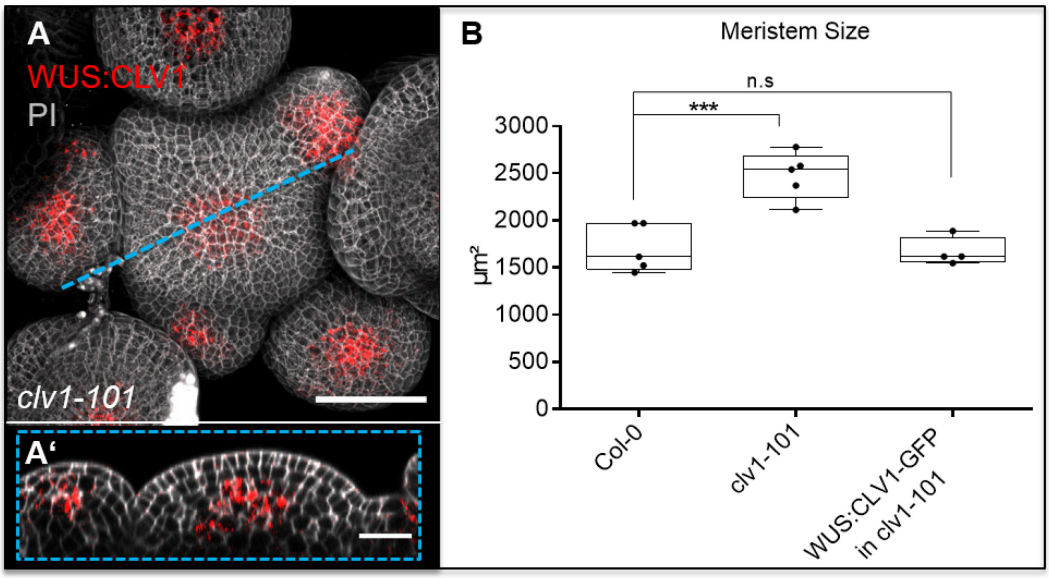

Fig. 22: *CLV1* expression in the center of the meristem can rescue the *clv1-101* meristem phenotype

(A) MIP of an inflorescence meristem expressing the *CLV1* gene under the control of the WUS promoter in a *clv1-101* mutant background (*WUS:CLV1-Venus//clv1-101*) shows expression in the center of the IFM and FMs. **(A')** The longitudinal section through the center of the meristem shows that *CLV1* is not PM localized. **(B)** At 6 WAG, z-stack of IFMs of *Col-0* (N=5), *clv1-101* (N=5), and *clv1-101* plants carrying the *WUS:CLV1-mVenus* construct (N=4) were imaged. *clv1-101* mutants show significantly increased meristems compared to *Col-0* and *clv1-101* plants expressing the *WUS:CLV1-mVenus* construct.

Scale bars: 50 µm (A), 20 µm (A') PI = Propidium iodide, Asterisks were assigned after calculating p-values by ANOVA and Dunnett's multiple comparison test (differential grouping from $p \leq 0.01$)

4.3.5 CLV1 restricts *WUS* expression

In wild type plants, WUS promoter activity is detected in the center of the meristem (Fig. 23, A-E) from where WUS protein moves through plasmodesmata to the tip of the meristem to activate *CLV3* expression. In *clv1-101* mutants, the main receptor for the CLV3p is missing and thus the downstream signaling of CLV1 cannot restrict WUS to the OC anymore. *WUS* is now expressed in an extended domain in the meristem center, but interestingly WUS promoter activity is also found in the L1 of *clv1-101* mutants. *WUS* expression leads to an over-proliferation of stem cells, resulting in an extended IFM along the apical-basal axis. Compared to wild type plants, 27 cells express WUS promoter activity in the meristem center (Fig. 23; SupplFig. 3). These results confirm the restricting effect of CLV1 on *WUS* expression in the IFM. IFMs of *WUS*-expressing cells in wild type plants are the same as presented in sections 4.1.4 and 4.2.6 (Fig. 11; Fig. 18).

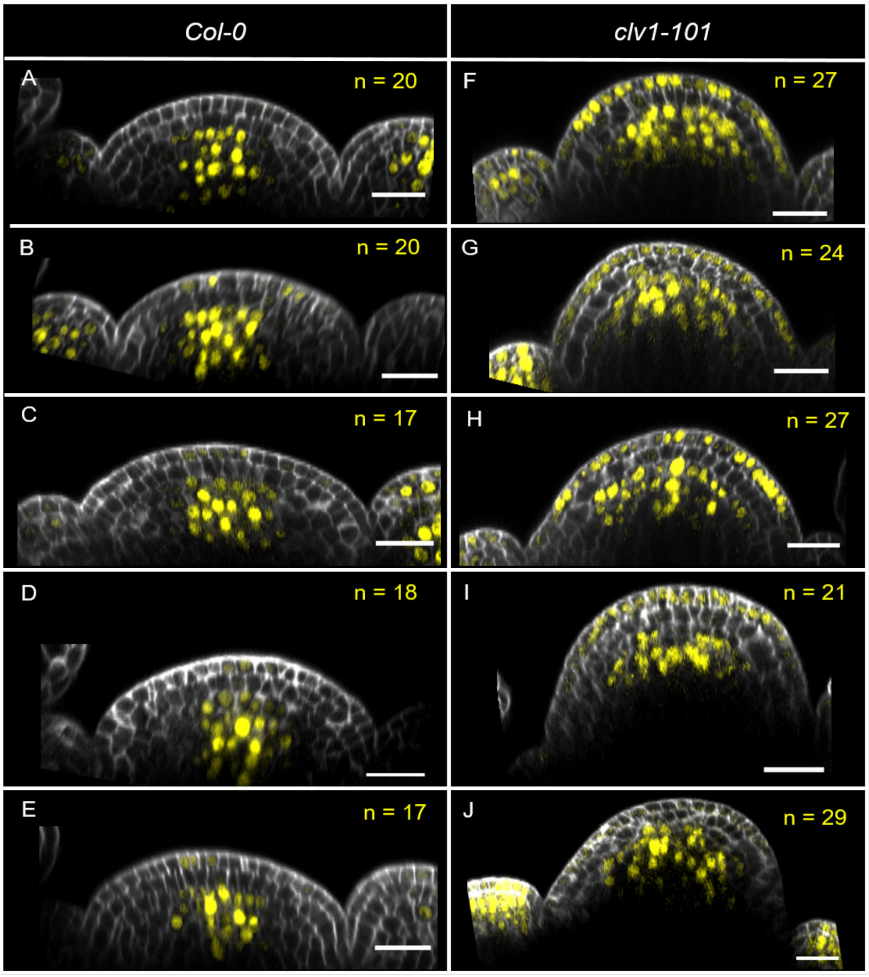

Fig. 23: CLV1 restricts *WUS* expression in the IFM

Longitudinal sections of **(A-E)** wild type (N=9) and **(F-J)** *clv1-101* (N=5) mutant plants expressing the reporter *WUS:NLS-GFP* are shown. Longitudinal sections were performed

through the middle of the meristem from P4 to P5 and *WUS* expressing cells in the meristem center were counted. On average wild type plants express WUS promoter activity in about 19 cells in the center of the meristem, whereas *clv1-101* mutants show an average WUS activity in approximately 27 cells in the meristem center. Notably, *WUS* expression is also found in the L1 in most of the *clv1-101* mutants. Scale bars: 20 µm (A-J), PI = Propidium iodide

4.4 The role of ACR4 in the IFM

ACR4 is a membrane-localized receptor kinase, which was shown to be exclusively expressed in the L1 of shoot meristems (SAM, IFM) and is mainly found on the lateral and basal surface of cells in the leave epidermis (Gifford et al., 2003; Roeder et al., 2012). In the root meristem, it was depicted that ACR4 might be triggered by CLE40 perception and is involved in stem cell fate (Berckmans et al., 2019; Stahl et al., 2009). Thus, ACR4 might also play a role in regulating stem cell maintenance in the IFM.

4.4.1 *acr4* mutants have smaller meristems compared to wild type plants

In order to analyze the role of ACR4 in the shoot, IFM measurements were performed on two different *acr4* mutant alleles at 6 WAG. Both mutant alleles showed a highly significant decrease in meristem size compared to wild type plants (Fig. 24). *acr4-8* mutants showed a stronger phenotype than the *acr4-2* mutants, although both mutations are supposed to be knock-out mutants (see section 3.1) (Gifford et al., 2003). Thus, loss of the ACR4 receptor promotes meristem growth, leading to the assumption that it either is involved in the CLV pathway or plays a role in maintaining the epidermis of the meristem.

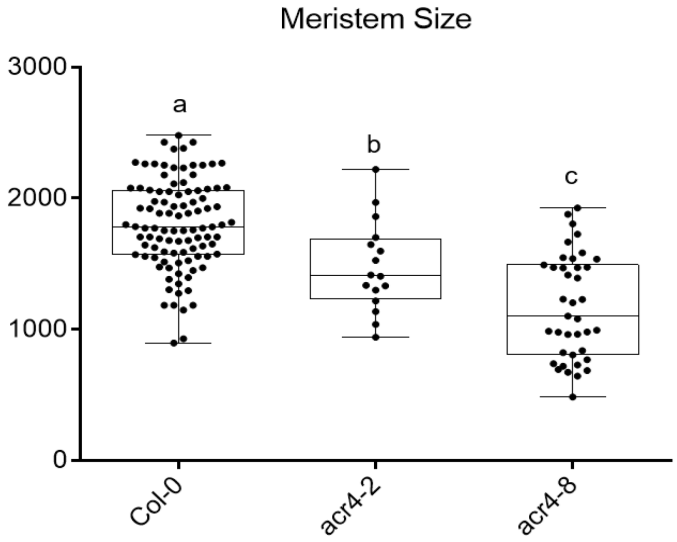

Fig. 24: The meristem area of *acr4* mutants is decreased compared to *Col-0* plants

At 6 WAG, the meristem size of *Col-0* (N=82), *acr4-2* (N=15) and *acr4-8* (N=39) mutants were measured by taking a z-stack of each meristem. *acr4-2* and *acr4-8* show significantly smaller

meristems compared to *Col-0* plants while *acr4-8* meristems are also significantly smaller compared to *acr4-2* mutants.

Statistical groups were assigned after calculating p-values by ANOVA and Turkey's multiple comparison test (differential grouping from $p \leq 0.01$).

4.4.2 *ACR4* is exclusively expressed in the L1 of the inflorescence

The MIP of an IFM at 5 WAG expressing *ACR4* under its endogenous promoter (*ACR4:ACR4-GFP//Col-0*) shows *ACR4* expression throughout the entire inflorescence (Fig. 25, A). In the epidermis, ACR4 is located at the PM of the meristem as well as in the cytosol, where it is being internalized (Fig. 25, B, C). Longitudinal optical sections of the meristem reveal *ACR4* expression exclusively in the L1 of the meristem (Fig. 25, C, P1 –P6). Expression of *ACR4* elevates at the flanks of the meristem, (Fig. 25, C) and at the border to new emerging primordia (Fig. 25, P3, P4), and is less expressed in the CZ. In older primordia, the *ACR4* expression level is consistently distributed through the epidermis (Fig. 25, P5, P6).

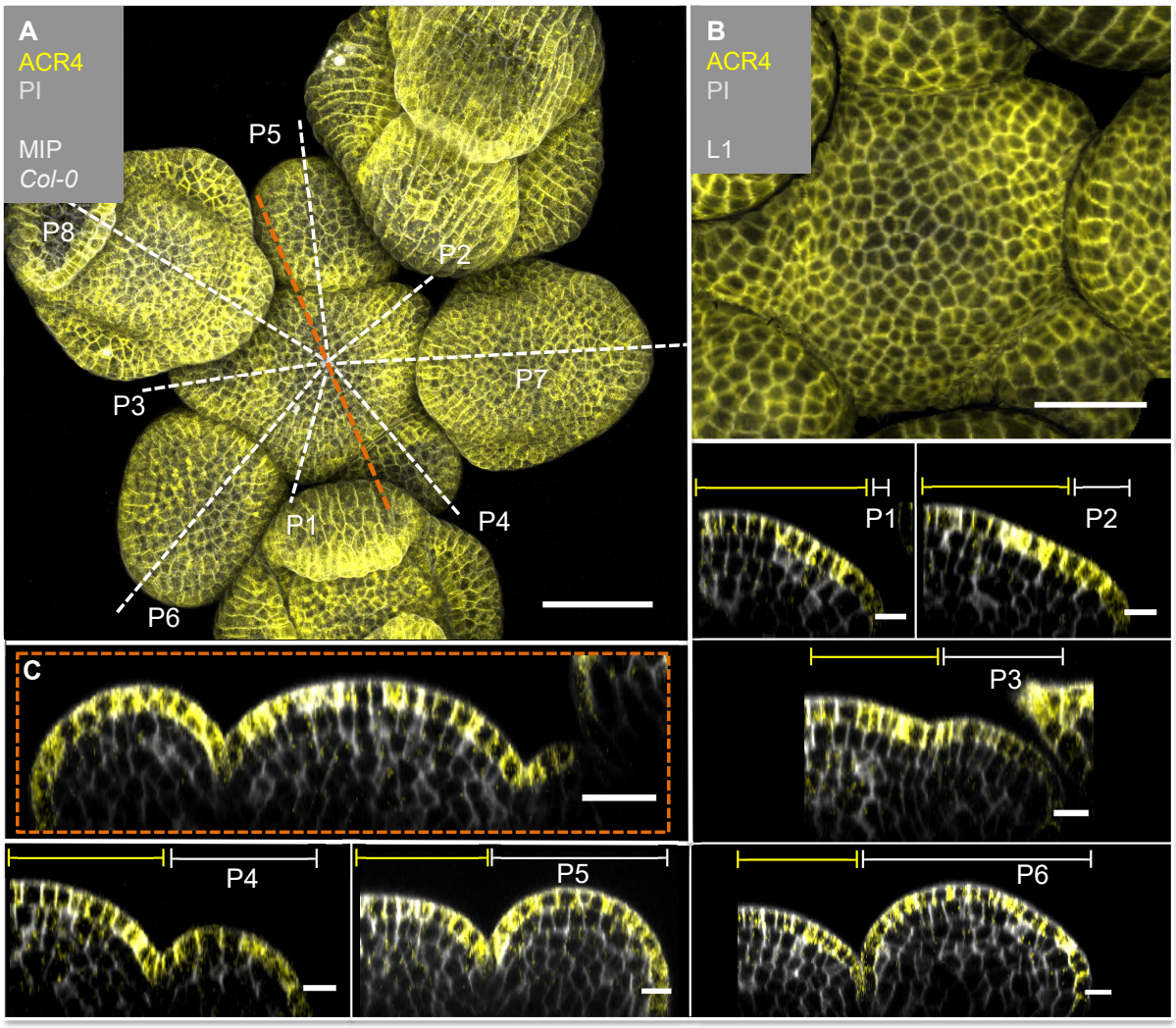

Fig. 25: *ACR4* is exclusively expressed in the L1 of the inflorescence.

(A) The MIP shows an inflorescence of an *A. thaliana* plant at 5 WAG expressing *ACR4* under its endogenous promoter (*ACR4:ACR4-GFP//Col-0*). *ACR4* expression is ubiquitously detected inflorescence (N=14). **(B)** In the L1 projection of the meristem, *ACR4* is all cells with elevated expression at the flanks of the meristem. **(C)** The longitudinal section through the meristem shows that ACR4 is exclusively expressed in the L1of the meristem. **(P1 – P4)** In all primordia, *ACR4* expression is exclusively found in the epidermis. In P1 to P4, elevated expression is detected at the flanks of the meristem while less *ACR4* expression is found in the center of the L1. **(P5-6)** ACR4 expression is equally distributed in the L1. Dashed white and orange lines indicate longitudinal sections.

Scale bars: 50 µm (A), 20 µm (B, C), 10 µm (P1 to P6), MIP = Maximum intensity projection, PI = Propidium iodide, L1 = layer 1 projection, P = Primordium

4.4.3 Expression of *ACR4* does not change in mutant backgrounds

In section 4.4.1, it could be demonstrated that the loss of ACR4 leads to a decrease in meristem size. Additionally, ACR4 was previously described to play a critical role in cell fate and positioning of cells in the distal root meristem (Berckmans et al., 2019; Stahl et al., 2009). Thus, the question remains if ACR4 is involved in the CLV pathway. Endogenous *ACR4* expression was analyzed in different mutant backgrounds, such as *clv1-101, clv3-9, cle40-2,* and *bam1-3* (Fig. 26). All longitudinal sections show expression of *ACR4* exclusively in the L1 of the meristem (Fig. 26, A-E).

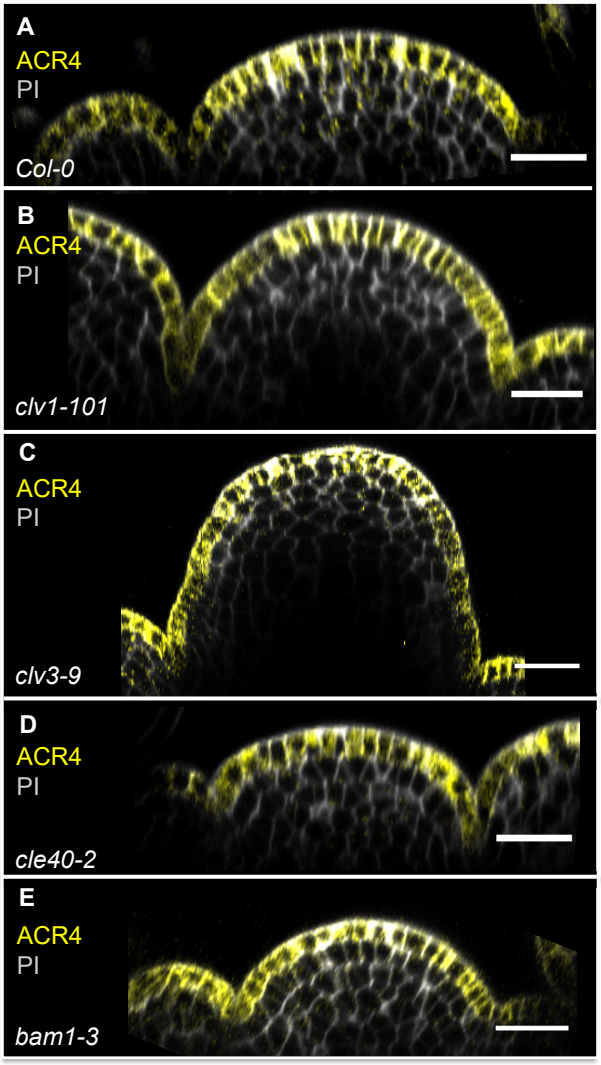

Fig. 26: The spatial distribution of *ACR4* expression in different mutant backgrounds does not change

The translational reporter *ACR4:ACR4-GFP* expressed in **(A)** wild type plants and in **(B)** *clv1-101* (N=15), **(C)** *clv3-9* (N=3), **(D)** *cle40-2* (N=15), **(E)** *bam1-3* (N=11) mutant backgrounds. **(A-E)** In wild type and all mutant backgrounds (*clv1-101, clv3-9, cle40-2,* and

bam1-3), *ACR4* expression is found exclusively in the L1 of the IFMs and FMs. No difference in the expression pattern between wild type and mutant backgrounds can be detected.

Scale bars: 20 µm (A-E), PI = Propidium iodide

No differences in *ACR4* expression can be detected comparing the expression pattern of *ACR4* in wild type plants (Fig. 26, A) to the expression pattern in the mutants *clv1-101, clv3-9, cle40-2, bam1-3* (Fig. 26, B-E). *ACR4* expression appears less in the CZ and elevated at the flanks of the meristem. Meristems of *clv1-101* and *clv3-9* mutants show a fasciated and enlarged meristem (Fig. 26, B, and C), while *bam1-3* and *cle40-2* mutants have smaller and flatter meristems (Fig. 26, D and E). Overall, no differences in the spatial distribution of *ACR4* could be detected in the single mutants of the CLV pathway presuming that ACR4 does not play a key role in stem cell signaling in the shoot meristem.

4.4.4 Ectopic expression of *ACR4* in the OC cannot rescue its meristem phenotype

In order to deduce the function of the ACR4, its normal expression pattern was miss localized by expressing the *ACR4* gene under the WUS promoter and was transformed into *acr4-8* mutants (*WUS:ACR4-GFP//acr4-8*). In those lines, the *ACR4* expression is shifted from its endogenous expression domain in the L1 to the WUS domain in the OC. Subcellular ACR4 localization is predominantly found at the PM and at a lower level in the cytosol (Fig. 27, A, A'). To test if the ectopic expression of *ACR4* in the OC can rescue its small meristem phenotype, we measured the IFM of wild type plants, *acr4-8* mutants, and *acr4-8* mutants carrying the *WUS:ACR4-GFP* construct at 6 WAG (Fig. 27, B). We found that *ACR4* expression in the L3 of the meristem is not sufficient to rescue the small meristem phenotype, since both, *acr4-8* mutants and *acr4-8* mutants carrying the *WUS:ACR4-GFP* construct, displayed a significantly smaller meristem size compared to wild type plants (Fig. 27, B). Hence, ACR4 protein in the OC of *acr4-8* mutants is not able to rescue its small meristem phenotype, suggesting that ACR4 does not play a critical role in the CLV pathway.

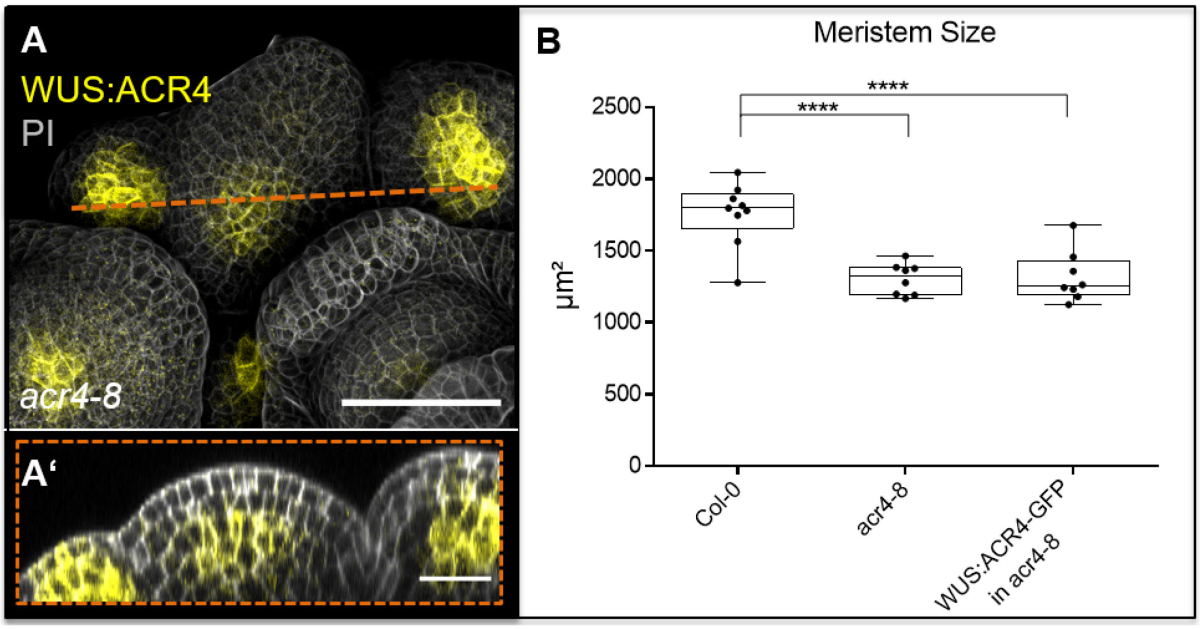

Fig. 27: *ACR4* expressed under the *WUS* promoter cannot rescue its small meristem phenotype.

(A) The MIP of an IFM expressing the *ACR4* gene under the control of the *WUS* promoter in an *acr4-8* mutant background (*WUS:ACR4-GFP//acr4-8*) shows expression in the center of the IFM and FMS. **(A‘)** The longitudinal section through the center of the meristem shows that the expression of *ACR4* is mainly PM localized. **(B)** After 6 weeks of plant growth, z-stack of IFMs of *Col-0* (N=9), *acr4-8* (N=8), and *acr4-8* plants carrying the *WUS:ACR4-GFP* construct (N=8) were imaged. *acr4-8* mutants expressing the *WUS:ACR4-GFP* construct showed significantly decreased meristem sizes compared to *Col-0* plants.

Scale bars: 50 µm (A), 20 µm (A’), PI = Propidium iodide

4.4.5. ACR4 does not alter *WUS* expression in the IFM

In wild type plants, WUS promoter activity is detected in the center of the meristem (Fig. 28). In *acr4-8* mutants, *WUS* expression is similar to *Col-0* plants (Fig. 28). *WUS* expression is in the center of the meristem in the same domain as in wild type plants. In line with that, the number of *WUS* expressing cells are comparable in *acr4-8* mutants and *Col-0* plants. While in wild type plants approximately 19 cells show *WUS* promoter activity, *acr4-8* mutants depict 18 cells expressing *WUS* in the meristem center (Fig. 28; SupplFig. 3). IFMs of *WUS*-expressing cells in wild type plants are the same as presented in sections 4.1.4 and 4.2.6 (Fig. 11; Fig. 18; Fig. 23). These results indicate that ACR4 does not have a direct impact on *WUS* expression and thus might not be involved in the CLV pathway. However, more replicates need to be performed to validate the hypothesis.

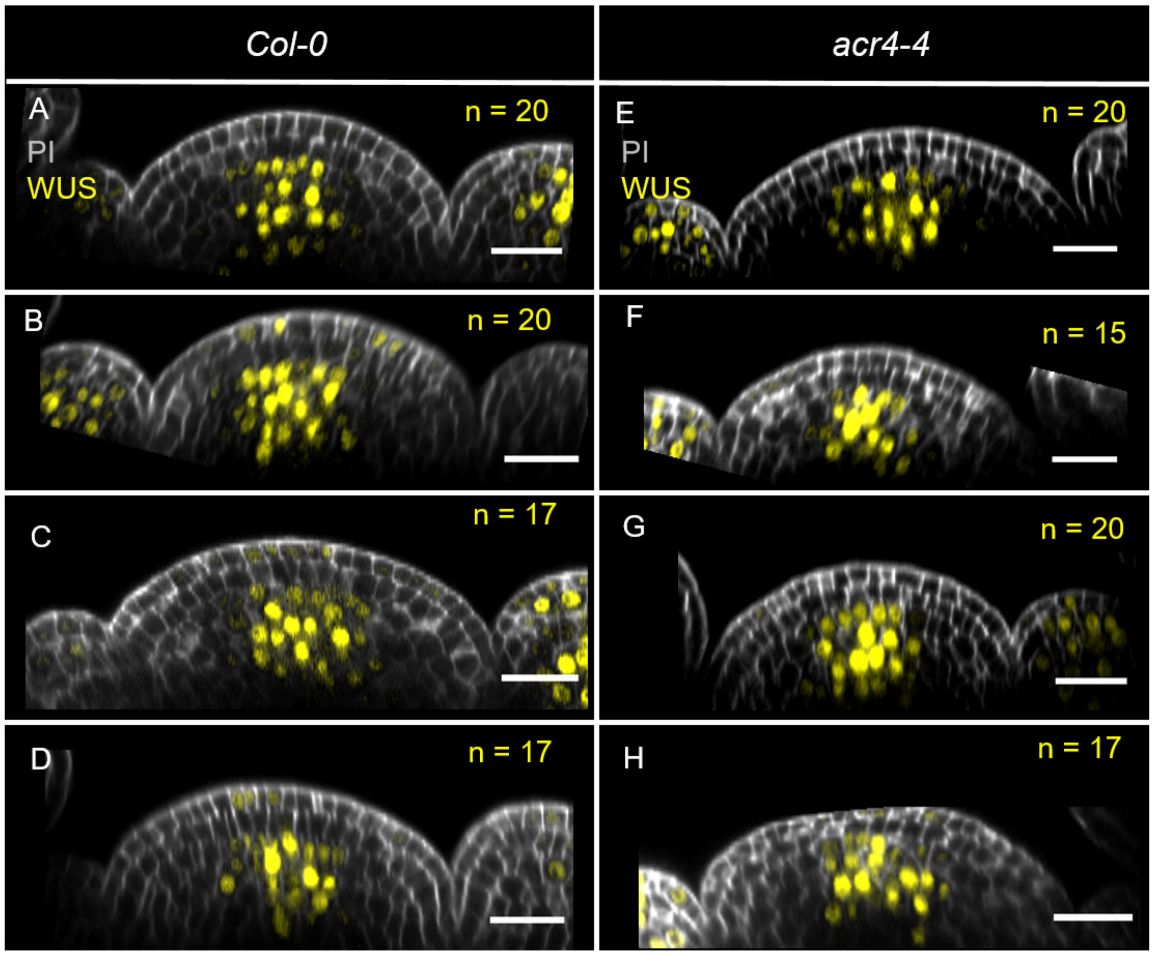

Fig. 28: ACR4 does not have an impact on the *WUS* promoter activity in the meristem center.

Longitudinal sections of wild type (N=9) **(A-D)** and *acr4-8* mutant (N=4) **(E-H)** plants expressing the reporter *WUS:NLS-GFP*. Longitudinal sections were made through the middle of the meristem from P4 to P5. *WUS* expressing cells were counted. On average wild type and *acr4-8* mutant plants show *WUS* promoter activity in about 18 to 19 cells in the center of the meristem. No significant change in *WUS* expressing cells can be detected between wild type and *acr4-8* mutants. Scale bars: 20 µm (A-H)

4.5 Analysis of *clv* mutant phenotypes

In angiosperms, the CLV pathway controls the maintenance of the stem cells in shoot meristems. PM-localized receptors that belong to the CLV family perceive peptides at the cell surface to trigger a signal transduction cascade to downregulate TFs like WUS in the OC of the meristem. However, the detailed regulation of each player within the signaling pathway remains unclear. To uncover the functional effects of the main players within the CLV pathway during IFM and flower development, we analyzed single, double, and triple mutants in terms of plant growth, meristem size, and leaf length.

4.5.1 Peptide and receptor mutants from the CLV pathway alter in their plant growth, organ production, and meristem size

A wild type *Col-0* Arabidopsis plant at 5 WAG is about 20 cm high, consists of 3 to 6 lateral branches and various siliques (Fig. 29, A). The inflorescence shows a highly organized positioning of flower organs in a radial growth pattern around the main axis (Fig. 29, A') and the number of carpels in a silique is always two (Fig. 29, A''). The highly organized radial growth pattern is also visible on the meristem level, where the position of the meristem is in the center and is surrounded by developing primordia (Fig. 29, A'''). In contrast to wild type plants, *clv3-9* plants usually grow higher than *Col-0* plants in the same period and have thicker stems (Fig. 29, B). The lack of CLV3p to activate the CLV signaling pathway reduces *WUS* repression. In turn, over-proliferation of stem cells and fast-differentiating cells occurs (Brand et al., 2002; Clark et al., 1995). Thus, the inflorescence of *clv3-9* mutants develops more flower organs, has more siliques and the siliques carry more than two carpels (Fig. 29, B', B''). In line with this, the meristem is extremely fasciated and increases in size (Fig. 29, B'''). In contrast, *cle40-2* mutants do not show a drastic phenotype compared to wild type plants. However, *cle40-2* mutant plants appear to be smaller in their overall growth, their inflorescence, and meristem size (Fig. 29, C, C', C'''). Carpel number of *cle40-2* mutants is WT-like (Fig. 29, C''). While *clv3-9* mutants are bigger than wild type plants and show additional flower organs in the inflorescence, the LRR receptor mutant *clv1-101* has on average the same plant size as wild type plants and appears to have only a few additional flowers in comparison to *Col-0* plants (Fig. 29, D, D'). Nevertheless, carpel numbers and IFM size is increased in *clv1-101* mutants, since also here, the absence of the main receptor for CLV3 leads to an over-proliferation of stem cells in the shoot meristem (Fig. 29, D'', D'''). On the other hand, *bam1-3* and *acr4-8* mutants show a similar phenotype as *cle40-2* mutants. Overall plant size, as well as the

inflorescence and the IFMs appear to be smaller compared to wild type plants (Fig. 29, E, E', E''', F, F', F'''). The carpel number of *bam1-3* and *acr4-8* mutants is always two, as it was shown for *cle40-2* mutants and *Col-0* plants (Fig. 29, E'', F''). Together, these results suggest two in parallel signaling pathways. The one signaling pathway is restricting meristem size via CLV3-CLV1 signaling, while the second one promotes meristem size by acting through CLE40-BAM1 and probably ACR4.

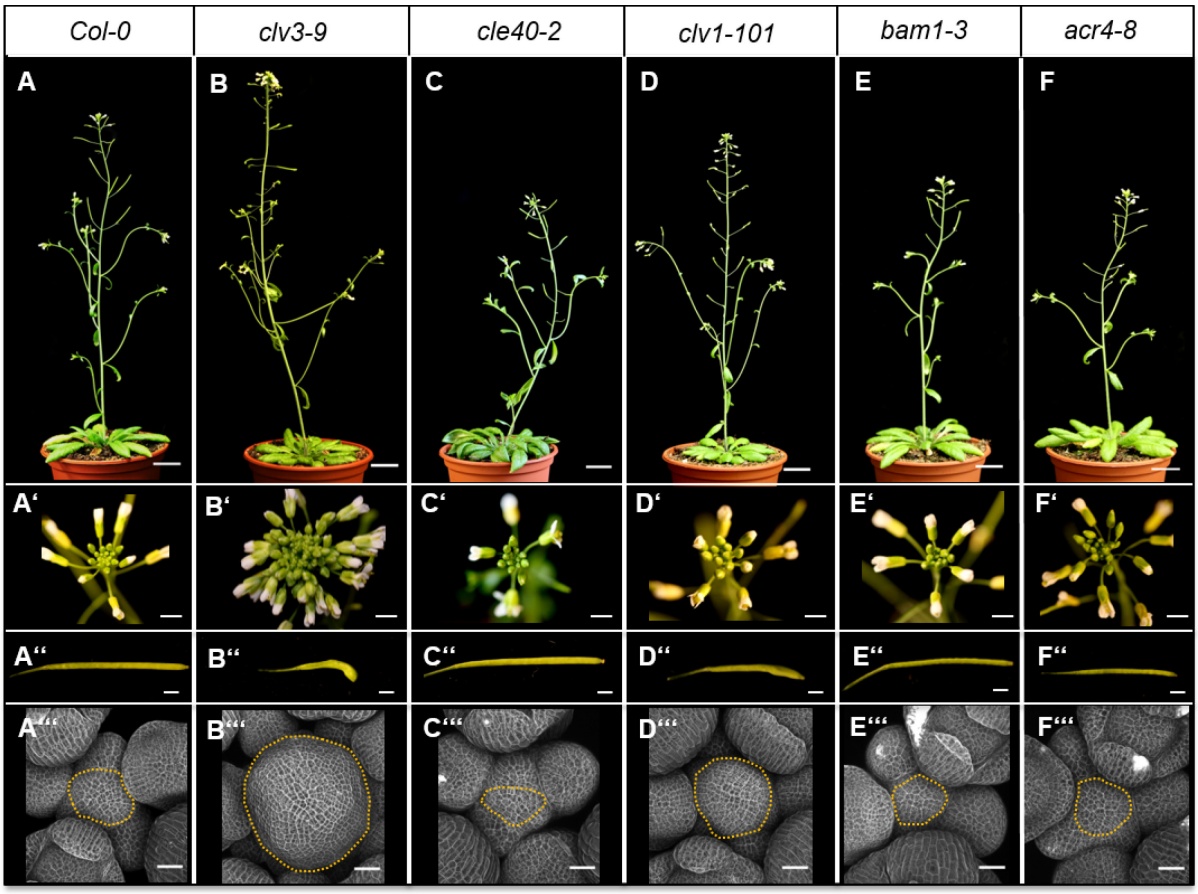

Fig. 29: Plant phenotypes of peptide and receptor mutants from the CLV pathway alter in their plant growth, inflorescence size, carpel number, and meristem sizes

(A) A wild type plant at 6 WAG is shown, with **(A')** inflorescence, **(A'')** siliques, and **(A''')** meristem structure. **(B)** A *clv3-9* mutant shows a thicker stem and higher plant growth, **(B')** a bigger and disorganized inflorescence, **(B'')** deformed siliques with a high number of carpels and, **(B''')** an extremely enlarged fasciated IFM compared to wild type plants. **(C)** A 6 WAG *cle40-2* mutant plant appears to be smaller in its overall growth and **(C')** its inflorescence compared to wild type plants. **(C'')** The siliques of *cle40-2* mutants are similar to wild type plants and always consist of two carpels. **(C''')** The IFM area size of *cle40-2* mutants is smaller compared to *Col-0* plants. **(D)** *clv1-101* mutant plants have a similar height and **(D')** inflorescence size as *Col-0* plants. **(D'')** The siliques of *clv1-101* plants are deformed and show additional carpels. **(D''')** The IFM of *clv1-101* plants is increased compared to wild type plants. **(E and F)** *bam1-3* and *acr4-8* mutants appear to be smaller than wild type plants and show a

(D' and F') a smaller inflorescence size as *Col-0* plants; similar to *cle40-2* plants. **(E'' and F'')** The siliques of *bam1-3* and *acr4-8* mutant plants are similar to wild type plants and consist of two carpels. **(E''' and F''')** The IFM of *bam1-3* and *acr4-8* plants is decreased in its size compared to *Col-0* plants. Scale bars: 20 mm (A-F), 2 mm (A'-F'), 1mm (A''-F''), 25µm (A'''-F''')

4.5.2 Leaf shape and length differ in various *clv* mutants

To additionally uncover functional effects of important players within the CLV pathway during flower development, we measured the leaf length of Arabidopsis mutant plants at 4 WAG. Leaf initiation starts at the flanks of the meristem where it is governed by the polar transport of the phytohormone auxin, and its influx and efflux transporters (Bayer et al., 2009; Guenot et al., 2012). The decision if a cell becomes a leaf primordia cell instead of a stem cell is regulated by the antagonistic relation between the two transcription factors KNOTTED-like homeobox (KNOX1) and ASYMMETRIC LEAF1/ROUGH SHEATH2/PHANTASTICA (ARP) proteins (Byrne et al., 2002; Hay & Tsiantis, 2006, 2010). While the KNOX gene *SHOOTMERISTEMLESS* (*STM*) is expressed throughout the entire meristem except in young primordia, *AS1* from the ARP family is not expressed in the meristem, but in cells forming new leaf primordia, resulting in a complementary pattern of both proteins (Byrne et al., 2000; Long et al., 1996). Thus, *KNOX* genes are important regulators for SAM and carpel development, since they maintain undifferentiated cells in the meristem while ARP proteins initiate differentiation in the leaf primordium (Byrne et al., 2002; Scofield & Murray, 2006). Mutants of *stm* fail to produce a SAM and thus do not form leaves, whereas *as1* and *as2* mutants produce small and round leaves (Byrne et al., 2002; Long et al., 1996). The dodecapeptide CLV3 is crucial for stem cell homeostasis and *clv3-9* mutants show an increase in flower organs, carpel number, and meristem size meristem (Fig. 29). Notably, *clv3-9* mutants show a similar leaf phenotype compared to *as1* and *as2* mutants. Leaves of *clv3-9* mutants also show smaller and rounder leaves compared to wild type plants (Fig. 30). This leaf shape phenotype is also observable in *bam1-3;clv1-101* double mutants. *clv1-101* mutants show a reduction in leaf length but do not have as round leaves as *clv3-9* mutants (Fig. 30). In contrast, single and double mutants of *cle40-2* and *bam1-3* mutants have the same leaf shape as wild type plants (Fig. 30). In summary, these results reveal that genes promoting meristem size do not have an obvious effect on organ development, while mutants from genes that restrict meristem growth display drastically shorter leaves. The short leaves in mutants of the CLV pathway could be explained by the elevated energy costs for the additional organ production and over-proliferation of the meristem. However, *clv3-9* and *as1* mutants show the same leaf phenotype

(small and round), even though their expression patterns and functions in the meristem are antagonistic, indicating a more complex system in regulating leaf initiation and development.

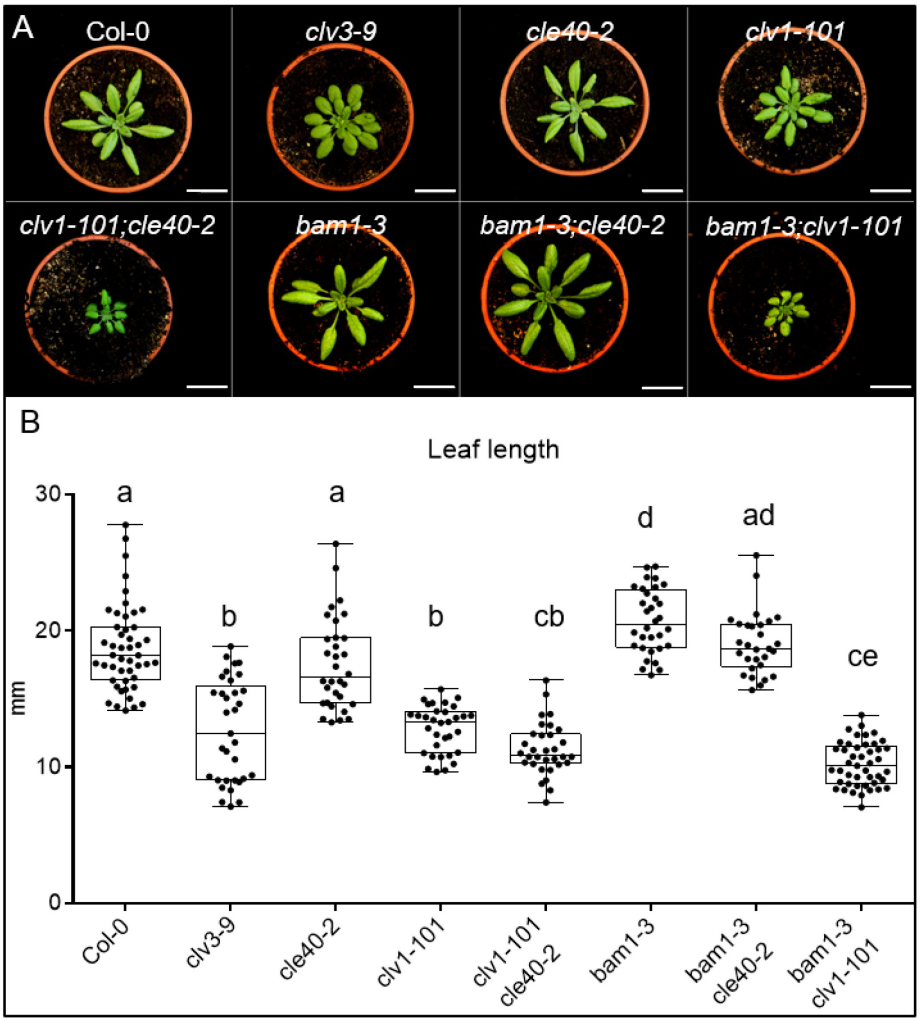

Fig. 30: Mutants of the *CLV* genes show different leaf length at 4 WAG

(A) Wild type (*Col-0*) and different single and double mutants (*clv3-9, cle40-2, clv1-101, clv1-101;cle40-2, bam1-3, bam1-3;cle40-2, bam1-3;clv1-101)* at 4 WAG. **(B)** Leaf lengths were measured and plotted. Wild type (*Col-0* N=47), *cle40-2* (N=32), and *bam1-3;cle40-2* (N=29) mutant plants do not show a significant difference in leaf length to each other. While *bam1-3* (N=32) mutants exhibit on average significantly longer leaves than wild type plants, the single mutants *clv3-9* (N=33) and *clv1-101* (N=33) and the double mutants *clv1-101;cle40-2* (N=32) and *bam1-3;clv1-101* (N=45) show significantly shorter leaves. Statistical groups were assigned after calculating p-values by ANOVA and Turkey's multiple comparison test (differential grouping from $p \leq 0.01$). Scale bar: 25 mm (A)

4.5.3 Differences in meristem area size of *clv* mutants imply antagonistic feedback regulations

The results described in sections 4.1.1, 4.2.1, and 4.3.1 show that single mutants of the CLV pathway differ in meristem size compared to wild type plants. As a result, *cle40-2, bam1-3,* and *acr4-8* single mutants have smaller meristems compared to wild type plants, i.e. the functional genes show a promoting effect on meristem size (Fig. 31). In contrast, *clv1-101* and *clv3-9* mutants have enlarged meristems, confirming that *CLV1* and *CLV3* genes have a repressing effect on meristem size in a (Fig. 31). More detailed analysis of double and triple mutants validated the promoting effect of the single mutants *cle40-2, bam1-3,* and *acr4-8*. Thus, double mutants of *bam1-3;cle40-2*, *acr4-8;cle40-2,* and *acr4-8;bam1-3* showed also a significant reduction in meristem size compared to wild type plants. However, no additive effect of the double mutants (*bam1-3;cle40-2*, *acr4-8;cle40-2,* and *acr4-8;bam1-3)* compared to the single mutants (*cle40-2, bam1-3,* and *acr4-8*) could be detected, suggesting that the proteins either act in the same signaling pathway or the difference in meristem size is too small to detect.

c*lv1-101* mutants have an enlarged meristem, while *acr4-8* mutants have smaller meristems. In line with that, double mutants of *acr4-8;clv1-101* can restore the meristem size to wild type level (Fig. 31). These results imply that the ACR4 and CLV1 receptors do not signal in the same pathway and have antagonistic effects on meristem size. ACR4 promotes meristem size, while the CLV1 pathway has a repressing effect on meristem size. Contrary to that, double mutants of *clv1-101;cle40-2* exhibit comparable meristem sizes as the single mutant *clv1-101*, indicating that CLE40 can act through the LRR-receptor kinase CLV1. In line with that, the triple mutant *acr4-4;cle40-2;clv1-101* is also able to rescue the enlarged meristem phenotype of *clv1-101* mutants, confirming the promoting effect of ACR4 on meristem size independently from the CLV3-CLV1-WUS signaling pathway.

Interestingly, the lack of both LRR receptors *CLV1* and *BAM1* leads to a severely fasciated meristem, resulting in an IFM area of about ~8300 µm², comparable to *clv3-9* mutants (Fig. 31). At first glance, this seems to contradict since the CLE40-BAM1 pathway has a promoting effect on meristem size and thus *bam1-3;clv1-101* double mutants should be smaller in their IFM size than *clv3-9* mutants. On the other hand, this effect indicates a strong cross-regulation between the receptors *CLV1* and *BAM1*. In the absence of both receptors, the perception of both CLV3 and CLE40 is disturbed. Thus, *WUS* expression is no longer restricted and leads to an over-proliferation of stem cells. In the presence of either BAM1 or CLV1, they could compensate each other.

In summary, we here present three independent but intertwined pathways. While the CLV3-CLV1 pathway restricts meristem size, the CLE40-BAM1 signaling pathway promotes meristem growth. ACR4 also promotes increased meristem size, but independently of the CLV3-CLV1 pathway. ACR4 could either act in the same pathway as CLE40 and BAM1 since we could not detect a significant difference between *acr4-8* single and *acr4-8;cle40-2* double mutants or in an independent pathway, since ACR4 is not able to bind CLE40 (Satohiro Okuda, Ludwig A. Hothorn, 2020).

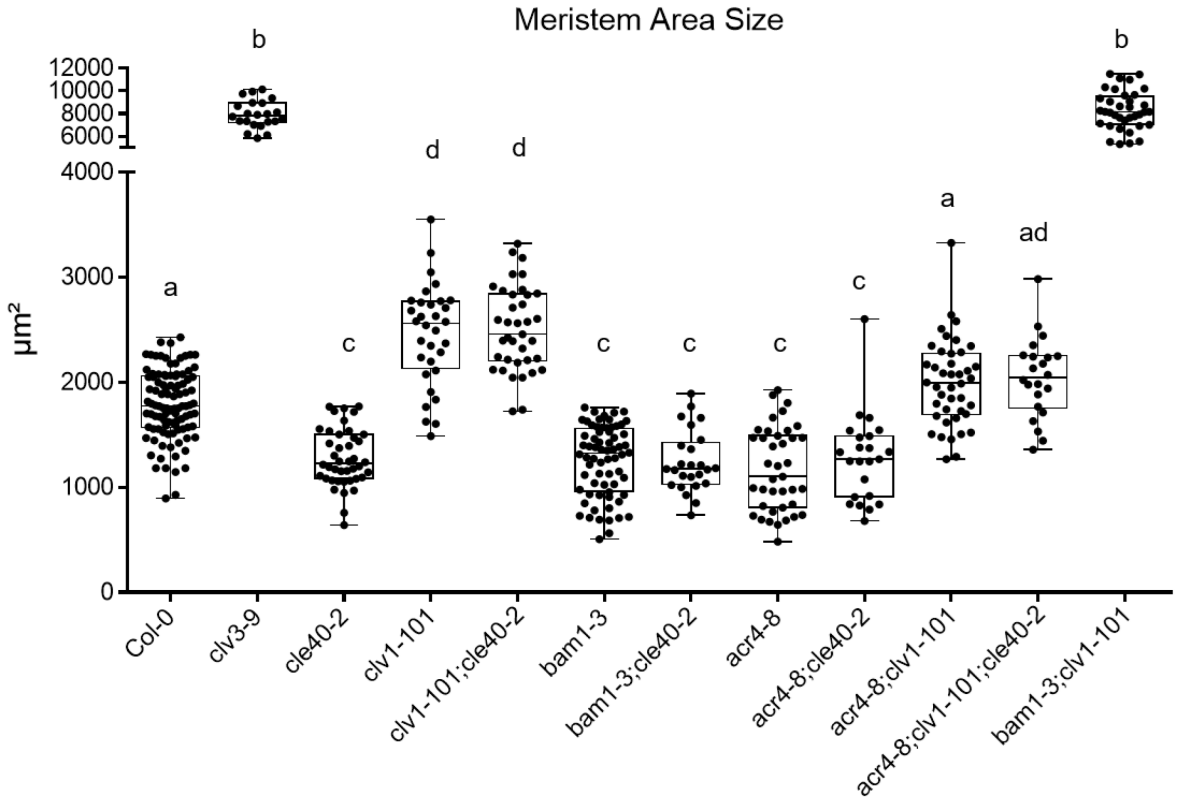

Fig. 31: Analysis of meristem area sizes of single and double mutants from the CLV pathway reveal antagonistic feedback regulations

The IFM area size *A. thaliana* plants at 6 WAG of *Col-0* (N=82) and different single mutants (*clv3-9* N=22*, cle40-2* N=42*, clv1-101* N=32*, bam1-3* N=68*, acr4-8* N=39), double mutants (*cle40-2;clv1-101* N=37*,cle40-2;bam1-3* N=25*, acr4-8;cle40-2* N=23*, acr4-8;clv1-101* N=42*, bam1-3;clv1-101* N=36), and the triple mutant *acr4-8;clv1-101;cle40-2* (N=22) was measured. The meristem size of the single *cle40-2, bam1-3,* and *acr4-8* mutants, as well as the double mutants *cle40-2;bam1-3* and *acr4-8; cle40-2* are approximately 1.5 times smaller than the IFM area size of wild type plants (*Col-0*). *clv1-101* and *clv1-101; cle40-2* mutant plants have an increased meristem area size compared to *Col-0* plants (about 1.4 times). The double and triple mutant *acr4;clv1-101* and *acr4-8;clv1-101; cle40-2* are at WT level. While the

acr4-8;clv101 double mutants have significantly smaller meristems than *clv1-101* plants, the triple mutant of *acr4-8;clv1-101; cle40-2* is not significantly different in its meristem size compared to the single *clv1-101* mutant. The single mutant *clv3-9* and the double mutant *bam1-3;clv1-101* have the biggest meristem size with approximately 5.5 times larger IFMs than wild type plants.

Statistical groups were assigned after calculating p-values by ANOVA and Turkey's multiple comparison test (differential grouping from $p \leq 0.001$).

4.2.4 The CLV pathway controls meristem shape along the apical-basal axis

The CLV pathway is known to regulate stem cell homeostasis and meristem size in *A. thaliana*. The balance between stem cells and *WUS* expressing cells is crucial to maintain the shape and size of a meristem. In wild type plants, the longitudinal section of a meristem displays a perfectly shaped hemisphere, while the longitudinal section of a *cle40-2* mutant shows not only a smaller but flatter meristem (Fig. 32, A-B'). In contrast, *clv3-9* and *bam1-3;clv1-101* mutants undergo an over-proliferation of stem cells, resulting in a fasciated, dome-shaped meristem, which expands along the apical-basal axis (Fig. 31, C', D'). While *clv3-9* mutants expand more along the apical-basal axis of the meristem, having a significant higher meristem compared to *bam1-3;clv1-101* mutants, the double receptor mutant (*bam1-3;clv1-101*) expands more along the radial axis, depicting the widest meristem with on average 115 µm (Fig. 31, E, F). Comparing the meristem size of both mutants (*clv3-9* and *bam1-3;clv1-101*) no significant difference can be detected (Fig. 31, G). These results indicate that the CLV pathway is not only responsible for the homeostasis of stem cells but also plays a crucial role in the spatial configuration of the meristem along its apical-basal axis and its radial axis. Our results suggest the presence of two parallel pathways, which are responsible for shaping the meristem. The CLV3-CLV1-WUS pathway forms the meristem along its apical-basal axis, while the CLE40-BAM1-WUS pathway acts from the periphery of the meristem to control meristem shape along the radial axis.

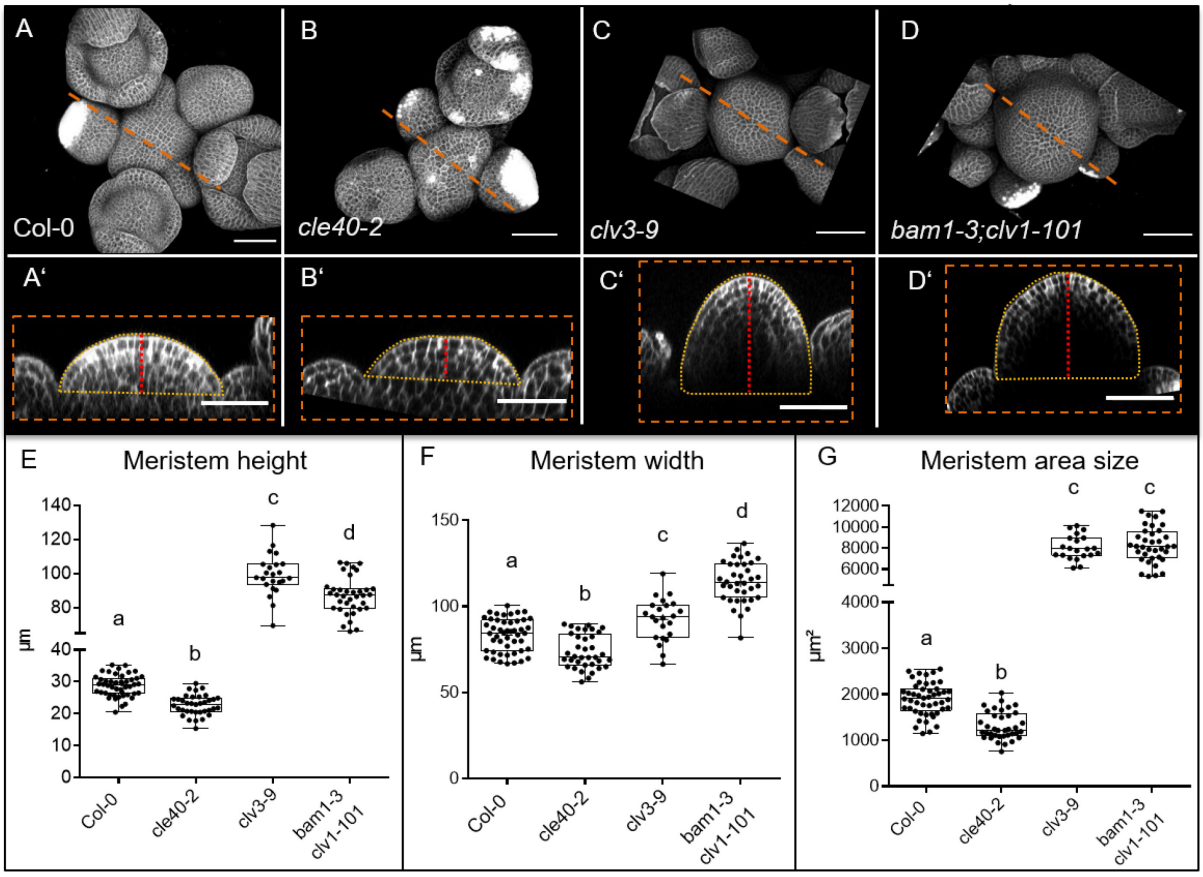

Fig. 32: The CLV pathway controls meristem shape along the apical-basal axis.

(A-D) MIP of inflorescences of a **(A)** wild type, **(B)** a *cle40-2* mutant, **(C)** a *clv3-9,* and **(D)** a *bam1-3;clv1-101* double mutant plant are shown. The meristem in the center is surrounded by developing primordia growing in a helicoidal pattern around the main axis. **(A')** The longitudinal section through the *Col-0* IFM is shaped in form of a hemisphere. **(B')** The longitudinal section through the *cle40-2* meristem shows a smaller and flatter meristem compared to *Col-0* plants. **(C')** The longitudinal section through a *clv3-9* meristem reveals an expansion of the meristem along the apical-basal axis in a dome-shaped way. **(D')** The XZ-view of *bam1-3;clv1-101* double mutants show a fasciated meristem with an expansion along the apical-basal and the radial axis of the meristem. **(E-G)** IFM heights **(E)**, width **(F),** and area **(G)** of 6 weeks old *Col-0* (N=48), *cle40-2* (N=36), *clv3-9* (N=27), and *clv1-101;bam1-3* (N=40) plants were measured and plotted. *cle40-2* mutants show a significantly smaller height, width, and area size compared to wild type plants. *clv3-9* mutants have the highest meristem with an average of 100 µm along the apical-basal axis of the meristem and *bam1-3;clv1-101* mutants have the widest IFMs of about 114 µm compared to wild type (83 µm), *cle40-2* (73 µm) and *clv3-9* (93 µm) mutant plants. No significant difference was detected between the area size of *clv3-9* and *bam1-3;clv1-101* double mutants.

Scale bars: 50 µm (A-D), 20 µm (A'-D')0 µm (P1 to P6) Statistical groups were assigned after calculating p-values by ANOVA and Turkey's multiple comparison test (differential grouping from $p \leq 0.01$)

4.6 Exogenous peptide treatment on IFMs can trigger receptor internalization

Cell-cell communication in plants is different from the animal kingdom since plant cells comprise a cell wall, which acts as a physical barrier. Thus, plants developed two main communication pathways. Macromolecules use plasmodesmata to traffic from cell to cell. The diameter of plasmodesmata is approximately 20 to 50 nm. They are formed during cytokinesis when dividing cells remain connected (Ehlers & Kollmann, 2001; Lucas et al., 2009). Small molecules, like peptides and phytohormones, are able to diffuse through the cell wall and membranes and are subsequently perceived by PM-located receptors of an adjacent cell. The binding of a peptide to its associated receptor is highly specific and triggers a downstream signaling cascade on the intracellular side of the PM, e.g. to activate or repress gene expression. After the peptide binds to the extracellular domain of a receptor, the complex undergoes internalization, which can be followed by receptor recycling and re-transport to the PM or by degradation in lytic vacuoles (Geldner et al., 2007; Wiley & Burke, 2001). This process can be imaged with high-resolution microscopy. If a receptor is able to bind a peptide, its activity is elevated, triggering receptor internalization from the PM. Potentially, the external addition of a peptide, which can bind to the receptor, can be detected in a reduced signal at the PM and an increased signal of vesicles within the cells. Similar to the mature peptide in wild type plants, we here used synthetic peptides of CLV3 and CLE40, which were modified by proline hydroxylation (CLV3hyp13p/CLV3p or CLE40hyp13p/CLE40p), for exogenous addition on IFMs at 5 WAG.

4.6.1 CLV1 internalization can be triggered by CLE peptides

Previous studies have shown that the binding of CLV3p to the extracellular domain of the LRR receptor *CLV1* triggers the activation of its intracellular kinase domain resulting in the internalization of *CLV1* from the PM in a VTI11/ZIG- dependent manner. *CLV1* traffics to the lytic vacuole where it gets degraded (Nimchuk et al., 2011). Here, we expanded those experiments to test if the external addition of CLE40p triggers internalization of CLV1, we used the *CLV1:CLV1-GFP* reporter line and added external CLV3hyp13p and *CLE40*hyp13p 48 h, 24 h, and 10 min before imaging on IFMs at 5 WAG. As a positive control, we also added external BFA on IFMs carrying the *CLV1:CLV1-GFP* transgene. BFA inhibits the activation of proteins involved in vesicle formation and thus is commonly used to disrupt the trafficking of internalized vesicles (Nebenführ et al., 2002; Samaj et al., 2004). In untreated plants, *CLV1*

expression was detected at the PM in L1/L2 and in the center of the meristem in the L3. Intracellular vesicles could not be detected in either the cross-section or in the MIP projection (Fig. 33, A-A’’’). Upon 10 µM CLV3p addition, more intracellular GFP signals could be detected in the L1/2 and L3 in form of small dots (white arrows, Fig. 33 B’ and B’’’). These dots indicate internalization of CLV1 upon CLV3p treatment. Similar observations were made when we added external CLE40p to the IFM (Fig. 33, C’, C’’’). We could observe increased punctate GFP signals within the cells compared to untreated plants, but fewer GFP signal dots compared to plants treated with CLV3p, indicating that CLV1 can bind also CLE40p, but less specifically than CLV3p. When we added BFA to the meristem, nearly no GFP signal was detected at the PM anymore (Fig. 33, D-D’’’). Instead, most of the cells accumulated GFP signal in many and big dots within the cells (Fig. 33, D’’’). BFA inhibits trafficking of internalized vesicles, thus after internalization, CLV1 cannot be transported back to the PM and hence accumulates within lytic vacuoles within the cell. Since we could see a strong effect in BFA treated IFMs, we demonstrated that it is possible to detect a change in GFP signal from the PM to the lytic vacuoles. BFA treatment on IFMs also allows us to estimate how strong the effect of internalization and recycling can be. Together this experiment shows that it is possible to image the internalization of a receptor upon peptide treatment, but that a quantitative read-out is still missing to draw precise conclusions about peptide and receptor binding. Our results suggest that CLV1 internalization is activated upon CLV3p addition and that CLV1 is also able to bind CLE40p, but in a less specific manner.

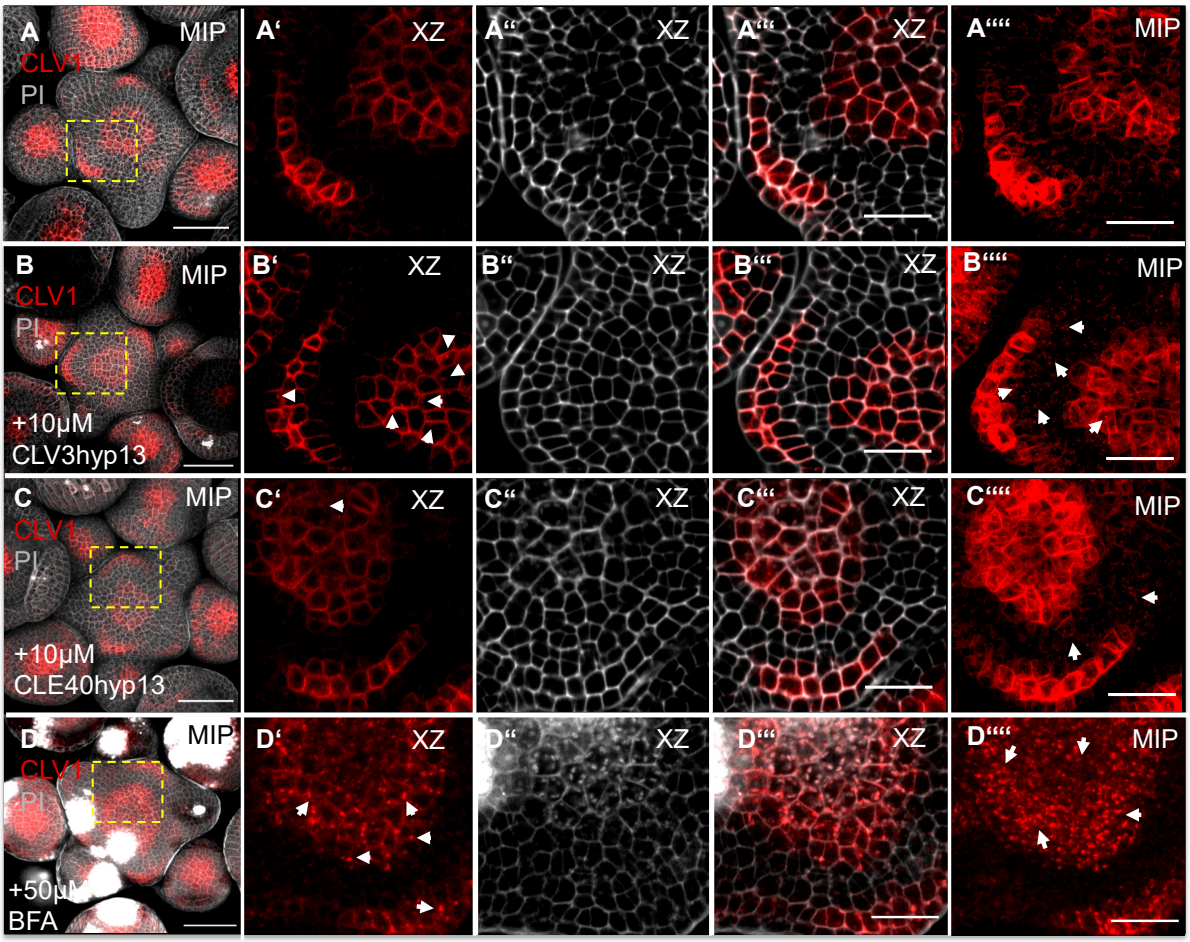

Fig. 33: External addition of CLV3p triggers internalization of the CLV1 receptor

(A) MIP of an IFM carrying the *CLV1:CLV1-GFP* transgene. *CLV1* expression is detected in the center of the meristem and in cells of the L1 and L2 layer where new primordia develop (N=7). **(A'-A''')** A cross-section of a part of the meristem shows *CLV1* expression localized to the PM. **(A'''')** MIP of *CLV1* expression in a zoom-in from A shows *CLV1* expression at the PM. **(B)** MIP of an IFM carrying the *pCLV1:CLV1-GFP* transgene was treated with 10 µM pCLV3hyp13p, 48 h, 24 h, and 10 min before imaging (N=13). **(B'-B''')** Cross-section of a close-up of the IFM from B shows *CLV1* expression at the PM and in vesicles in the cytoplasm (white arrows). **(B'''')** MIP of the zoom-in from B shows multiple vesicles within the cells (white arrows). **(C)** MIP of an IFM carrying the *pCLV1:CLV1-GFP* transgene was treated with 10 µM p*CLE40*hyp13p, 48 h, and 10 min before imaging (N=6). **(C'-C''')** The cross-section of the zoom-in of the IFM from C shows *CLV1* expression at the PM and a couple of vesicles in the cytoplasm (white arrows). **(C'''')** MIP of the zoom in from B shows a few vesicles within the cells (white arrows). **(D)** MIP of an IFM carrying the *pCLV1:CLV1-GFP* transgene treated with 50 µM BFA 15 min before imaging (N=6). **(D'-D''')** The cross-section of a close-up of the IFM from D shows nearly no *CLV1* expression at the PM but various intracellular vesicles (white arrows). **(D'''')** The MIP of the zoom-in from B shows high *CLV1* expression within multiple intracellular vesicles (white arrows) and no expression of *CLV1* at the PM.

Scale bars: 50 µm (A-D), 20 µm (A’’’-D’’’’), MIP = Maximum intensity projection, PI = Propidium iodide

4.6.2 ACR4 internalization can be triggered by CLE40 peptide

To determine whether its potential ligand CLE40 can activate ACR4 kinase internalization, we imaged IFMs at 5 WAG carrying the translational *ACR4:ACR4-GFP* reporter and added exogenous CLE40p. It was previously reported that *ACR4* expression was increased by ectopic CLE40p in the root and that that CLV1 and ACR4 can form heteromeric complexes in the distal root meristem to perceive CLE40p (Stahl et al., 2013). As a control, we first imaged an IFM carrying the *ACR4:ACR4-GFP* reporter line without any treatment (Fig. 34, A). ACR4 was localized mainly at the PM. After imaging, the same IFM was treated for 1 min with mock and imaged again. No change in the *ACR4* expression pattern was observed (Fig. 34, A’). After 30 min of mock treatment, the same IFM was imaged again and the GFP signal could still be detected mainly at the PM of the cells (Fig. 34, A’’). Next, we imaged a second IFM carrying the *ACR4:ACR4-GFP* reporter and could detect GFP signals mostly at the PM, but also in small dots within the cells (Fig. Fig. 34, B). After 1 min of 10 µM CLE40p treatment, the same IFM was imaged again and obvious changes in ACR4 localization were observed (Fig. 34, B’). After 30 min CLE40p treatment, much more GFP signal was detected in small dots within the cell and less GFP signal could be seen at the PM (Fig. 34, B’’ red arrows) compared to the GFP signal before treatment with CLE40p. These results indicate that the ACR4 receptor was activated upon CLE40p treatment and subsequently was internalized. However, it was reported previously (section 1.2.1.3) that CLE40 is unlikely to bind ACR4 directly, and thus CLE40 might bind to a CLV1/ACR4 complex and triggers ACR4 internalization indirectly.

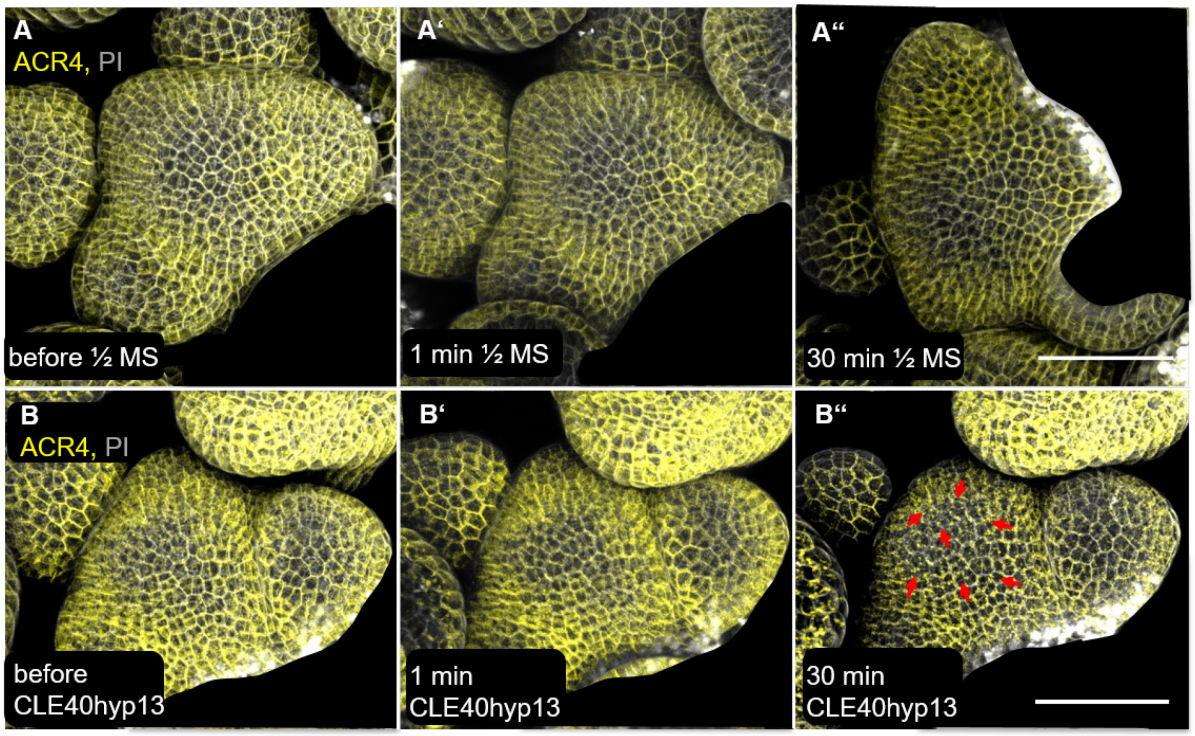

Fig. 34: External addition of *CLE40p* on the same meristem over time alters ACR4 localization

(A-A'') The MIP of the same IFM expressing the translational reporter *ACR4:ACR4-GFP* is shown, **(A)** before, **(A')** after 1 min, and **(A'')** after 30 min of mock treatment. *ACR4* expression is found in all cases through the entire L1 of the IFM, with less expression in the center of the meristem. The ACR4 receptor localized at the PM, even after 30 min of mock treatment (N=2). **(B-B'')** The MIP of the same IFM expressing the translational reporter *ACR4:ACR4-GFP* is shown, **(B)** before, **(B')** after 1 min and **(B'')** after 30 min of 10 µM *CLE40*hyp13 treatment. **(B-B')** Before and 1 min after *CLE40*hyp13 treatment, ACR4 is mainly localized to the PM in the L1 of the meristem. A few vesicles within the cells showing an ACR4 signal can be detected. **(B'')** After 30 min of 10 µM *CLE40*hyp13p treatment, ACR4 expression is detected in many vesicles within the cells and less ACR4 is found at the PM, indicating internalization of the ACR4 receptor upon *CLE40*p treatment (N=4).

Scale bar: 50µm, MS = Murashige & Skoog media

To validate our previous observation, we imaged only a few cells of an IFM plant expressing *ACR4:ACR4-GFP*. This time, multiple IFMs were imaged after 5, 10, or 20 min of mock or 10 µM CLE40p treatment. At least three different regions from each meristem were imaged. In order to quantify the effect of internalization upon exogenous CLE40p treatment the grey value intensity profiles of the GFP signal across a PM were measured and plotted as mean values of nine independent measurements (Fig. 35, C, F, I, L). Before treatment, ACR4 localizes mainly to the PM but was also detected in small vesicles within the cells (Fig. 35, A-B''). The

intensity plots of two different IFMs before treatment did not show a difference in their profiles (Fig. 35, C). After 5 min of CLE40p treatment, no visible differences in the expression pattern of *ACR4* could be detected compared to 5 min of mock treatment (Fig. 35, D-E'). Interestingly, the quantification of the GFP signal showed a wider amplitude and a reduced signal in plants treated with CLE40p compared to plants treated with ½ MS media (Fig. 35, F). This shows that more GFP signal was detected within the cell and less GFP signal was measured at the PM, indicating internalization of the ACR4 receptor. However, after 10 min of treatment, no visible and quantifiable effect could be detected between IFMs treated with ½ MS media or CLE40p (Fig. 35, G-I). After 20 min of CLE40p treatment, ACR4-GFP was still visible at the PM but appeared to be reduced compared to IFMs with shorter or no treatments (Fig. 35, K''). Nevertheless, quantification of the plants treated with 20 min of ½ MS media showed a wider amplitude and a decreased GFP signal, indicating that the treatment without peptide also affects the imaging of *ACR4* expression over time. In comparison, the amplitude of IFMs treated with CLE40p is even wider, demonstrating that the GFP signal was evenly distributed throughout the cell and did not accumulate at the PM as strongly as it was shown in untreated plants (Fig. 35, C, L). Considering that also the mock-treated plants showed a wider amplitude no precise conclusions can be driven. In summary, our results indicate that ACR4 might be internalized upon CLE40p treatment, but better quantificational read-outs need to be established and negative controls with other CLE peptides should be performed.

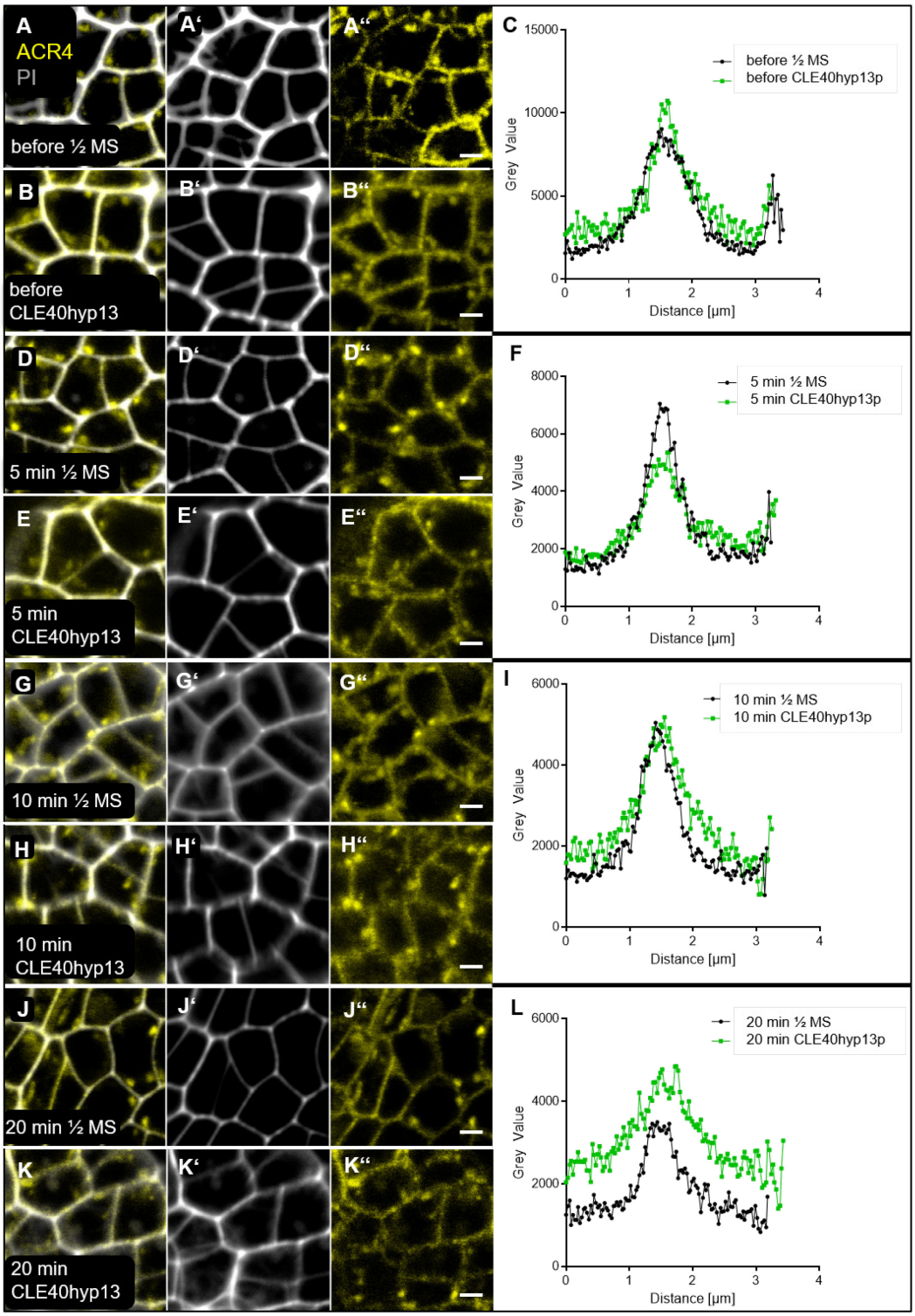

Fig. 35: External addition of CLE40p on IFMs does not increase *ACR4* expression within the cell

(A-K'') Cross-sections of IFMs expressing the translational *ACR4:ACR4-GFP* line are shown **(A-B'')** before (N=5), **(D-D'')** after 5 min of mock (N=3), **(E-E'')** after 5 min of 10 µM

*CLE40*hyp13 (N=5), **(G-G'')** after 10 min of mock (N=3), **(H-H'')** after 10 min of 10 µM *CLE40*hyp13 (N=5), **(J-J'')** after 20 min of mock (N=3), and **(K-K'')** after 20 min of 10 µM *CLE40*hyp13 treatment (N=3). The first row shows the merge of ACR4 expression and PI, while the second row depicts only the PI expression at the PM and the third row shows only *ACR4* expression. **(C, F, I, L)** The plots show the mean of 9 independent grey value intensity profiles of *ACR4* expression that were measured by randomly drawing a line across a PM in either ½ MS media or *CLE40*hyp13 treated plants **(C)** before, **(F)** after 5 min, **(I)** after 10 min, and after **(L)** 20 min of treatment.

Scale bar = 2 µm (A-K''), MS = Murashige & Skoog media

4.6.3 Peptides tagged to small fluorophores allow *in vivo* visualization

Mature CLE peptides consist of 5 to 20 aa, while commonly used fluorophores like GFP comprise ~240 aa (Breiden & Simon, 2016; Zimmer, 2002). This size discrepancy between the target and the 20-times bigger tag makes it challenging to ensure peptide functionality *in vivo*. The tag most likely affects the physical behaviors of the peptide such as mobility and receptor binding specificity. Nevertheless, it would be of great importance to be able to image the *in vivo* function and diffusion of a peptide within a specific tissue and thus tag a peptide with a small fluorophore without losing its *in vivo* functionality and mobility. Another problem with exogenous peptide treatment on IFMs is the fact that we cannot ensure that the addition of exogenous peptides reaches the PM of the organs. Until now, most experiments with exogenous peptide addition were performed in roots and only a few studies reported experiments on shoot meristems (Nimchuk et al., 2011). The root takes up water and nutrients from its surroundings, while the shoot is not adapted to take up nutrients from the environment (H. Wang et al., 2006).

4.6.3.1 CLV3p-Tamra is not functional

Here, we (Centic Biotec®) tagged the second aa of the CLV3p to the small, red Tamra fluorophore that has a size of ~ 430 Dalton (GFP ~26kDa) (SupplFig. 4). To test the functionality of the CLV3p-Tamra, *Col-0* and *clv2-101* seedlings were sown on ½ MS media, ½ MS media containing 100 nM or 1 µM CLV3hyp13p Tamra, and on ½ MS media containing free Tamra. The root length of wild type plants is shorter upon CLV3p treatment, while *clv2-101* mutants are resistant to CLV3p treatment (Fiers et al., 2005). No significant decrease in root length of *Col-0* compared to *clv2-101* plants could be measured when seedlings were grown on ½ MS media containing 100 nM or 1 µM of CLV3hyp13-Tamra or on ½ MS media containing

free Tamra (Fig. 36, A). The negative control, where seedlings were sown on ½ MS media did not show a significant difference in root length of *Col-0* seedlings compared to *clv2-101* plants, while the positive control showed a significant root length decrease of *Col-0* plants compared to *clv2-101* seedlings (½ MS media with CLV3hyp13p 100 nm and 1 µM). These results demonstrate that the CLV3p tagged to the Tamra fluorophore is not functional, as it did not show a decrease in the root length of wild type plants (Fig. 36, A).

Nevertheless, we tested how the CLV3p tagged to Tamra diffuses into the root of wild type plants. *Col-0* plants were treated for 5 min with 1 µM of pCLV3hyp13p-Tamra and imaged with a confocal microscope. The peptide tagged to the Tamra fluorophore entered the root tissue and located mainly at the PM of the cells. Most Tamra signal could be detected in the stele of the root but was also visible in the cortex, endodermis, and QC cells. Besides the localization at the PM, the Tamra signal accumulated in small dots within the cells, indicating that CLV3p was located also in intracellular vesicles (Fig. 36, B). Since CLV3 was shown to bind to the LRR receptor CLV1, 7 DAG wild type plants expressing the translational *CLV1:CLV1-GFP* reporter were treated for 5 min with 1 µM pCLV3-hyp13p-Tamra and were imaged subsequently. While the *CLV1*-GFP signal was mainly detected at the PM of columella stem cells, Tamra accumulated in large dots in the QC and in low levels at the PM of cells in the stele (Fig. 36, C). These results suggest that the CLV3p-Tamra is indeed not functional, since no co-localization of CLV3-Tamra with CLV1-GFP was observed.

.

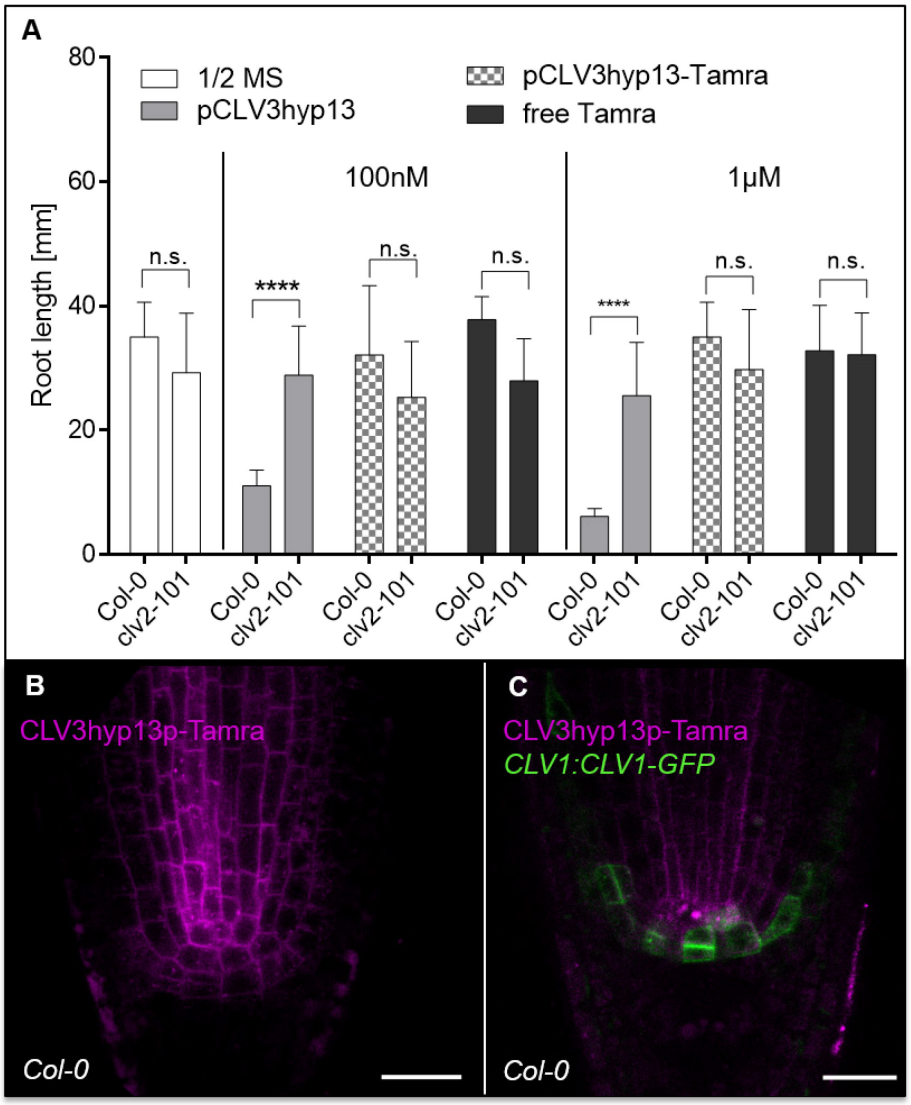

Fig. 36: CLV3p-Tamra is not functional

(A) Seedlings of wild type (*Col-0*) and *clv2-101* plants were sown on ½ MS media, ½ MS media containing 100 nM and 1 µM CLV3yp13p tagged to Tamra and on ½ MS media containing free Tamra. Root lengths were measured after 10 DAG. *Col-0* roots (N=26) were shorter compared to *clv2-101* (N=25) seedlings when plants were grown on ½ MS media containing 100 nM or 1 µM CLV3hyp13p. No significant decrease in root length of *Col-0* compared to *clv2-101* plants could be measured when seedlings grew on either ½ MS media containing 100 nM or 1 µM of CLV3hyp13p tagged to Tamra or on ½ MS media containing free Tamra. The control, where seedlings were sown on only ½ MS media did not show a significant difference in root length. **(B)** A 7 DAG *Col-0* root was treated for 5 min with 1 µM of pCLV3hyp13p-Tamra (N=10). The peptide is visible at the PM of the cells, especially in the stele of the root. Expression of pCLV3hyp13-Tamra is also detected in some dots within the cells (white arrows). **(C)** A 7 DAG root expressing the translational *CLV1:CLV1-GFP* reporter line treated with 5 min of 1 µM CLV3hyp13p-Tamra is shown (N=6). While the GFP signal of the *CLV1* receptor is mainly

found at the PM of columella stem cells, CLV3hyp13-Tamra expression is detected in large dots in the QC and in low levels at the PM of cells in the stele of the root.

Scale bars: 20 µm (B, C), MS = Murashige & Skoog media

4.6.3.2 CLV3p-Atto488 is functional

In a second approach, the CLV3p was tagged at its second aa to the small, green fluorescent marker Atto488. To test the functionality of the tagged CLV3p, wild type (*Col-0*) and *clv2-101* mutant seeds were sown on ½ MS media and ½ MS media containing 200nM of CLV3p-Atto488. Root length of wild type and *clv2-101* mutants were measured and plotted after 7, 10, and 14 DAG. Already, after 7 DAG a significant decrease in root length of *clv2-101* mutants compared to wild type plants could be detected when seedlings were grown on CLV3p-Atto488 (Fig. 37). After 10 and 14 DAG, the difference between the root length of wild type and *clv2-101* mutants was even more pronounced since *clv2-101* plants were ~ 50% reduced in their root length compared to *Col-0* plants when grown on CLV3p-Atto488 (Fig. 37). As a control, *Col-0* and *clv2-101* seedlings grown on ½ MS media did not show a significant difference in their root length after 7, 10, or 14 DAG (Fig. 37). These results suggest that the CLV3p tagged to Atto488 is still functional since shorter roots could be observed in wild type plants.

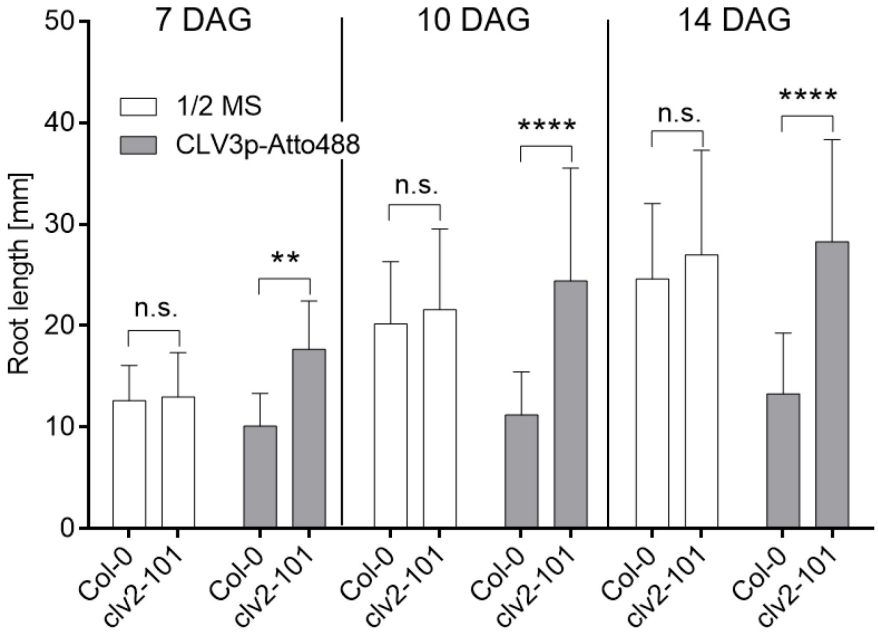

Fig. 37: CLV3p tagged to the small fluorescent marker Atto488 is functional

Wild type (*Col-0* N=25) and *clv2-101* (N=24) seedlings were sown on ½ MS media and ½ MS media containing 200nM of pCLV3p-Atto488. Root length was measured and plotted after 7

DAG, 10 DAG, and 14 DAG. While wild type and *clv2-101* mutants did not show a significant change in root length grown on ½ MS media after 7, 10, and 14 DAG, a significant change in root length between *Col-0* and *clv2-101* mutants could be detected after 7, 10 and 14 DAG when the roots were grown on ½ MS media containing 200nM of pCLV3p-Atto488.

To test the CLV3p-Atto488 *in vivo,* wild type (*Col-0*), *bam1-3, clv1-101,* and *bam1-3;clv1-101* mutants were grown for 7 days on ½ MS media and were treated for 10 min with 1 µM of CLV3p-Atto488 before the roots were imaged. Previous studies reported that CLV1 and BAM1 can bind CLV3p and thus a change in the localization of the CLV3p would be expected in the different mutants compared to wild type plants (Shinohara & Matsubayashi, 2015). In wild type plants, CLV3p-Atto488 was mainly found in the QC and in the stele with subcellular localization at the PM and in some intracellular vesicles indicating trafficking of the CLV3p (Fig. 38). In *bam1-3* mutants, the CLV3p-Atto488 accumulated in large vesicles of many cells in the outer cell layers of the root and could only be detected in the QC cells at the PM. The accumulation of CLV3-Atto488 in large vesicles in the outer layers of the root may indicate that the peptide is degraded to a large extent and is not functional (i.e. does not activate signaling cascades). However, *clv1-101* roots showed CLV3p-Atto488 signal only at the PM of cells through the entire root, with elevated signal in the QC and no small vesicles within the cells as it could be seen in wild type plants (Fig. 38). These observations suggest that the lack of the CLV1 receptor inhibits active trafficking of the CLV3p and thus CLV3p-Atto488 was only detected at the PMs but not in small vesicles within the cells. On the other hand, double mutants of *bam1-3;clv1-101* showed CLV3p-Atto488 signal in vesicles within the cells, indicating a high trafficking activity, even though the main two receptors for CLV3 are missing (Fig. 38). In summary, the CLV3p-Atto488 seems to be functional and can diffuse into the root tissue. It mainly accumulates in cells of the stele and the QC, reflecting the *BAM1* expression domain in the root (Breiden et al., 2021). The detection of CLV3p-Atto488 throughout the entire root cap in *clv1-101* mutants, where it only localized to the PM, indicates a major effect of CLV1 in CLV3 signaling. Future experiments can help to understand peptide signaling in detail. A functional peptide tagged to a fluorophore could show how far peptides diffuse in various tissues, where they activate signaling pathways, and which receptors are necessary for signaling (co-localization studies).

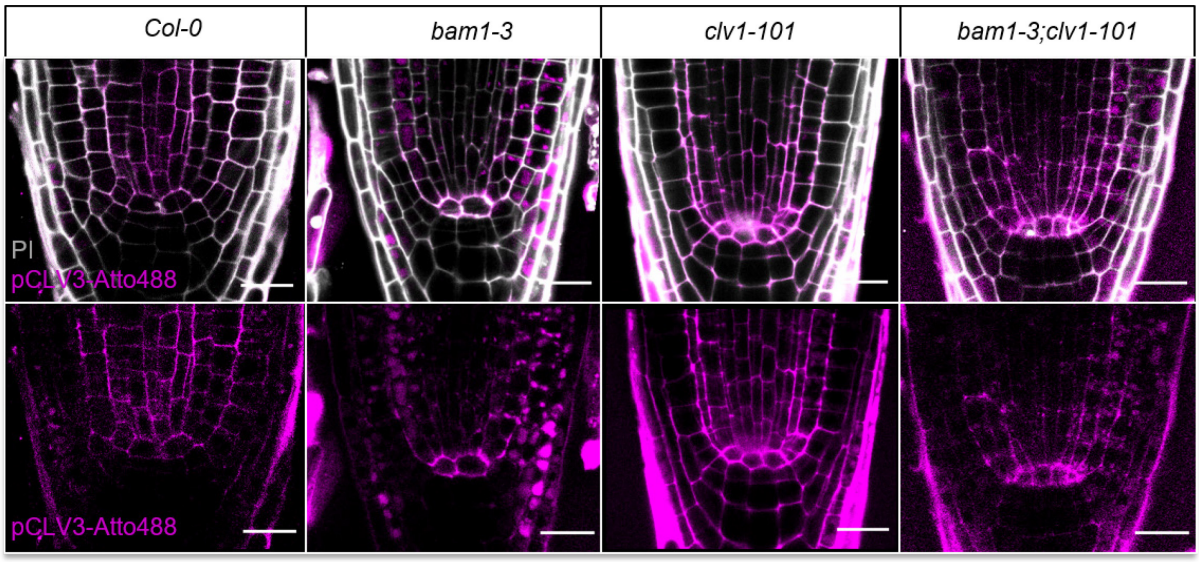

Fig. 38: Absence of different CLV receptors influence CLV3-Atto488 localization in the root of *A. thaliana*

Seedlings of wild type (*Col-0*), *bam1-3, clv1-101,* and *bam1-3;clv1-101* mutants were grown for 7 dag ½ MS media. Before imaging, roots were treated for 10 min with 1 µM of CLV3p-Atto488 and were afterwards washed twice with H_2O. In wild type plants, the signal of CLV3-Atto488 peptide was mainly found at the PM of the QC and stele and also in some vesicles within the cells (N=9). In *bam1-3* mutants, the CLV3p-Atto488 accumulated in big vesicles of many cells in the outer cell layers of the root and only a high signal at the PM could be detected in the QC (N=5). *clv1-101* roots showed CLV3p-Atto488 signal only at the PM of the cells through the entire root, with elevated signal in the QC (N=5). *bam1-3;clv1-101* double mutants showed high CLV3p-Atto488 signal in the QC at the PM and in many vesicles within the cells (N=6). Scale bar: 20 µm, PI = Propidium iodide

4.7 Auxin distribution in wild type and *cle40-2* mutants

The phytohormone auxin plays a crucial role in various processes during shoot development. For instance, auxin signals were reported to be involved in governing the phyllotactic patterning of the meristem and thus in the initiation of new organs, and in the differentiation of the vascular strand in cells of the L3 of the SAM (De Reuille et al., 2006; Reinhardt et al., 2003). In the root of *A. thaliana*, expression of the translational auxin efflux transporter *PIN-FORMED1* (PIN1) was found to be downregulated in *cle40-2* mutants compared to wild type plants, suggesting that CLE40 is able to regulate *PIN1* expression in the root (Wink, 2013). Also, the *DR5rev:GFP* reporter in *cle40-2* mutants showed a reduction in the GFP signal in the proximal root meristem compared to *Col-0* (Wink, 2013). In the shoot, *CLE40* shows a broad expression pattern in the IFM and since its role is still largely unknown, *CLE40* could also be involved in auxin regulation and thereby in cell differentiation and organ initiation. Therefore, two different auxin reporter

lines were introduced into *cle40-2* mutants and were compared to their wild type expression pattern.

4.7.1 Expression pattern of *DR5rev:GFP* does not change in *cle40-2* mutants

The DR5 reporter was cloned from a highly active synthetic auxin response element found in the soybean GH3 promoter and fused to a GFP to study auxin expression *in vivo* (Ulmasov et al., 1997). Wild type inflorescences expressing the reporter *DR5rev:GFP* show auxin expression in a patchy pattern in the IFM and in older primordia from P6 onwards. Nearly no *GFP* expression under the DR5 promoter is detected in the CZ but rather in areas where new organs develop (Fig. 39, A). Similarly, *cle40-2* mutants also show a patchy *DR5rev:GFP* expression pattern in the IFM (Fig. 39, B). However, in *cle40-2* mutants, *GFP* signal is also detected where new organs will form, but also in cells of the CZ (Fig. 39, B). The longitudinal sections through the IFM of a *Col-0* and a *cle40-2* plant show *GFP* expression exclusively in the L1 and mostly in the PZ. Some cells in the CZ also express *GFP* in both IFMs (Fig. 39, A', B'). In wild type and *cle40-2* mutants, no expression of *GFP* is detected in the longitudinal sections of primordia P1 to P5. GFP expression is detected in the L1 of the IFM next to emerging primordia in P1, P2, and P3 (white arrows). In primordia P4 and P5, cells next to the primordia do not express *GFP* in the IFM, confirming that auxin initiates organ development. Cells close to the stem cell zone express elevated GFP signal in the L1 of the IFM since auxin precedes organ development. At P6, *GFP* signal is detected in L1 cells at the adaxial domain in wild type (*Col-0*) and *cle40-2* mutants, marking the border between emerging sepals and FMs (Fig. 39). Overall, no differences in *GFP* expression pattern between wild type and *cle40-2* mutants were observed, indicating that auxin signaling is not impaired by the loss of CLE40.

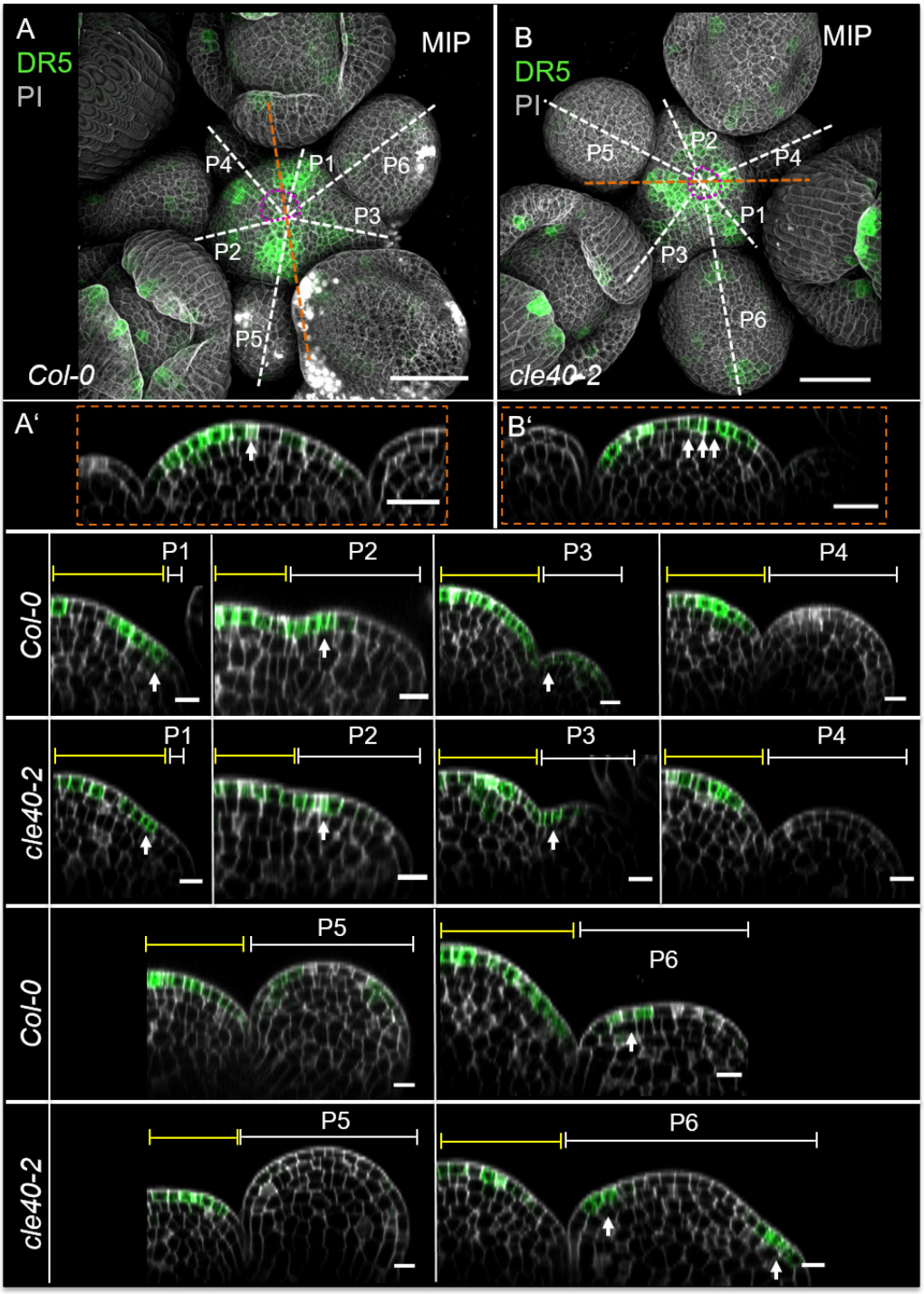

Fig. 39: No differences in *GFP* expression pattern under the control of DR5rev promoter in *Col-0* and *cle40-2* mutants are detectable

(A) MIP of a wild type inflorescence at 5 WAG carrying the transcriptional reporter *DR5rev:GFP*. *DR5* expression can be found in the IFM in a patchy pattern and in older organ primordia from P6 on (N=8). **(A')** The longitudinal section through the IFM shows *DR5rev:GFP* expression exclusively in the L1 in the PZ and only in a few cells in the CZ of the IFM (white arrow). **(B)** The MIP of a 5 weeks old *cle40-2* mutant inflorescence carrying the transcriptional

reporter *DR5rev:GFP* is shown. *GFP* expression can be found in the IFM and in older organ primordia from P6 on in a patchy pattern (N=9). **(B')** The longitudinal section through the *cle40-2* mutant IFM shows *GFP* expression exclusively in the L1 in nearly all cells but not in cells that are close to the P4 and P5. **(P1-P5)** In wild type and *cle40-2* mutants, no expression of *DR5-GFP* is detected in the longitudinal sections of primordia P1 to P5. *GFP* expression can be detected in the L1 of the IFM next to emerging primordia in P1, P2, and P3 (white arrows). In primordia P4 and P5, cells next to the primordia do not express DR5 in the IFM. However, cells close to the stem cell zone express elevated DR5 signal in the L1 of the IFM. **(P6)** At P6, the DR5 signal is detected in L1 cells at the adaxial domain in wild type (*Col-0*) and *cle40-2* mutants (white arrows).

Dashed white and orange lines indicate longitudinal sections. The pink dashed line marks the CZ. Scale bars: 50 µm (A, B), 20 µm (A', B'), 10 µm (P1 to P6), MIP = Maximum intensity projection, PI = Propidium iodide, L1 = layer 1 projection, P = Primordium

4.7.2 *PIN1* expression pattern in *cle40-2* mutants is similar to wild type plants

The *PIN1* gene in *A. thaliana* encodes for an auxin efflux carrier and thus accumulation of PIN1 in the PM serves as a read-out for auxin transport. *PIN1* is expressed through the entire inflorescence of wild type and *cle40-2* plants (Fig. 40, A, B). The longitudinal section through the IFM shows that *PIN1* expression is mainly found in the L1 but could also be detected in a few cells in the PZ in L2 and L3 of wild type plants (Fig. 40, A'). In *cle40-2* plants, *PIN1* localization was evenly distributed through the L1 layer, exclusively (Fig. 40, B'). In all primordia (P1 –P6) of wild type and in *cle40-2* mutants, *PIN1* expression was detected throughout the entire L1 (Fig. 40, P1-P6). In young primordia P1 and P2, faint *PIN1* expression could also be found in the L2 and L3 in cells where the new organs form. In older primordia, *PIN1* expression was observed in the adaxial domain where new sepals will emerge (Fig. 40, P6). In summary, *PIN1* expression is detected in the entire L1 and in cells where new organs (primordia or sepals) will emerge. No difference in the expression pattern of *PIN1* in wild type and *cle40-2* mutants could be discovered, indicating that auxin is not a downstream signal of the CLE40 pathway.

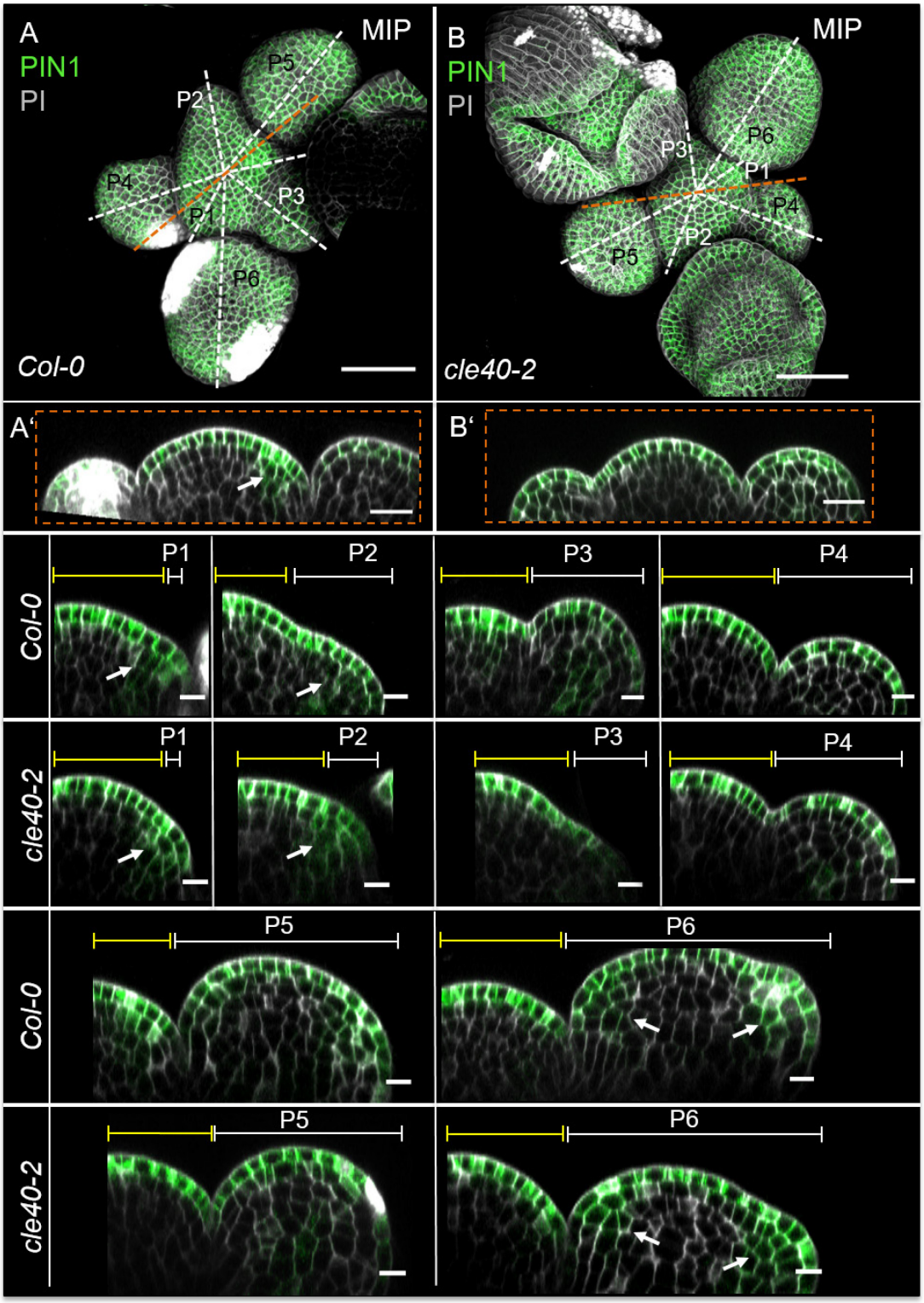

Fig. 40: The expression pattern of the translational *PIN1:PIN1-GFP* line does not alter between wild type and *cle40-2* mutants.

(A) MIP of a wild type inflorescence at 6 WAG carrying the translational reporter *PIN1:PIN1-GFP*. *PIN*1 expression is detected in the entire L1 of the IFM and all flower organs (N=6). **(A')**

The longitudinal section through the IFM of a *Col-0* plant shows *PIN1* expression mainly in the L1 and in a few cells of the L2 and L3 in the PZ of the IFM (right side). **(B)** The MIP of a 6 weeks old *cle40-2* mutant inflorescence carrying the translational reporter *PIN1:PIN1-GFP* is shown. *PIN1* expression can be detected in all cells of the L1 of the inflorescence except for old sepals. **(B')** The longitudinal section through the *cle40-2* mutant IFM shows *PIN1* expression exclusively in the L1 of the IFM and flower primordia (N=5). **(P1 to P6)** In all flower organs of wild type and *cle40-2* mutants, *PIN1* expression is detected through the entire L1. **(P1 and P2)** Besides the expression of *PIN1* in the L1, cells at the border to emerging primordia in layers L2 and L3 express *PIN1* in *cle40-2 2* mutants and *Col-0* plants (white arrows). **(P6)** From P6 on *PIN1* expression was also detected in the adaxial domain of the flower primordia, where new sepals will emerge in wild type and *cle40-2* mutant plants.

Dashed white and orange lines indicate longitudinal sections. Scale bars: 50 µm (A, B), 20 µm (A', B'), 10 µm (P1 to P6), MIP = Maximum intensity projection, PI = Propidium iodide, L1 = layer 1 projection, P = Primordium

5. Discussion

5.1 CLV3 and CLE40 antagonistically control meristem size

The *CLV3* gene encodes for a small peptide, which is expressed in the CZ of the IFM regulating stem cell maintenance. In this study, we analyzed the expression pattern and the function of its closest homologue *CLE40* in the shoot. *clv3-9* mutants show an increased and fasciated IFM compared to wild type plants (Brand et al., 2002; Clark et al., 1995). Our analysis confirms these results, showing a fivefold increase in the area of secondary *clv3-9* IFMs compared to wild type (*Col-0*) meristems. In contrast, we found that *cle40* meristems show smaller IFM areas in comparison to wild type plants. *cle40-2* and three independent *CLE40*-CRISPR alleles (*cle40-cr1, cle40-cr2, cle40-cr3*) IFMs showed a decrease in area size compared to wild type and *clv3-9* mutant plants (Fig. 7; Fig. 8). Using a *CLE40* promoter reporter line we could show that *CLE40* expression is detected in a broad pattern through the inflorescence. *CLE40* expression is found within the periphery of the meristem, in the center of flower primordia, and mature sepals, but not in the OC, CZ, and young flower organs until P5 (Fig. 9, A-C, P1-P6). These findings demonstrate that CLE40 plays an important role during IFM development. However, *CLE40* expression was not only found in a broad expression pattern within the inflorescence, but also in other parts of the plant, such as leaves and roots, which leads to the assumption that *CLE40* performs numerous tasks in plant signaling (Stahl et al., 2009; Wink, 2013). In this study, we focused on the role of *CLE40* within the IFM.

CLV3 and CLE40 are highly similar in their processed peptide structure, as they only differ in 4 aa and share 64% sequence similarity (Fiers et al., 2005). Previous studies showed that expression of *CLE40* under the control of the *CLV3* promoter can rescue *clv3-2* mutants regarding IFM size, but that overexpression of *CLE40* (35S:*CLE40*) causes a developmental arrest of the shoot meristems (Hobe et al., 2003). These results indicate that meristem development is maintained by i) the precise spatio-temporal availability of a peptide and ii) is highly sensitive towards the dosage of an expressing peptide. Using a double reporter line of *CLE40:Venus-H2B*;*CLV3:NLS-3xmCherry*, we depicted a precise complementary pattern in the IFM (Fig. 9, D-F''). While *CLV3* is specifically expressed in the stem cells at the tip of the meristem, *CLE40* expression is found in the periphery. These results suggest that *CLV3*, being expressed in only a small domain at the tip of the meristem, is required in high dosage to maintain stem cell fate, while *CLE40*, being expressed in various cells in the IFM, is only expressed in low dosage to regulate meristem development.

Hence, our results show two peptides regulating meristem size in an antagonistic manner. CLV3 in the CZ has a restricting effect on meristem size while *CLE40* from the PZ shows a promoting effect on meristem size and thus the localization rather than the structure determines the function of CLE peptides.

5.1.2 *CLE40* activity is repressed by WUS and in turn promotes *WUS* expression

Signals from the CZ and the PZ are transported to the center of the meristem. Here, TFs like WUS control gene expression to maintain the stem cell population (Lohmann et al., 2001; Schoof et al., 2000). Hence, *WUS* expression can be detected in the L3 in the center of the IFM (Fig. 11; SupplFig. 1), while WUS protein moves through plasmodesmata to the CZ. Interestingly, *CLE40* expression is not detectable in these cells. *CLE40* expression is not found in either the OC, the CZ, or in early flower primordia, P1 to P4 (Fig. 9). In *clv3-9* mutants, the IFM has an expanded dome-shaped structure along the apical-basal axis and shows an enlarged stem cell domain as well as an extended expression domain of the *WUS* promoter (Fig. 10; SupplFig. 1) and *WUS* mRNA (Brand et al., 2000; Busch et al., 2010). However, no *CLE40* can be detected in the tip of the extended stem cell domain of *clv3-9* mutants (Fig. 10, B'; SupplFig. 1). *CLE40* expression is only found at the flanks of the IFM, suggesting a repressing effect of WUS on *CLE40* expression (Fig. 10, B, B'; SupplFig. 1). In a previous study, Su et al. showed that WUS and STM in the stem cell domain maintain *CLV3* expression and stem cell identity (Su et al., 2020). Here, we suggest that WUS represses *CLE40* activity in the stem cells and the OC to maintain meristem homeostasis and size. To confirm our hypothesis that *CLE40* is negatively regulated by WUS, we expressed *WUS* under the control of the *CLV3* promoter to increase the *WUS*-expressing cells within the meristem. Since overexpression of *WUS* leads to a termination of the plant after seedling stage, we analyzed *CLE40* expression in the vegetative meristem and found no *CLE40* expression within the meristem area of *CLV3:WUS//Col-0* plants, while in a wild type plant *CLE40* expression was detected at the flanks of the vegetative meristem (Fig. 10, E-F'). In a complementary experiment, we then crossed the *CLE40* reporter into *wus-7* mutants and could detect an expansion of the *CLE40* domain in the meristem area. *CLE40* was detected in the entire meristem of *wus-7* mutants (Fig. 10, G-H', S4). These results demonstrate a direct or indirect repression of WUS on *CLE40* promoter activity.

To answer the question of whether *CLE40* regulates *WUS* expression in a promoting manner, we expressed a *WUS:NLS-GFP* construct in *cle40-2* mutants (Fig. 11, F). In all *cle40-2* IFMs, we found a reduced number of *WUS*-expressing cells in the longitudinal section of the meristem compared to wild type plants, confirming a promoting effect of *CLE40* on WUS.

5.1.3 CLE40 signals through the CLV-family receptors BAM1 and CLV1

CLV1 is the main receptor for CLV3 signaling and both proteins play a crucial role in maintaining stem cell homeostasis in the meristem (Clark et al., 1997; Ogawa et al., 2008). Also *BAM1* and its related (receptor-encoding) genes *BAM2* and *BAM3* are expressed in the IFM and play an important role in regulating meristem development (DeYoung et al., 2006; DeYoung & Clark, 2008). Our mutant studies revealed that double mutants of *clv1-101;cle40-2* and *bam1-3;cle40-2* did not show any significant differences compared to the single mutants (*clv1-101* and *bam1-3*) in terms of meristem size, carpel number, and leaf length (Fig. 31; Fig. 30). These results indicate that CLE40 acts in the same pathway as CLV1 and BAM1. Analyzing their expression patterns in the IFM in detail showed that *CLV1* and *CLE40* overlap in a few cells in the L1 and L2 close to emerging primordia and that *BAM1* and *CLE40* expression overlap in most cells of the meristem (Fig. 12; Fig. 15). Accordingly, BAM1 might be the main receptor for CLE40 signaling. However, it is also likely that CLV1 can bind CLE40 since CLE40 under the control of the *CLV3* promoter is able to compensate for the *clv3-2* mutant phenotype (Hobe et al., 2003). Thus, it is possible that the receptors *CLV1* and *BAM1* can act in a promiscuous manner, being able to bind both peptides (CLV3 and CLE40).

In *bam1-3* mutants, the putative main receptor for CLE40 is missing, and thus CLE40 signals through CLV1, which leads to a smaller meristem area (Fig. 13). In *clv1* mutants, *BAM1* is able to partly compensate for *CLV1* (Nimchuk, 2017) and thus CLV3 can now signal through *BAM1,* restricting WUS and leading to an increase in meristem size (Fig. 19). In *clv1* mutants, *BAM1* is no longer expressed in the PZ of meristems, and thus CLE40 signaling through BAM1 might be impaired (Fig. 16). This could also explain why we did not observe a change in meristem area size between *clv1-101* and c*lv1-101;cle40-2* mutants, since CLE40 cannot signal through BAM1 in the PZ of the meristem. When both receptors, *CLV1* and *BAM1*, are absent, CLE40 and CLV3 are not able to signal at all, which leads to an over-proliferation of stem cells and a fasciated meristem comparable in its size *to clv3-9* mutants (Fig. 31). Consequently, it is probably not only the specific interaction between one peptide-receptor pair which defines the

downstream signaling but also the localization and the concentration of the incoming peptide signal. Hence we conclude that CLV1 and BAM1 are promiscuous receptors, which signal in a concentration-depended manner.

5.1.4 The RLK ACR4 is not involved in stem cell homeostasis in the shoot meristem

In the root, ACR4 was shown to control cell fate in the columella lineage in the root apex, where it regulates QC activity and position. It was suggested that ACR4 is triggered by CLE40 signaling (Berckmans et al., 2019; De Smet et al., 2009; Stahl et al., 2009). For the shoot, no specific role for ACR4 was reported and thus we asked if ACR4 is involved in regulating stem cell fate in the shoot via CLE40 signaling. We found that the loss of ACR4 leads to a reduced meristem size and that *ACR4* is exclusively expressed in the L1 of the meristem (Fig. 24; Fig. 25). Interestingly, *ACR4* expression is reduced in the CZ of the L1, but elevated in the PZ of the epidermis similar to that of *CLE40* expression (Fig. 25). *CLE40* is not expressed in the CZ but shows elevated expression in the PZ and like *acr4* mutants, *cle40* mutants show a reduction in meristem size (Fig. 8; Fig. 9). However, no effect of *ACR4* expression was detected in the mutant backgrounds of the CLV pathway. *ACR4* expression was not altered in *clv1-101, clv3-9, cle40-2* or *bam1-3* mutants (Fig. 26). Elevated *ACR4* expression was found at the flanks of the meristem and less in the CZ. Besides this, a lack of *ACR4* expression in an *acr4-8* mutant background did not affect *WUS* expression (Fig. 28). Indeed, *acr4-8* mutants expressed *WUS* in a similar number of cells in the OC compared to wild type plants (Fig. 28; SupplFig. 3). Together these results indicate that ACR4 is not directly involved in CLV signaling since no effect on WUS could be observed and also no change in the spatial distribution of *ACR4* in *clv* mutant backgrounds. Interestingly, double mutants of *acr4-8;clv1-101* showed a similar meristem size as wild type plants and smaller meristems compared to *clv1-101* plants (Fig. 31). These results confirm a promoting effect of ACR4 on meristem size and demonstrate that ACR4 and CLV1 do not act in the same pathway since no additive effect was observed in the double mutant *acr4-8;clv1-101* (Fig. 31). Previous studies reported that ACR4 is required for normal cell organization during ovule integument development and the formation of sepal margins as well as in the formation of giant cells in the sepal endodermis(Gifford et al., 2003; Roeder et al., 2012). Taking all results into account, we show that ACR4 is a positive regulator of meristem size, but does not act via the CLV pathways (CLV3-CLV1-WUS or CLE40-BAM1-WUS). While ACR4 does not directly influence WUS activity in the OC, it might affect meristem size by regulating cell proliferation and organization in the epidermis of the shoot meristem.

5.1.5 CLV-family receptors and cognate peptides regulate the meristem shape

In the IFM, stem cells and the underlying organizing cells maintain a fine balance between stem cell maintenance and cell differentiation to establish the correct architecture of the inflorescence. The meristem in the middle of the inflorescence is surrounded by developing flower primordia in a helicoidal pattern around the main axis (Bowman et al., 1989). In wild type plants, the longitudinal section of the meristem from primordium P4 to P5 shows a shaped hemisphere (Fig. 32, A A'), while the longitudinal section of a *cle40-2* mutant shows a smaller and flatter meristem compared to *Col-0* plants (Fig. 32, B, B'). In contrast, the loss of the CLV3 peptide leads to an expansion of the meristem along the apical-basal axis in the early stages of the development, resulting in a dome-shaped meristem (Fig. 32, C, C'). While *CLE40* expression is found in the PZ and the flanks of the meristem, *CLV3* expression is only located in the stem cells at the tip of the meristem. Hence, if cells at the tip of the meristem lose their cell fate (*clv3-9*), expansion takes place along the apical-basal axis, whereas a peptide deficiency in the periphery of the meristem (*cle40-2*) leads to a decrease along the apical-basal axis and thus to flatter meristems. These results support the antagonistic effect of the two closely related peptides on meristem size and shape. Similar to *clv3-9* meristems, the double receptor mutant *bam1-3;clv1-101* undergoes over-proliferation of stem cells, due to the loss of CLV3 signaling. However, the meristem shape of *bam1-3;clv1-101* mutants expand during early development in the radial direction of the meristem. While *clv3-9* mutants have the tallest meristem with ~100 µm, *bam1-3;clv1-101* mutants depict the widest meristem with 115 µm. Hence, losing the signal from the tip and the periphery of the meristem leads to an expansion in both, the apical-basal direction and the lateral direction (*bam1-3;clv1-101*), while the loss of a signal from the stem cells leads to a prioritized expansion along the apical-basal axis (*clv3-9*). Only in later stages of development does the expansion of the meristem (*clv3-9* and *bam1-3;clv1-101*) take place in all directions, since cell fate and meristem organization are then totally lost. A similar effect was observed for the EPFL/Erf system. *EPFL* peptides are expressed in the periphery of the IFM and triple mutants of their corresponding receptors ER, ERL1, and ERL2 showed an expansion along the lateral axis of the meristem compared to wild type plants (Zhang et al., 2021). However, here we demonstrate that a signal from the stem cell domain, the CLV3 peptide, has a restricting effect on meristem size, and an antagonistic signal from the periphery of the meristem, CLE40, has a promoting effect on meristem size. We also propose that the putative CLE40 receptor BAM1 is regulating the shape of the meristem along its lateral axis, while the CLV3-CLV1 signaling cascade is responsible for the shape of the meristem along its apical-basal axis.

5.1.6 Schematic models of two antagonistic pathways acting in the IFMs of *clv* mutants

Our results showed that the complementary expression patterns of *CLE40* in the PZ and *CLV3* in the stem cells of the meristem (Fig. 9) lead i) to an opposite meristem phenotype regarding its size and shape (Fig. 31; Fig. 32) and ii) to a decrease of *WUS* expressing cells within the OC in *cle40-2* mutants and an increase in *clv3-9* mutants (Fig. 11; SupplFig. 1). While CLV3 signals through its main receptor CLV1, the peptide CLE40 signals in an autocrine manner through its receptor BAM1. Thus, signals from the stem cell domain (CLV3-CLV1) promote *WUS* expression, while the activation of a signal cascade from the periphery of the meristem (CLE40-BAM1) restricts *WUS* activity (Fig. 11; Fig. 18; Fig. 23; SupplFig. 1).

Hence, our model shows two antagonistic signaling pathways that control meristem growth and development. In wild type plants, CLE40 signals from the periphery through its main receptor BAM1 promoting *WUS* activity in the OC and WUS in a negative feedback loop represses *CLE40* expression in the stem cell domain and the OC directly or indirectly (Fig. 41). Furthermore, our results show that *BAM1* and *CLE40* are highly overlapping in the periphery of the meristem, while both expression patterns do not overlap with the expression of *WUS* (Fig. 15). Thus, we postulate that i) CLE40 acts in an autocrine manner and ii) CLE40-BAM1 signaling activates an unknown diffusible factor X, which can move either symplastically or apoplastically to the OC to promote *WUS* activity. In the center of the meristem, CLV3 signals through CLV1 to repress *WUS* activity in the OC, while WUS protein moves through plasmodesmata to the tip of the meristem to promote stem cell identity together with *CLV3* expression. Hence, our model presents two intertwined pathways that serve to adjust *WUS* activity in the OC and incorporate information on the actual size of the stem cell domain, via CLV3-CLV1 and the growth requirements from the PZ via CLE40-BAM1.

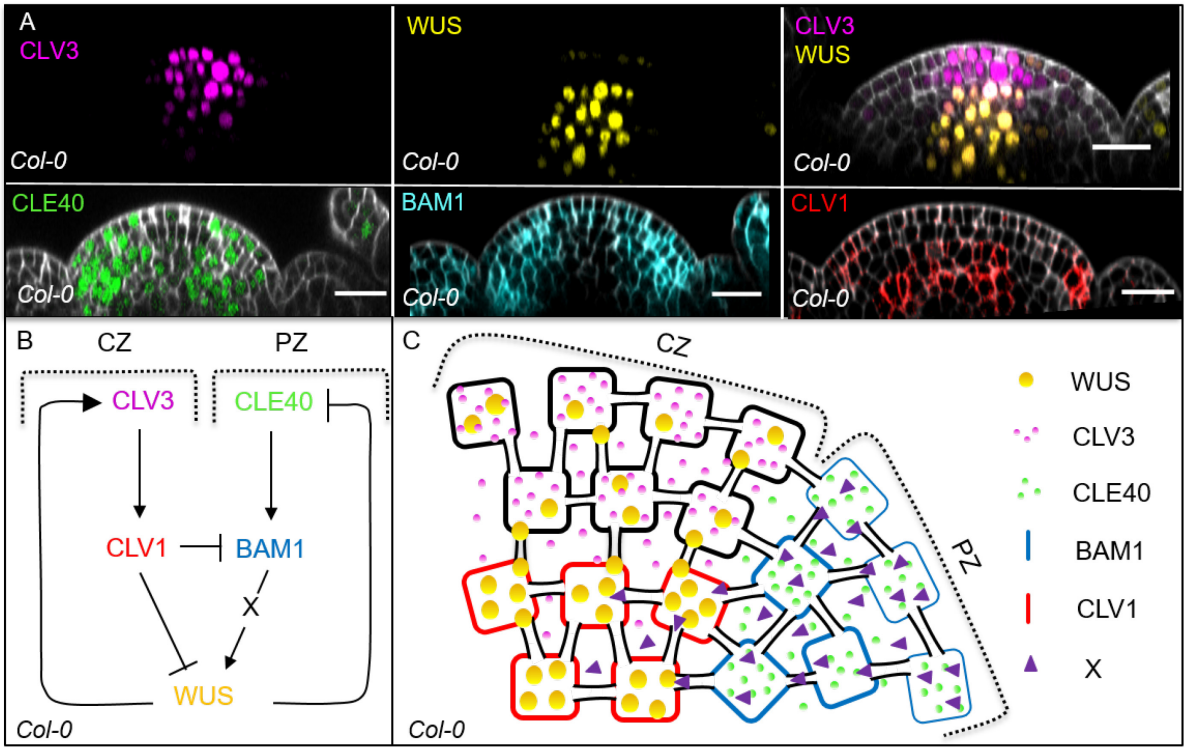

Fig. 41: Schematic model of the intertwined signaling pathways in a wild type plant

(A) The expression patterns of *CLV3, WUS, CLE40, BAM1,* and *CLV1* are shown in a wild type background. **(B and C)** Schematic representation of two intertwined negative feedback loops in the IFM of *Arabidopsis thaliana*. CLV3 in the CZ binds to the LRR receptor CLV1 activating a downstream signaling cascade that leads to the repression of the TF WUS. In a negative feedback loop WUS protein moves through the plasmodesmata to activate *CLV3* gene expression in the stem cells. In the PZ of the IFM, a second negative feedback loop controls meristem growth by the dodecapeptide CLE40 and its putative LRR receptor BAM1. CLE40 binds to BAM1 leading to the activation of a downstream signal "X" that promotes *WUS* activity. WUS protein, in turn, represses the expression of the *CLE40* gene. Scale bars: 20 µm (A), CZ =Central Zone, PZ = Peripheral Zone

Our new model now gives us a better understanding of the *clv* mutant phenotypes that were observed previously and in this study. For instance, *clv1-101* mutants show an increase in meristem size and an additional number of carpels, but their phenotype is not as severe as *clv3-9* mutants, even though the main receptor for CLV3 is missing in *clv1* mutants (Fig. 29). Using our new knowledge we could show that in *clv1* mutants, a shift of *BAM1* expression to the center of the meristem and an elevated expression in the L1 is detected (Fig. 42). Expression of *BAM1* in the L3 is now able to partly substitute for CLV1 signaling and thus BAM1 can perceive CLV3 to repress *WUS* activity. The elevated expression of *BAM1* in the L1 overlaps in a few cells with *CLE40* expression in the periphery and leads to weak activation

of the downstream signal “X” that promotes *WUS* activity. Since WUS is only partly repressed by the *CLV3-BAM1* signaling pathway, the activity of *WUS* is increased compared to wild type plants and hence leads to an over-proliferation of stem cells and thereby to an increase in meristem size. The increase in WUS activity leads to an increase in CLV3 activity and thus to an expanded expression domain of *CLV3* and *WUS* in *clv1-101* mutants. *WUS* expression is not only found in an extended domain in the meristem center but also in a patchy pattern of the L1, where it is highly overlapping with *BAM1* expression (Fig. 42). Notably, *WUS* expression is excluded from the L2, indicating a very specific role for the L2 in development. Likely, the L2 is not involved in the regulation of stem cell homeostasis during development but rather is involved in other developmental processes, such as the formation of gametophytes and mesophyll cells (Torregrosa et al., 2010).

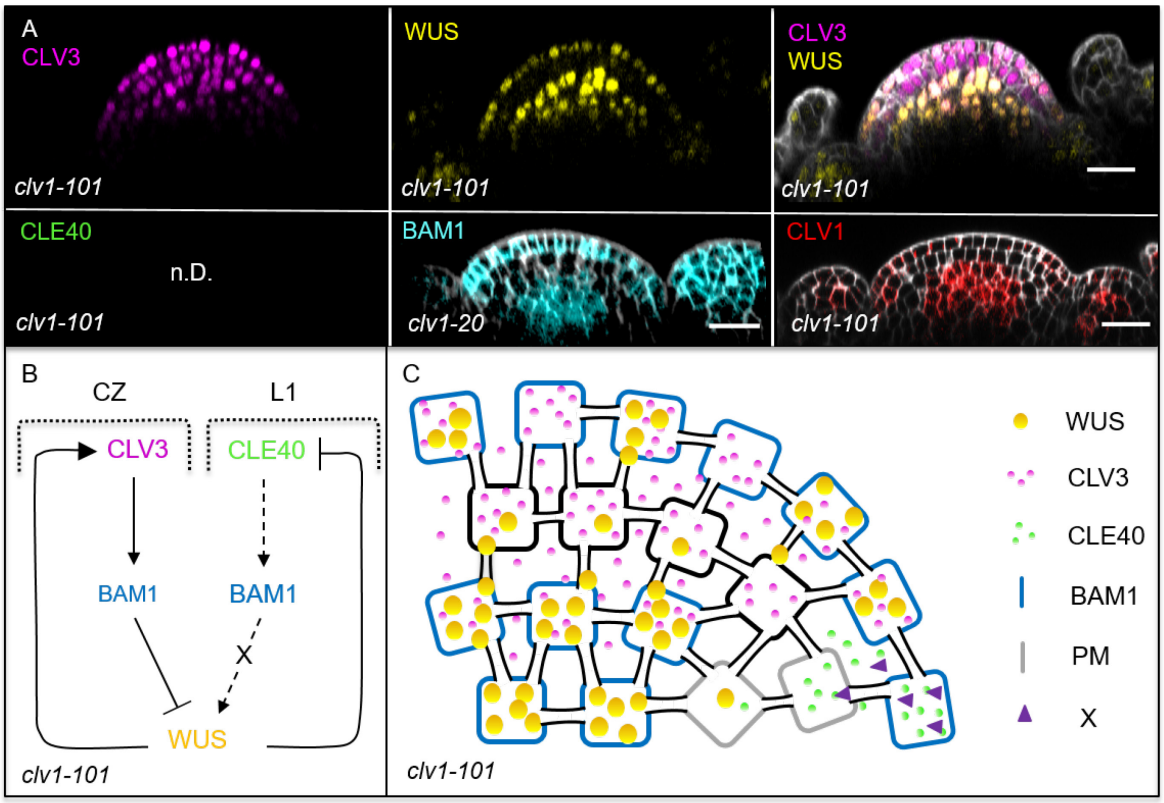

Fig. 42: Schematic model of the intertwined signaling pathways in a *clv1-101* mutant background

(A) Optical sections of through IFMs show the expression patterns of *CLV3* (N=8), *WUS* (N=8), *BAM1* (N=9), and *CLV1* (N=5) in a *clv1* mutant. Compared to wild type plants, the expression of *CLV3* and *WUS* is expanded and *WUS* is found in a patchy pattern in the L1. *BAM1* expression shifts to the CZ and is found in an elevated expression in the L1. **(B and C)** Schematic representation of two intertwined negative feedback loops in the IFM of a *clv1-101* mutant. The lack of CLV1 leads to a shift of *BAM1* expression to the OC and an elevated

expression in the L1. In the L3, BAM1 can partly substitute for CLV1 and thus CLV3 can act via BAM1 to repress WUS activity. The elevated expression of *BAM1* in the L1 overlaps in very few cells with *CLE40* expression in the periphery and leads to weak activation of the downstream signal “X” that promotes WUS activity. Since *WUS* expression is only partly repressed by the *CLV3-BAM1* signaling pathway, the WUS domain is extended and leads to an increase in stem cells (expanded *CLV3* expression). *WUS* is now also detected in the L1 of the meristem, together with *BAM1* expression.

Scale bars: 20µm (A), CZ =central zone, L1 =layer 1

In contrast to *clv1-101* mutants, *clv3-9* mutants exhibit extremely fasciated meristems and, multiple additional organs, like numerous carpels per silique (Fig. 29). Since no CLV3 peptide is available in *clv3-9* mutants, the downstream signaling of CLV1 is not activated, and thus, the expression of *CLV1* shifts from the OC to the tip of the CZ (Fig. 43). Through the shift of *CLV1* expression, *BAM1* is no longer detected at the tip of the meristem since it is repressed by *CLV1* (Nimchuk, 2017). *BAM1* expression shifts to the inner layers of the PZ, while *CLE40* expression is now only found in the outer layers of the PZ due to the expanded *WUS* domain in the center of the meristem (Fig. 43). Thus, only very few cells express both, *BAM1* and *CLE40,* and hence, barely any WUS promoting factor “X” is produced. Due to the lack of CLV3 peptide, the CLV1 downstream signaling cascade does not restrict WUS to the OC anymore which leads to an expansion of the *WUS* domain and thereby to an over activation of *CLV3* activity and thus an over-proliferation of stem cells.

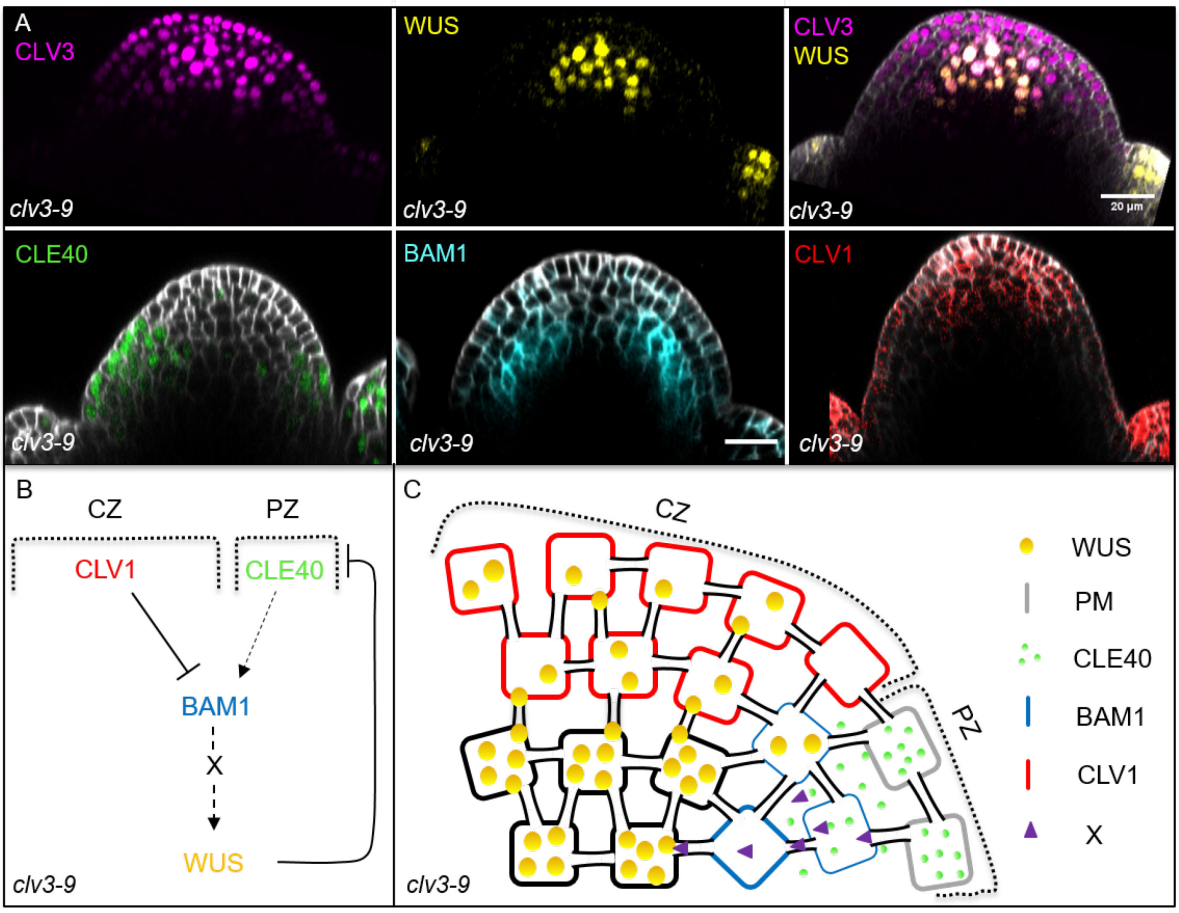

Fig. 43: Schematic model of the intertwined signaling pathways in a clv3-9 mutant background

(A) Optical sections of through IFMs show the expression patterns of *CLV3* (N=5), *WUS* (N=5), *CLE40* (N=6), *BAM1* (N=5), and *CLV1* (N=5) in a *clv3-9* mutant. Compared to wild type plants, the meristem is highly increased in its size along the apical-basal axis and the expression of *CLV3* and *WUS* is expanded in the CZ and OC. *CLE40* expression is limited to the outer layers of the meristems´ periphery and excluded from the CZ and OC, while *BAM1* expression shifts towards the inner layers of the PZ. *CLV1* expression is found at the tip and not in the center of the fasciated meristem. **(B and C)** Schematic representation of two intertwined negative feedback loops in the IFM of a *clv3-9* mutant. The lack of CLV3 leads to a fasciated meristem with an increased number of stem cells and thus an expanded CZ and a decreased PZ. Since no CLV3 peptide is available, CLV1 is not activated, and expression of *CLV1* shifts from the OC to the tip of the CZ, where it represses *BAM1* expression. *BAM1* is expressed in the inner layers of the PZ, while *CLE40* expression is found in the outer layers of the PZ since it is repressed by the expanded WUS domain in the center of the meristem. Thus only very few cells express both, *BAM1* and *CLE40,* and hence, nearly no WUS promoting factor “X” is produced and the CLV3-CLV1 signaling pathway does not repress WUS activity.

Scale bars: 20µm (A), CZ = central zone, PZ = peripheral zone

While *clv1-101* and *clv3-9* mutants lead to an increase in meristem size and organ production, *cle40-2* mutants have smaller and flatter meristems. The expression of the CLV3 domain in *cle40-2* mutants does not show an obvious difference compared to wild type plants, while the number of cells expressing *WUS* is decreased compared to *Col-0* (Fig. 44). *WUS* expressing cells are detected in the center of the OC, but were found in a narrow domain (Fig. 44, A). Interestingly, *CLV1* expression seems to be downregulated in *cle40-2* mutants, while *BAM1* appears to be expressed in a broader pattern (Fig. 44, A). These observations fit the assumption that CLV1 represses *BAM1*. Thus, more *BAM1* expression is found in the CZ where *CLV3* is expressed, and hence CLV3 can signal via BAM1 and CLV1 from the center of the meristem to repress WUS activity in the OC. Since CLE40 is not present, the promoting signaling pathway from the PZ on WUS activity is lacking and thus *WUS* expression is confined to the center of the OC (Fig. 44, B, C).

Similar to *cle40-2* plants, *bam1-3* mutants display a smaller and flatter meristem (Fig. 13; Fig. 45). In contrast to *cle40-2* mutants, where *CLV1* expression appeared to be decreased, *CLV1* expression seems to be increased in *bam1-3* mutants, indicating that BAM1 can repress CLV1 activity (Fig. 45). However, with the absence of BAM1 in the periphery of the meristem, the diffusible factor “X”, that promotes WUS activity, is not produced and thus *WUS* is only expressed in the center of the OC in fewer cells compared to *Col-0* plants (Fig. 18; Fig. 45). *CLV3* expression is found in a similar pattern in *bam1-3* mutants and in wild type plants and it can signal, as in *Col-0* plants, through its main receptor CLV1 to repress *WUS* activity in the OC (Fig. 45). BAM1 and CLV1 share a high structural similarity and thus CLE40 might also be able to signal through CLV1 in the absence of BAM1 in order to repress the TF WUS in the OC (Fig. 45).

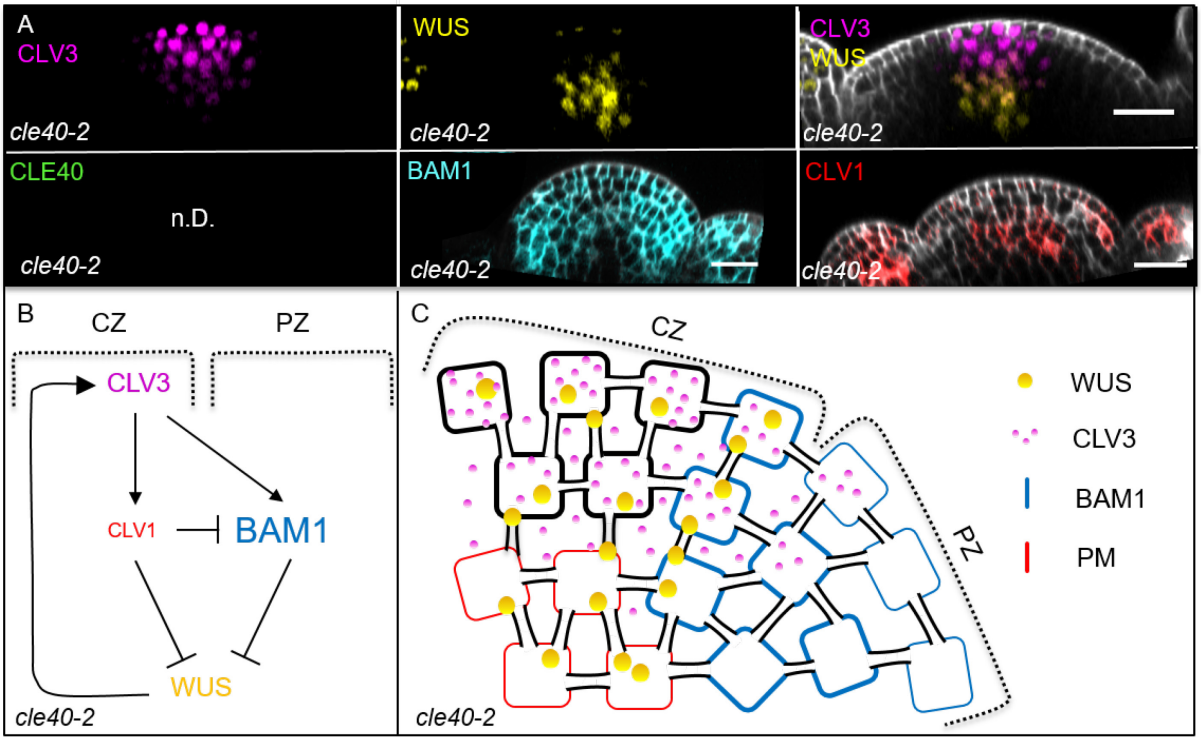

Fig. 44: Schematic model of the intertwined signaling pathways in a *cle40-2* mutant background

(A) Optical sections through IFMs show the expression patterns of *CLV3* (N=9), *WUS* (N=9), *BAM1* (N=7), and *CLV1* (N=9) in a *cle40-2* mutant. *CLV3* expression is similar to wild type plants, in the CZ. *WUS* expression is found in the OC, but in fewer cells than in *Col-0* plants. *BAM1* expression appears to be broader compared to wild type plants, while *CLV1* expression seems to be decreased in its intensity. **(B and C)** Schematic representation of two intertwined negative feedback loops in the IFM of a *cle40-2* mutant. In *cle40-2* mutants, *CLV1* expression seems to be decreased and leads to a broader *BAM1* expression compared to wild type plants. Since expression of *BAM1* is now also found in the CZ, CLV3 is able to bind CLV1 and BAM1 in the OC and CZ (respectively), leading to a double repression signaling cascade from the center of the meristem. In the PZ, the downstream signaling cascade of BAM1 is not activated through CLE40 and thus the WUS promoting factor "X" is not being expressed and the WUS domain is confined to the center of the OC.

Scale bars: 20µm (A), CZ = central zone, PZ = peripheral zone

In summary, the expression pattern of the key players in mutant backgrounds together with our model, allows us to better understand stem cell regulation in the shoot meristem. We postulate a second negative feedback loop that promotes *WUS* activity from the periphery of the meristem, while WUS feeds back to negatively regulate *CLE40* expression.

In addition, our results suggest a tight cross-regulation between CLV1 and BAM1. It was shown that BAM1 can partly substitute for CLV1 and shifts its expression pattern in a *clv1* mutant,

while at the same time expression of *CLV1* represses *BAM1* activity. Our expression analyses suggest that *BAM1* is also able to repress *CLV1* expression, at least partially.

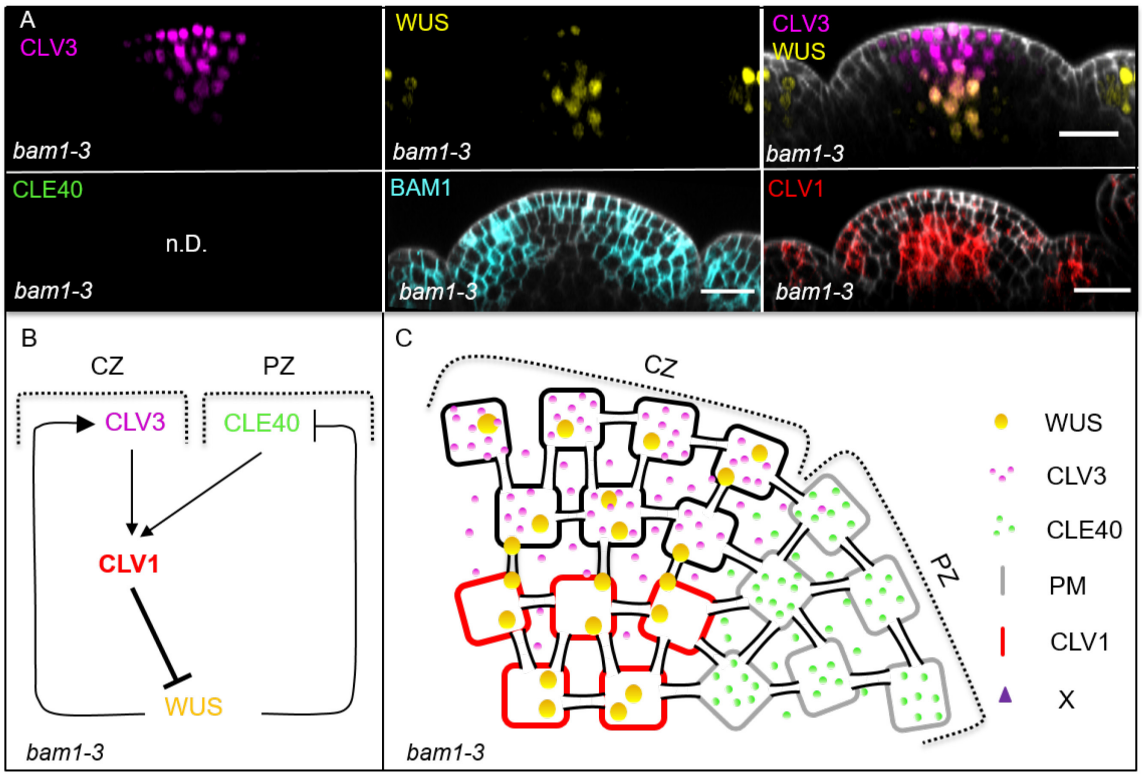

Fig. 45: Schematic model of the intertwined signaling pathways in a *bam1-3* mutant background

(A) Optical sections of through IFMs show the expression patterns of *CLV3* (N=9), *WUS* (N=9), *BAM1* (N=15), and *CLV1* (N=7) in a *bam1-3* mutant. *CLV3* expression is similar to wild type plants, at the tip of the meristem in a cone-shaped domain. *WUS* expression is found in the OC, but in fewer cells than in *Col-0* plants. *CLV1* expression seems to increase in its intensity compared to wild type plants. **(B and C)** Schematic representation of two intertwined negative feedback loops in the IFM of a *bam1-3* mutant. In *bam1-3* mutants, *CLV1* expression appears to be increased. Since BAM1 is lacking in the periphery, the *WUS* promoting diffusion factor "X" is not being produced and thus *WUS* expression is decreased and confined to the center of the OC, similar to *cle40-2* plants. With the loss of BAM1, the main receptor for CLE40 is missing, and thus CLE40 peptide now might signal through CLV1 leading to a stronger repression of *WUS* from the center of the meristem.

Scale bars: 20µm (A), CZ = central zone, PZ = peripheral zone

5.1.7 Cytokinin but not auxin might be the downstream target of CLE40 in the IFM

In the proximal root meristem of *Arabidopsis*, auxin plays an important role in regulating and maintaining stem cell homeostasis (Sauer et al., 2006; Scarpella et al., 2006). The auxin efflux carriers PIN1, PIN3, and PIN7 transport auxin through the root, which results in an auxin maximum in the QC of the root (Billou et al., 2005; Petersson et al., 2009). One of the main functions of CLE40 in the root is the positioning of the QC at the root tip. In line with this, CLE40 is also involved in regulating the auxin distribution in the proximal root meristem (Wink, 2013). In the shoot, local accumulations of auxin in the flanks of the meristem trigger organ initiation that leads to the radial pattern of flower primordia (Heisler et al., 2005). Here, we could demonstrate that elevated *CLE40* expression is found in the flanks of the meristem and at borders to emerging primordia. We, therefore, asked if CLE40 also regulates auxin distribution in the shoot of the meristem. Therefore, we analyzed the auxin marker lines *DR5rev:GFP* and *PIN1:PIN1-GFP* in wild type and *cle40-2* mutant backgrounds. Our results showed no differences in the spatial expression pattern of both reporter lines between wild type and *cle40-2* mutants (Fig. 39; Fig. 40). We concluded that auxin is not regulated by CLE40 in the shoot.

Like auxin, the phytohormone CK is involved in many developmental processes in plants. While CK leads to the differentiation of the proximal meristem of the root, it promotes the proliferation of meristematic cells in the shoot, thus inhibiting the effect on cell division activity (Dello Ioio et al., 2007). It was shown that the ARABIDOPSIS RESPONSE REGULATOR genes (ARR5, ARR6, ARR7, and ARR15), which are negative regulators of CK signaling, are directly repressed by *WUS* (Leibfried et al., 2005). ARR1 on the other hand has been reported to be activated by CK signaling and to directly bind to the *WUS* promoter region to start *de novo* activation of *WUS* expression in leaf axils and probably also during FM formation (J. Wang et al., 2017) (Fig. 46). It was suggested that CLE40 might be a negative regulator of CK signaling to promote columella stem cell fate, since the expression of ARR5 was upregulated in the root *of cle40-2* mutants, suggesting that ARR5 is a downstream target of CLE40 signaling (Wink, 2013). Developmental regulation in the shoot and root meristem is often regulated oppositely. Thus, CLE40 might repress CK signaling in the root, while it has a promoting effect on CK expression in the shoot. Here, we suggest that the diffusible factor X, which was postulated in our model as a potential downstream target of the CLE40-BAM1 pathway (Fig. 41), might be CK (Fig. 46). Notably, the TF STM was proposed to promote CK biosynthesis in the leaf axil (J. Wang et al., 2017).

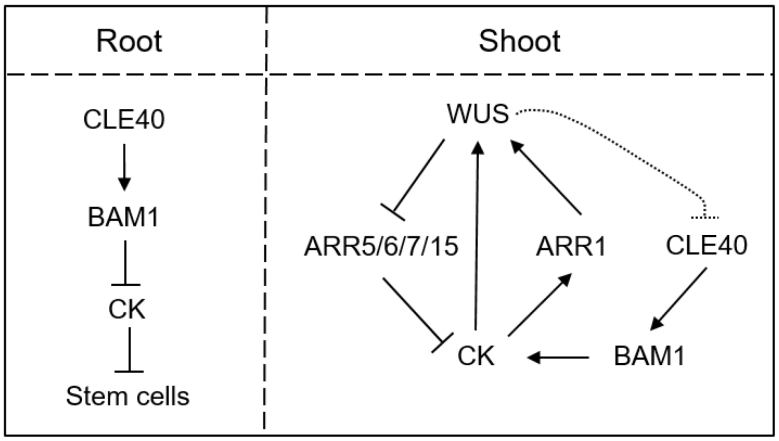

Fig. 46: Schematic model of root and shoot meristem regulation by CLE40 signaling via its potential downstream target CK.

(left) In the root, CLE40 acts via BAM1 to repress CK signaling, which is a negative regulator of stem cells. **(right)** In the shoot, WUS directly represses ARR5/6/7/15, which are negative regulators of CK signaling. Biosynthesis of CK, in turn, activates ARR1, which directly binds to the WUS promoter to activate *WUS* expression. WUS on the other hand represses CLE40 in the CZ and OC. In the PZ, CLE40 signals through BAM1 to activate CK synthesis, which promotes WUS.

5.1.8 TFs and miRNA regulate *CLE* signaling in the shoot

Recent publications reported that the homeobox TF WUS can interact with the homeobox TF STM and with the GRAS family TF HAM1 (Su et al., 2020). While *WUS* expression is restricted to the OC of the shoot meristem, *STM* expression was found throughout the entire shoot meristem, except for young primordia (Long et al., 1996; Yadav et al., 2011). *HAM1* expression was detected in the entire L3 of the shoot meristem and its flower primordia (Han, Geng, et al., 2020). Furthermore, Su and colleagues could show that STM interaction with WUS in the CZ of the meristem is required to activate *CLV3* expression, while the interaction between HAM1 and WUS in the OC of the meristem represses *CLV3* expression despite the presence of STM (Su et al., 2020). In addition, the TF TOPLESS (TPL/WSIP1) can also interact with WUS (Kieffer et al., 2006). *TPL* is expressed in the PZ in the L1 and L2 of the shoot meristem and thus might also be involved in the regulation of CLE peptides in the shoot (personal communication Jan Maika). Interestingly, *CLE40* expression is not detected in the CZ, OC and, young primordia until P4, but in high levels in the PZ of the meristem (Fig. 9). Here, we provide evidence that CLE40 is repressed in a WUS-dependent manner in the OC and CZ of the meristem. Thus, WUS activity represses CLE40 regardless of whether HAM1 or STM is

present. Hence, it is possible that in the L1 and L2 of the PZ, TPL interacts with STM to promote *CLE40* expression, while in the L3 STM and HAM1 together promote CLE40 activity. Thus, the complex of STM-HAM1-WUS represses *CLV3* and *CLE40* expression in the OC, while the complex STM-HAM1 or STM1-TPL might promote *CLE40* expression in the PZ. However, it is likely that only complexes of specific TFs are able to up or downregulate the expression of CLE peptides. It will be intriguing to test how different combinations of these TFs (WUS, STM, HAM, TPL) regulate *CLE40* expression in the shoot.

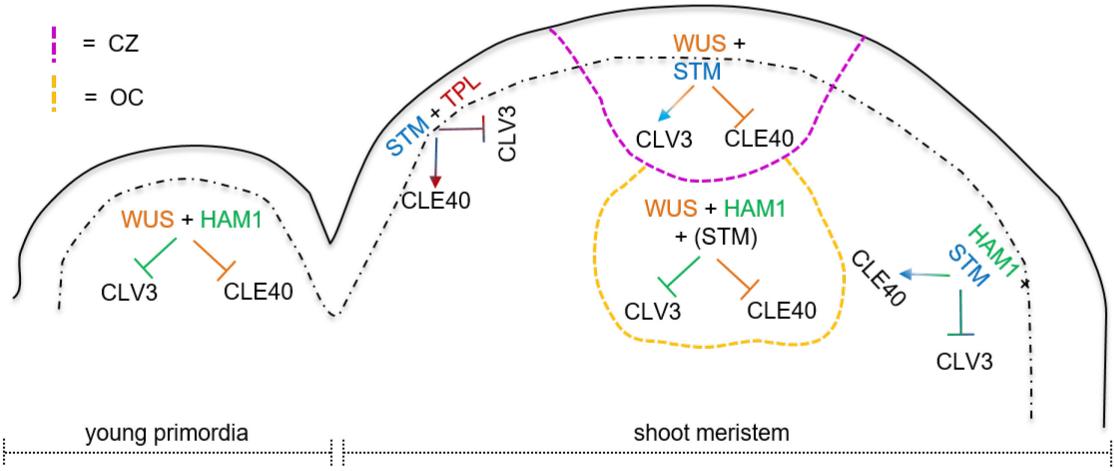

Fig. 47: Schematic model of CLE signaling regulation in the shoot via TF complexes of variating composition.

In the OC of the shoot meristem and in young primordia a complex of WUS and HAM1 represses *CLV3* and *CLE40* expression. In the CZ, a complex of WUS and STM activates *CLV3* expression and might repress the expression of *CLE40*. In the L1 and L2, the TFs STM and TPL could form a complex to repress *CLV3*, while activating the expression of *CLE40*. In the L3, a putative complex of HAM1 and STM could activate *CLE40* expression and at the same time repress *CLV3* activity.

It is also known that microRNAs (MIRs) negatively regulate TFs in plants (Carlsbecker et al., 2010). For instance, it was recently reported that the MIR171 originating from the epidermal layer of the shoot meristem moves to the L2 and to cells located at the upper corpus. There it represses the expression of *HAM2* in the L1 and L2 strongly and in a moderate way in the L3 cells (Han, Yan, et al., 2020). Additionally, it was recently published that BAM1 is involved in the transportation of miRNAs through PD and thus, this would increase the mobility of MIR171 in the periphery of the meristem after activation of CLE40 (Fan et al., 2021). The increase of HAM2 in the OC would consequently reduce *WUS* expression and thereby promote stem cell activity. This hypothesis underpins the promoting effect of BAM1 on *WUS* activity, which we presented in this work. It would be of great interest to further study if MIRs have an impact on the CLE40-BAM1-WUS signaling pathway.

5.1.9 Evolutionary perspective and comparison to other plant families

In Arabidopsis, the *CLV3* and *CLE40* genes are highly similar in exon-intron structure, while all other CLE-genes are intronless, indicating that CLE40 and CLV3 have arisen from a gene duplication event in the land plant lineage, and have functionally diverged since then to repress or promote stem cell maintenance (Goad et al., 2017; Hobe et al., 2003). In the land plant lineage, the shoot meristems of bryophytes such as the moss *Physcomitrium patens* appear less complex than those of angiosperms and carry only a single apical stem cell which ensures organ initiation by continuous asymmetric cell divisions (Harrison et al., 2009). Broadly expressed CLE peptides were here found to restrict stem cell identity and act in division plane control (Whitewoods et al., 2018). Proliferation of the apical notch cell in the liverwort *Marchantia polymorpha* is promoted by *MpCLE2* peptide which acts from outside the stem cell domain via the receptor *MpCLV1*, while cell proliferation is confined by *MpCLE1* peptide through a different receptor (Hata & Kyozuka, 2021; Hirakawa et al., 2019, 2020). Thus, antagonistic control of stem cell activities through diverse CLE peptides is conserved between distantly related land plants. In the grasses, several CLEs were found to control the stem cell domain. In maize, *ZmCLE7* is expressed from the meristem tip, while *ZmFCP1* is expressed in the meristem periphery and its center. Both peptides restrict stem cell fate via independent receptor signaling pathways (L. Liu et al., 2021; Rodriguez-Leal et al., 2019). In rice, overexpression of the CLE peptides OsFCP1 and OsFCP2 downregulates the homeobox gene *OSH1* and arrests meristem function (Ohmori et al., 2013; Suzaki et al., 2008). In rice and maize, CLE peptide signaling often restricts stem cell activities in the shoot meristem, but a stem cell promoting pathway has so far not been identified. We here showed that CLV3 and CLE40 do not only have an opposite shoot meristem phenotype but also show a complementary expression pattern in the shoot meristem (Fig. 9; Fig. 29). Thus the antagonistic effects of Arabidopsis CLV3 and CLE40 on meristem size can only be compared to the antagonistic functions of MpCLE1 and MpCLE2 on the gametophytic meristems of *Marchantia polymorpha*, which signal through two distinct receptors, *MpTDR* and *MpCLV1*, respectively (Hata & Kyozuka, 2021). So far, only signaling pathways repressing *WUS* activity have been identified in angiosperms and grasses. Hence, with this work, we broaden our perspective by proposing that a WUS promoting pathway is conserved in the plant lineage to fine-tune stem cell homeostasis in the SAM.

6. Summary

This study broadens our knowledge on how stem cell homeostasis in the shoot meristem of plants is achieved. Here, we provide evidence that the CLE40 peptide and its cognate receptor BAM1 antagonizes the well-studied CLV3-CLV1 pathway in stem cell regulation in the shoot meristem by the opposing regulation of the transcription factor WUS.

Using translational and transcriptional reporter lines, we analyzed the expression patterns of the main players of the CLV pathway in the IFM and combined these experiments with mutant studies. We were able to describe a new role for the CLE40 peptide, the closest homologue of CLV3, and its putative receptor BAM1, which belongs to the CLV-family receptors. *CLE40* is expressed in the PZ of the IFM in an expression pattern precisely complementary to that of CLV3. Furthermore, loss of the *CLE40* and *CLV3* gene, respectively, have opposing impacts on the meristem morphology in mutant plants. While *clv3* mutants have enlarged and fasciated IFMs, meristems of *cle40* mutants are smaller than wild type plants. Additionally, we could show that CLE40 signaling promotes *WUS* expression, while CLV3 signaling is known to restrict *WUS* expression via CLV1. In a negative feedback loop, WUS activity represses *CLE40* expression and CLE40 activity seems to be at least in part mediated by BAM1. *BAM1* is, like *CLE40*, also expressed in the PZ and *bam1* mutants have, like *cle40* mutants, smaller meristems compared to wild type plants. Additionally, BAM1 has, similar to CLE40, a promoting effect on WUS promoter activity. Besides that, ectopic expression of *BAM1* in the center of the meristem is able to rescue its small meristem phenotype and can partly substitute CLV1 in a *clv1* mutant background. *CLV1* is expressed in the center of meristems and in incipient organ primordia. Unlike *cle40* and *bam1* mutants, *clv1* mutants show enlarged IFMs. Together, these results show that shoot meristem development is controlled by two intertwined peptide signaling pathways that integrate signals from the stem cell zone and the meristem periphery to WUS and that WUS feeds back to regulate the expression of the two peptides to maintain a functional stem cell domain.

We provide further evidence that the RLK ACR4 has a promoting effect on shoot meristem size. However, the number of *WUS*-expressing cells was not altered in *acr4* mutants and ectopic expression of *ACR4* in the center of the meristem did not rescue its small meristem phenotype. Therefore, we conclude that ACR4 promotes meristem size in a pathway independent of the CLV3-CLV1-WUS and the CLE40-BAM1-WUS pathways.

Signaling events in plants can be controlled by receptor turnover/translocation upon ligand binding. For example, exogenous treatment of CLV3 peptide triggers the internalization of

CLV1-GFP in IFMs. Here, we extended these experiments to include CLE40 and ACR4. After CLV3 and CLE40 peptide treatment, we detected an increased accumulation of fluorescence signals of the receptors CLV1 and ACR4 in lytic vacuoles, respectively. To precisely track the local and subcellular dispersion of the peptide, we tagged the peptide with a small fluorophore. In the past, it appeared to be challenging to modify CLE peptides by introducing tags without losing binding specificity. However, here we managed to show the functionality of CLV3p tagged with the small, green fluorophore Atto488. These chimeric CLE peptides were able to trigger typical CLE responses *in planta* and were shown to diffuse into the root tissue.

Taken together, we here uncovered a new signaling pathway (CLE40-BAM1-WUS) that promotes meristem size and thus acts antagonistically to the well-known CLV3-CLV1-WUS pathway. We could further show that ACR4, most probably, acts independently of these pathways to promote meristem size and hence might also be involved in other developmental processes in the IFM. Additionally, the identification of functional peptides tagged to fluorophores was an important step to precisely visualize how peptides diffuse and interact on a subcellular level in future experiments. This will help to answer fundamental questions in plant development, for example, how, where, and when signaling cascades are activated.

7. Zusammenfassung

Die Regulation der Stammzellhomöostase in pflanzlichen Sprossmeristemen basiert auf dem gut charakterisierten CLV3-CLV1 Signalweg. In der vorliegenden Arbeit wurde das Gesamtverständis der zugrundeliegenden regulatorischen Mechanismen durch die Charackterisierung eines homologen, jedoch antagonistisch wirkenden CLE40-BAM1 Signalweges erweitert.

Mit Hilfe von transkriptionalen und translationalen Reporterlinien und der Analyse verschiedener Mutanten des CLV Signalwegs im Infloreszenzmeristem (IFM) konnte eine neue Rolle für CLE40 und seinen putativen Rezeptor BAM1 identifiziert werden. Obwohl CLE40 innerhalb der CLE-Familie die größte Sequenzähnlichkeit zum CLV3-Peptid aufweist, zeigen die beiden Peptide ein komplementäres Expressionsmuster im IFM. Auch funktional sind die beiden Peptide konträr: während *clv3* Mutanten ein vergrößertes und fasziiertes Meristem aufweisen, sind die Meristeme von *cle40* Mutanten kleiner. Des Weiteren zeigen beide Peptide eine gegensätzliche Wirkung auf den Transkriptionsfaktor WUS: während CLE40 die Aktivität von WUS erhöht, wirkt CLV3 reprimierend auf die Expression von *WUS*. Gleichzeitig reprimiert WUS die Aktivität von CLE40 und fördert die von CLV3, wodurch zwei negative Feedbacksignale entstehen. Die CLE40 Aktivität scheint, zumindest teilweise, durch den Rezeptor BAM1 reguliert zu werden. Wie CLE40 ist auch BAM1 in der Peripherie des IFM exprimiert. *bam1* Mutanten zeigen, wie *cle40* Mutanten, kleinere Meristeme und BAM1 selbst scheint ebenfalls, wie CLE40, eine fördernde Aktivität auf den Transkriptionsfaktor WUS zu haben. Die ektopische Expression von *BAM1* unter dem *WUS* Promoter rettet die phänotypische Ausprägung von *bam1* Mutanten im Bezug auf die Meristemgröße und kann zumindest teilweise die CLV1 Funktion in *clv1* Mutanten übernehmen. *CLV1* wird im Zentrum von Meristemen exprimiert und zeigt im Gegensatz zu CLE40 und BAM1 vergrößerte IFMs. CLV1 reprimiert außerdem die *WUS*-Expression, während CLE40 und BAM1 diese fördern. Zusammengefasst zeigen diese Ergebnisse, dass die Stammzellhomöostase im Sprossapikalmeristem durch zwei ineinandergreifende Signalwege reguliert wird. Dabei gelangen Signale von der zentralen und peripheren Zone zu WUS, welches wiederum die Expression der beiden Peptide kontrolliert, um eine funktionierende Stammzelldomäne zu erhalten.

Darüber hinaus konnten wir zeigen, dass der Rezeptor ACR4 zwar einen positiven Effekt auf die Sprossmeristemgröße hat, jedoch weder die Anzahl der *WUS*-exprimierenden Zellen verändert, noch konnte die ektopische Expression von *ACR4* im Zentrum des Meristems die wildtypische Meristemgröße wieder herstellen. Dies deutet darauf hin, das der positive Effekt

von ACR4 auf die Meristemgröße unabhängig von den CLV3-CLV1-WUS und CLE40-BAM1-WUS Signalwegen ist.

Die Aktivierung von Signalwegen kann durch den Abbau oder die Translokation eines Rezeptors nach Bindung des Liganden reguliert werden. Beispielsweise löst die Zugabe von CLV3 Peptid die Internalisierung von CLV1-GFP im IFM aus. In dieser Arbeit, haben wir diese Experimente auf das Peptid CLE40 und den Rezeptor ACR4 erweitertt. Nach der Zugabe von exogenem CLV3 oder CLE40 Peptid konnten wir eine erhöhte Akkumulation von Fluoreszenzsignalen der Rezeptoren CLV1 bzw. ACR4 in lytischen Vakuolen feststellen. Um die lokale und subzelluläre Dispersion des Peptids genau zu verfolgen, wurde das CLV3-Peptid mit einem kleinen Fluorophor markiert. In der Vergangenheit, stellte es eine Herausforderung dar CLE-Peptide mit einem Tag zu versehen ohne die Bindungsspezifität an den Rezeptor zu verlieren. In dieser Arbeit, ist es uns jedoch gelungen ein funktionales CLV3-Peptid, das mit dem Fluorophor Atto488 markiert wurde, zu identifizieren. Dieses chimäre CLE-Peptid war in der Lage die typischen Reaktionen von CLE-Peptiden in Pflanzen auszulösen (wie z.B. verkürztes Wurzelwachstum). Gleichzeitig haben wir nun die Möglichkeit die Diffusion des Peptids in das Wurzelgewebe zu visualisieren.

Zusammenfassend, konnte in dieser Arbeit gezeigt werden, dass es neben dem etablierten CLV3-CLV1-WUS Signalweg einen zweiten, antagonistisch wirkenden Signalweg bestehend aus CLE40-BAM1-WUS gibt, der einen positiven Effekt auf die Meristemgröße hat. Wir konnten außerdem zeigen, dass die Rezeptorkinase ACR4 ebenfalls einen positiven Effekt auf die Meristemgröße hat. Dieser Effekt scheint jedoch unabhängig von den beiden zuvor genannten Signalwegen zu agieren. Darüber hinaus konnten wir ein funktionelles fluoreszenz-markiertes Peptidid identifizieren, welches ermöglicht, präzise zu visualisieren, wie Peptide diffundieren und auf subzellulärer Ebene interagieren. Damit könnten grundlegende Fragen der Pflanzenentwicklung beantwortet werden, wie beispielsweise wo, wann und wie Signalkaskaden aktiviert werden.

8. Literature

Bayer, E. M., Smith, R. S., Mandel, T., Nakayama, N., Sauer, M., Prusinkiewicz, P., & Kuhlemeier, C. (2009). Integration of transport-based models for phyllotaxis and midvein formation. *Genes and Development*, *23*(3), 373–384. https://doi.org/10.1101/gad.497009

Becraft, P. W., Stinard, P. S., & McCarty, D. R. (1996). Crinkly4: A TNFR-like receptor kinase involved in maize epidermal differentiation. *Science*, *273*(5280), 1406–1409. https://doi.org/10.1126/science.273.5280.1406

Benfey, P. N., & Scheres, B. (2000). Root development. *Current Biology*, *10*(22), 813–815. https://doi.org/10.1016/S0960-9822(00)00814-9

Berckmans, B., Kirschner, G., Gerlitz, N., Stadler, R., & Simon, R. (2019). CLE40 signalling regulates the fate of root stem cells in Arabidopsis. *Plant Physiology*, pp.00914.2019. https://doi.org/10.1104/pp.19.00914

Berckmans, B., Kirschner, G., Gerlitz, N., Stadler, R., & Simon, R. (2020). CLE40 signaling regulates root stem cell fate. *Plant Physiology*, *182*(4), 1776–1792. https://doi.org/10.1104/PP.19.00914

Besnard, F., Refahi, Y., Morin, V., Marteaux, B., Brunoud, G., Chambrier, P., Rozier, F., Mirabet, V., Legrand, J., Lainé, S., Thévenon, E., Farcot, E., Cellier, C., Das, P., Bishopp, A., Dumas, R., Parcy, F., Helariutta, Y., Boudaoud, A., … Vernoux, T. (2014). Cytokinin signalling inhibitory fields provide robustness to phyllotaxis. *Nature*, *505*(7483), 417–421. https://doi.org/10.1038/nature12791

Betsuyaku, S., Takahashi, F., Kinoshita, A., Miwa, H., Shinozaki, K., Fukuda, H., & Sawa, S. (2011). Mitogen-activated protein kinase regulated by the CLAVATA receptors contributes to shoot apical meristem homeostasis. *Plant and Cell Physiology*, *52*(1), 14–29. https://doi.org/10.1093/pcp/pcq157

Billou, I., Xu, J., Wildwater, M., Willemsen, V., Paponov, I., Frimi, J., Heldstra, R., Aida, M., Palme, K., & Scheres, B. (2005). The PIN auxin efflux facilitator network controls growth and patterning in Arabidopsis roots. *Nature*, *433*(7021), 39–44. https://doi.org/10.1038/nature03184

Bleckmann, A., Weidtkamp-Peters, S., Seidel, C. a M., & Simon, R. (2010). Stem cell signaling in Arabidopsis requires CRN to localize CLV2 to the plasma membrane. *Plant Physiology*, *152*(1), 166–176. https://doi.org/10.1104/pp.109.149930

Blümke, P., Schlegel, J., Gonzalez-Ferrer, Carmen Becher, S., Gustavo Pinto, K., Monaghan, J., & Simon, R. (2021). Receptor-like cytoplasmic kinase MAZZA mediates developmental processes with CLAVATA1-family receptors in Arabidopsis. *Journal of Experimental Botany*. https://doi.org/10.1093/jxb/erab183

Bommert, P., Je, B. Il, Goldshmidt, A., & Jackson, D. (2013). The maize Gα gene COMPACT PLANT2 functions in CLAVATA signalling to control shoot meristem size. *Nature*, *502*(7472), 555–558. https://doi.org/10.1038/nature12583

Bowman, J. L., Smyth, D. R., & Meyerowitz, E. M. (1989). Genes directing flower development in arabidopsis. *Plant Cell*, *1*, 37–52. https://doi.org/10.1105/tpc.19.00276

Bowman, J. L., Smyth, D. R., & Meyerowitz, E. M. (1991). Genetic interactions among floral homeotic genes of Arabidopsis. *Development*, *112*(1), 1–20.

Brand, U., Fletcher, J. C., Hobe, M., Meyerowitz, E. M., & Simon, R. (2000). Dependence of

stem cell fate in Arabidopsis on a feedback loop regulated by CLV3 activity. *Science*, *289*(5479), 617–619. https://doi.org/10.1126/science.289.5479.617

Brand, U., Grünewald, M., Hobe, M., & Simon, R. (2002). Regulation of CLV3 expression by two homeobox genes in Arabidopsis. *Plant Physiology*, *129*(2), 565–575. https://doi.org/10.1104/pp.001867

Breiden, M., Olsson, V., Gustavo-Pinto, K., Schultz, P., Schlegel, J., Dietrich, P., Butenko, M. A., & Simon, R. (2021). The cell fate controlling CLE40 peptide requires CNGC9 to trigger highly localized Ca2+ transients in Arabidopsis thaliana root meristems. *Plant and Cell Physiology*, 1–30. https://doi.org/10.1101/2020.11.13.381111

Breiden, M., & Simon, R. (2016). Q&A: How does peptide signaling direct plant development? *BMC Biology*, *14*(1), 1–7. https://doi.org/10.1186/s12915-016-0280-3

Busch, W., Miotk, A., Ariel, F. D., Zhao, Z., Forner, J., Daum, G., Suzaki, T., Schuster, C., Schultheiss, S. J., Leibfried, A., Haubeiß, S., Ha, N., Chan, R. L., & Lohmann, J. U. (2010). Transcriptional control of a plant stem cell niche. *Developmental Cell*, *18*(5), 841–853. https://doi.org/10.1016/j.devcel.2010.03.012

Butenko, M. A., Vie, A. K., Brembu, T., Aalen, R. B., & Bones, A. M. (2009). Plant peptides in signalling: looking for new partners. *Trends in Plant Science*, *14*(5), 255–263. https://doi.org/10.1016/j.tplants.2009.02.002

Byrne, M. E., Barley, R., Curtis, M., Arroyo, J. M., Dunham, M., Hudson, A., & Martienssen, R. A. (2000). Asymmetric leaves1 mediates leaf patterning and stem cell function in arabidopsis. *Nature*, *408*(6815), 967–971. https://doi.org/10.1038/35050091

Byrne, M. E., Simorowski, J., & Martienssen, R. A. (2002). ASYMMETRIC LEAVES1 reveals know gene redundancy in Arabidopsis. *Development*, *129*(8), 1957–1965. https://doi.org/10.1242/dev.129.8.1957

Carlsbecker, A., Lee, J. Y., Roberts, C. J., Dettmer, J., Lehesranta, S., Zhou, J., Lindgren, O., Moreno-Risueno, M. A., Vatén, A., Thitamadee, S., Campilho, A., Sebastian, J., Bowman, J. L., Helariutta, Y., & Benfey, P. N. (2010). Cell signalling by microRNA165/6 directs gene dose-dependent root cell fate. *Nature*, *465*(7296), 316–321. https://doi.org/10.1038/nature08977

Clark, S. E., Running, M. P., & Meyerowitz, E. M. (1993). CLAVATA1, a regulator of meristem and flower development in Arabidopsis. *Development*, *119*, 397–418.

Clark, S. E., Running, M. P., & Meyerowitz, E. M. (1995). CLAVATA3 is a specific regulator of shoot and floral meristem development affecting the same processes as CLAVATA1. *Development*, *121*(7), 2057–2067.

Clark, S. E., Williams, R. W., & Meyerowitz, E. M. (1997). The CLAVATA1 Gene Encodes a Putative Receptor Kinase That Controls Shoot and Floral Meristem Size in Arabidopsis. *Cell*, *89*, 575–585.

Clough, S. J., & Bent, A. F. (1998). Floral dip: A simplified method for Agrobacterium-mediated transformation of Arabidopsis thaliana. *Plant Journal*, *16*(6), 735–743. https://doi.org/10.1046/j.1365-313X.1998.00343.x

Cock, J. M., & McCormick, S. (2001). A large family of genes that share homology with Clavata3. *Plant Physiology*, *126*(3), 939–942. https://doi.org/10.1104/pp.126.3.939

Coen, E. S., & Meyerowitz, E. M. (1991). The war of the whorls: genetic interactions controlling flower development. *Nature*, *353*(6339), 31.

Crook, A. D., Willoughby, A. C., Hazak, O., Okuda, S., Van Der Molen, K. R., Soyars, C. L., Cattaneo, P., Clark, N. M., Sozzani, R., Hothorn, M., Hardtke, C. S., & Nimchuk, Z. L. (2020). BAM1/2 receptor kinase signaling drives CLE peptide-mediated formative cell divisions in Arabidopsis roots. *Proceedings of the National Academy of Sciences of the United States of America*, *117*(51), 32750–32756. https://doi.org/10.1073/pnas.2018565117

Cruz-Ramírez, A., Díaz-Triviño, S., Wachsman, G., Du, Y., Arteága-Vázquez, M., Zhang, H., Benjamins, R., Blilou, I., Neef, A. B., Chandler, V., & Scheres, B. (2013). A SCARECROW-RETINOBLASTOMA Protein Network Controls Protective Quiescence in the Arabidopsis Root Stem Cell Organizer. *PLoS Biology*, *11*(11). https://doi.org/10.1371/journal.pbio.1001724

Czyzewicz, N., Nikonorova, N., Meyer, M. R., Sandal, P., Shah, S., Vu, L. D., Gevaert, K., Rao, A. G., & De Smet, I. (2016). The growing story of (ARABIDOPSIS) CRINKLY 4. *Journal of Experimental Botany*, *67*(16), 4835–4847. https://doi.org/10.1093/jxb/erw192

Daum, G., Medzihradszky, A., Suzaki, T., & Lohmann, J. U. (2014). A mechanistic framework for noncell autonomous stem cell induction in Arabidopsis. *Proceedings of the National Academy of Sciences of the United States of America*, *111*(40), 14619–14624. https://doi.org/10.1073/pnas.1406446111

Davies, P. J. (1995). The Plant Hormone Concept:Concentration, Sensitivity and Transport. In P. J. Davies (Ed.), *Plant Hormones: Physiology, Biochemistry and Molecular Biology* (pp. 13–38). Springer Netherlands. https://doi.org/10.1007/978-94-011-0473-9_2

De Reuille, P. B., Bohn-Courseau, I., Ljung, K., Morin, H., Carraro, N., Godin, C., & Traas, J. (2006). Computer simulations reveal properties of the cell-cell signaling network at the shoot apex in Arabidopsis. *Proceedings of the National Academy of Sciences of the United States of America*, *103*(5), 1627–1632. https://doi.org/10.1073/pnas.0510130103

de Reuille, P. B., Routier-Kierzkowska, A. L., Kierzkowski, D., Bassel, G. W., Schüpbach, T., Tauriello, G., Bajpai, N., Strauss, S., Weber, A., Kiss, A., Burian, A., Hofhuis, H., Sapala, A., Lipowczan, M., Heimlicher, M. B., Robinson, S., Bayer, E. M., Basler, K., Koumoutsakos, P., … Smith, R. S. (2015). MorphoGraphX: A platform for quantifying morphogenesis in 4D. *ELife*, *4*, 1–20. https://doi.org/10.7554/eLife.05864

De Smet, I., Voß, U., Jürgens, G., & Beeckman, T. (2009). Receptor-like kinases shape the plant. *Nature Cell Biology*, *11*(10), 1166–1173. https://doi.org/10.1038/ncb1009-1166

Defalco, T. A., Anne, P., James, S. R., Willoughby, A., Johanndrees, O., Genolet, Y., Pullen, A.-M., Zipfel, C., Hardtke, C. S., & Nimchuk, Z. L. (2021). A conserved regulatory module regulates receptor kinase signaling in immunity and development. *BioRxiv*, 2021.01.19.427293. https://doi.org/10.1101/2021.01.19.427293

Dello Ioio, R., Linhares, F. S., Scacchi, E., Casamitjana-Martinez, E., Heidstra, R., Costantino, P., & Sabatini, S. (2007). Cytokinins Determine Arabidopsis Root-Meristem Size by Controlling Cell Differentiation. *Current Biology*, *17*(8), 678–682. https://doi.org/10.1016/j.cub.2007.02.047

Denay, G., Chahtane, H., Tichtinsky, G., & Parcy, F. (2017). A flower is born: an update on Arabidopsis floral meristem formation. *Current Opinion in Plant Biology*, *35*(Figure 1), 15–22. https://doi.org/10.1016/j.pbi.2016.09.003

DeYoung, B. J., Bickle, K. L., Schrage, K. J., Muskett, P., Patel, K., & Clark, S. E. (2006). The CLAVATA1-related BAM1, BAM2 and BAM3 receptor kinase-like proteins are required

for meristem function in Arabidopsis. *Plant Journal*, *45*(1), 1–16. https://doi.org/10.1111/j.1365-313X.2005.02592.x

DeYoung, B. J., & Clark, S. E. (2008). BAM receptors regulate stem cell specification and organ development through complex interactions with CLAVATA signaling. *Genetics*, *180*(2), 895–904. https://doi.org/10.1534/genetics.108.091108

Dolan, L., Janmaat, K., Willemsen, V., Linstead, P., Poethig, S., Roberts, K., & Scheres, B. (1993). Cellular organisation of the Arabidopsis thaliana root. *Development*, *119*(1), 71–84.

Drisch, R. C., & Stahl, Y. (2015). Function and regulation of transcription factors involved in root apical meristem and stem cell maintenance. *Frontiers in Plant Science*, *6*(JULY), 1–8. https://doi.org/10.3389/fpls.2015.00505

Durbak, A. R., & Tax, F. E. (2011). CLAVATA signaling pathway receptors of arabidopsis regulate cell proliferation in fruit organ formation as well as in meristems. *Genetics*, *189*(1), 177–194. https://doi.org/10.1534/genetics.111.130930

Ehlers, K., & Kollmann, R. (2001). Primary and secondary plasmodesmata: Structure, origin, and functioning: Review article. *Protoplasma*, *216*(1–2), 1–30. https://doi.org/10.1007/BF02680127

Endrizzi, K., Moussian, B., Haecker, A., Levin, J. Z., & Laux, T. (1996). The SHOOT MERISTEMLESS gene is required for maintenance of undifferentiated cells in Arabidopsis shoot and floral meristems and acts at a different regulatory level than the meristem genes WUSCHEL and ZWILLE. *The Plant Journal*, *10*, 967–979.

Fan, P., Aguilar, E., Bradai, M., Xue, H., Wang, H., Xu, L., & Lozano-Duran, R. (2021). The receptor-like kinases BAM1 and BAM2 are required for root xylem patterning. *Proceedings of the National Academy of Sciences*, *118*(12), 2–7. https://doi.org/10.1073/pnas.2022547118/-/DCSupplemental.Published

Farrokhi, N., Whitelegge, J. P., & Brusslan, J. A. (2008). Plant peptides and peptidomics. *Plant Biotechnology Journal*, *6*(2), 105–134. https://doi.org/10.1111/j.1467-7652.2007.00315.x

Fiers, M., Golemiec, E., Xu, J., Geest, L. Van Der, Heidstra, R., Stiekema, W., & Liu, C. (2005). *The 14 – Amino Acid CLV3 , CLE19 , and CLE40 Peptides Trigger Consumption of the Root Meristem in Arabidopsis through a CLAVATA2 -Dependent Pathway*. *17*(September), 2542–2553. https://doi.org/10.1105/tpc.105.034009.1

Fletcher, J. C., Brand, U., Running, M. P., Simon, R., & Meyerowitz, E. M. (1999). Signaling of Cell Fate Decisions by \emph{CLAVATA3} in \emph{Arabidopsis} Shoot Meristems. *Science*, *19*(5409), 1911–1914. https://doi.org/10.1126/science.283.5409.1911

Geldner, N., Hyman, D. L., Wang, X., Schumacher, K., & Chory, J. (2007). Endosomal signaling of plant steroid receptor kinase BRI1. *Genes and Development*, *21*(13), 1598–1602. https://doi.org/10.1101/gad.1561307

Gifford, M. L., Dean, S., & Ingram, G. C. (2003). The Arabidopsis ACR4 gene plays a role in cell layer organisation during ovule integument and sepal margin development. *Development*, *130*(18), 4249–4258. https://doi.org/10.1242/dev.00634

Gifford, M. L., Robertson, F. C., Soares, D. C., & Ingram, G. C. (2005). ARABIDOPSIS CRINKLY4 function, internalization, and turnover are dependent on the extracellular crinkly repeat domain. *The Plant Cell*, *17*(4), 1154–1166. https://doi.org/10.1105/tpc.104.029975

Goad, D. M., Zhu, C., & Kellogg, E. A. (2017). Comprehensive identification and clustering of CLV3/ESR-related (CLE) genes in plants finds groups with potentially shared function. *New Phytologist*, *216*(2), 605–616. https://doi.org/10.1111/nph.14348

Gómez-Gómez, L., & Boller, T. (2000). FLS2: An LRR receptor-like kinase involved in the perception of the bacterial elicitor flagellin in Arabidopsis. *Molecular Cell*, *5*(6), 1003–1011. https://doi.org/10.1016/s1097-2765(00)80265-8

Graf, P., Dolzblasz, A., Würschum, T., Lenhard, M., Pfreundt, U., & Laux, T. (2010). MGOUN1 encodes an Arabidopsis type IB DNA topoisomerase required in stem cell regulation and to maintain developmentally regulated gene silencing. *Plant Cell*, *22*(3), 716–728. https://doi.org/10.1105/tpc.109.068296

Guenot, B., Bayer, E., Kierzkowski, D., Smith, R. S., Mandel, T., Zádníková, P., Benková, E., & Kuhlemeier, C. (2012). Pin1-independent leaf initiation in arabidopsis. *Plant Physiology*, *159*(4), 1501–1510. https://doi.org/10.1104/pp.112.200402

Hall, P., & Watt, F. (1989). Stem cells: the generation and maintenance of cellular diversity. *Development*, *106*(4), 619–633. http://dev.biologists.org/content/106/4/619.abstract

Han, H., Geng, Y., Guo, L., Yan, A., Meyerowitz, E. M., Liu, X., & Zhou, Y. (2020). The Overlapping and Distinct Roles of HAM Family Genes in Arabidopsis Shoot Meristems. *Frontiers in Plant Science*, *11*(541968). https://doi.org/10.3389/fpls.2020.541968

Han, H., Yan, A., Li, L., Zhu, Y., Feng, B., Liu, X., & Zhou, Y. (2020). A signal cascade originated from epidermis defines apical-basal patterning of Arabidopsis shoot apical meristems. *Nature Communications*, *11*(1), 1–17. https://doi.org/10.1038/s41467-020-14989-4

Harrison, C. J., Roeder, A. H. K., Meyerowitz, E. M., & Langdale, J. A. (2009). Local Cues and Asymmetric Cell Divisions Underpin Body Plan Transitions in the Moss Physcomitrella patens. *Current Biology*, *19*(6), 461–471. https://doi.org/10.1016/j.cub.2009.02.050

Hata, Y., & Kyozuka, J. (2021). Fundamental mechanisms of the stem cell regulation in land plants: lesson from shoot apical cells in bryophytes. *Plant Molecular Biology*. https://doi.org/10.1007/s11103-021-01126-y

Hay, A., & Tsiantis, M. (2006). The genetic basis for differences in leaf form between Arabidopsis thaliana and its wild relative Cardamine hirsuta. *Nature Genetics*, *38*(8), 942–947. https://doi.org/10.1038/ng1835

Hay, A., & Tsiantis, M. (2010). KNOX genes: Versatile regulators of plant development and diversity. *Development*, *137*(19), 3153–3165. https://doi.org/10.1242/dev.030049

Heisler, M. G., Ohno, C., Das, P., Sieber, P., Reddy, G. V., Long, J. A., & Meyerowitz, E. M. (2005). Patterns of auxin transport and gene expression during primordium development revealed by live imaging of the Arabidopsis inflorescence meristem. *Current Biology*, *15*(21), 1899–1911. https://doi.org/10.1016/j.cub.2005.09.052

Hempel, F. D., & Feldman, L. J. (1994). Bi-directional inflorescence development in Arabidopsis thaliana: Acropetal initiation of flowers and basipetal initiation of paraclades. *Planta*, *192*(2), 276–286. https://doi.org/10.1007/BF01089045

Hirakawa, Y., Fujimoto, T., Ishida, S., Uchida, N., Sawa, S., Kiyosue, T., Ishizaki, K., Nishihama, R., Kohchi, T., & Bowman, J. L. (2020). Induction of Multichotomous Branching by CLAVATA Peptide in Marchantia polymorpha. *Current Biology*, *30*(19), 3833-3840.e4. https://doi.org/10.1016/j.cub.2020.07.016

Hirakawa, Y., Uchida, N., Yamaguchi, Y. L., Tabata, R., Ishida, S., Ishizaki, K., Nishihama, R., Kohchi, T., Sawa, S., & Bowman, J. L. (2019). Control of proliferation in the haploid meristem by CLE peptide signaling in marchantia polymorpha. *PLoS Genetics*, *15*(3), 1–20. https://doi.org/10.1371/journal.pgen.1007997

Hobe, M., Müller, R., Grünewald, M., Brand, U., & Simon, R. (2003). Loss of CLE40, a protein functionally equivalent to the stem cell restricting signal CLV3, enhances root waving in Arabidopsis. *Development Genes and Evolution*, *213*(8), 371–381. https://doi.org/10.1007/s00427-003-0329-5

Hord, C. L. H., Chen, C., DeYoung, B. J., Clark, S. E., & Ma, H. (2006). The BAM1/BAM2 receptor-like kinases are important regulators of Arabidopsis early anther development. *Plant Cell*, *18*(7), 1667–1680. https://doi.org/10.1105/tpc.105.036871

Ishida, T., Tabata, R., Yamada, M., Aida, M., Mitsumasu, K., Fujiwara, M., Yamaguchi, K., Shigenobu, S., Higuchi, M., Tsuji, H., Shimamoto, K., Hasebe, M., Fukuda, H., & Sawa, S. (2014). Heterotrimeric G proteins control stem cell proliferation through CLAVATA signaling in Arabidopsis. *EMBO Reports*, *15*(11), 1202–1209. https://doi.org/10.15252/embr.201678010

Ito, Y., & Fukuda, H. (2006). Dodeca-CLE Peptides as Suppressors. *Science*, *August*, 842–845. https://doi.org/10.1126/science.1128436

Je, B. Il, Gruel, J., Lee, Y. K., Bommert, P., Arevalo, E. D., Eveland, A. L., Wu, Q., Goldshmidt, A., Meeley, R., Bartlett, M., Komatsu, M., Sakai, H., Jönsson, H., & Jackson, D. (2016). Signaling from maize organ primordia via FASCIATED EAR3 regulates stem cell proliferation and yield traits. *Nature Genetics*, *48*(7), 785–791. https://doi.org/10.1038/ng.3567

Jenik, P. D., & Irish, V. F. (2000). *Regulation of cell proliferation patterns by homeotic genes during Arabidopsis floral development*. *1276*, 1267–1276.

Jeong, S., Trotochaud, A. E., & Clark, S. E. (1999). The Arabidopsis CLAVATA2 gene encodes a receptor-like protein required for the stability of the CLAVATA1 receptor-like kinase. *Plant Cell*, *11*(10), 1925–1933. https://doi.org/10.1105/tpc.11.10.1925

Jin, P., Guo, T., & Becraft, P. W. (2000). The maize CR4 receptor-like kinase mediates a growth factor-like differentiation response. *Genesis*, *27*(3), 104–116. https://doi.org/10.1002/1526-968x(200007)27:3<104::aid-gene30>3.0.co;2-i

Kaufmann, K., Wellmer, F., Muiñ, J. M., Ferner, T., Wuest, S. E., Kumar, V., Serrano-Mislata, A., Madueño, F., Kraiewski, P., Meyerowitz, E. M., Angenent, G. C., & Riechmann, J. L. (2010). Orchestration of floral initiation by APETALA1. *Science*, *328*(5974), 85–89. https://doi.org/10.1126/science.1185244

Kayes, J. M., & Clark, S. E. (1998). CLAVATA2, a regulator of meristem and organ development in Arabidopsis. *Development*, *125*(19), 3843–3851.

Kieffer, M., Stern, Y., Cook, H., Clerici, E., Maulbetsch, C., Laux, T., & Davies, B. (2006). Analysis of the transcription factor WUSCHEL and its functional homologue in Antirrhinum reveals a potential mechanism for their roles in meristem maintenance. *Plant Cell*, *18*(3), 560–573. https://doi.org/10.1105/tpc.105.039107

Kinoshita, A., Betsuyaku, S., Osakabe, Y., Mizuno, S., Nagawa, S., Stahl, Y., Simon, R., Yamaguchi-Shinozaki, K., Fukuda, H., & Sawa, S. (2010). RPK2 is an essential receptor-like kinase that transmits the CLV3 signal in Arabidopsis. *Development*, *137*(24), 4327–4327. https://doi.org/10.1242/dev.061747

Krizek, B. A. (2009). AINTEGUMENTA and AINTEGUMENTA-LIKE6 act redundantly to regulate arabidopsis floral growth and patterning. *Plant Physiology*, *150*(4), 1916–1929. https://doi.org/10.1104/pp.109.141119

Lampropoulos, A., Sutikovic, Z., Wenzl, C., Maegele, I., Lohmann, J. U., & Forner, J. (2013). GreenGate - A novel, versatile, and efficient cloning system for plant transgenesis. *PLoS ONE*, *8*(12). https://doi.org/10.1371/journal.pone.0083043

Lee, H., Jun, Y. S., Cha, O. K., & Sheen, J. (2019). Mitogen-activated protein kinases MPK3 and MPK6 are required for stem cell maintenance in the Arabidopsis shoot apical meristem. *Plant Cell Reports*, *38*(3), 311–319. https://doi.org/10.1007/s00299-018-2367-5

Leibfried, A., To, J. P. C., Busch, W., Stehling, S., Kehle, A., Demar, M., Kieber, J. J., & Lohmann, J. U. (2005). WUSCHEL controls meristem function by direct regulation of cytokinin-inducible response regulators. *Nature*, *438*(7071), 1172–1175. https://doi.org/10.1038/nature04270

Lenhard, M., Jürgens, G., & Laux, T. (2002). The WUSCHEL and SHOOTMERISTEMLESS genes fulfil complementary roles in Arabidopsis shoot meristem regulation. *Development*, *129*(13), 3195–3206.

Liu, L., Gallagher, J., Arevalo, E. D., Chen, R., Skopelitis, T., Wu, Q., Bartlett, M., & Jackson, D. (2021). Enhancing grain-yield-related traits by CRISPR–Cas9 promoter editing of maize CLE genes. *Nature Plants*, *7*(3), 287–294. https://doi.org/10.1038/s41477-021-00858-5

Liu, X., Kim, Y. J., Müller, R., Yumul, R. E., Liu, C., Pan, Y., Cao, X., Goodrich, J., & Chen, X. (2011). AGAMOUS terminates floral stem cell maintenance in arabidopsis by directly repressing WUSCHEL through recruitment of Polycomb Group proteins. *Plant Cell*, *23*(10), 3654–3670. https://doi.org/10.1105/tpc.111.091538

Lohmann, J. U., Hong, R. L., Hobe, M., Busch, M. A., Parcy, F., Simon, R., & Weigel, D. (2001). A molecular link between stem cell regulation and floral patterning in Arabidopsis. *Cell*, *105*(6), 793–803. https://doi.org/10.1016/S0092-8674(01)00384-1

Long, J. A., Moan, E. I., Medford, J. I., & Barton, M. K. (1996). A member of the KNOTTED class of homeodomain proteins encoded by the STM gene of Arabidopsis. *Nature*, *379*(6560), 66–69. https://doi.org/10.1038/379066a0

Lucas, W. J., Ham, B. K., & Kim, J. Y. (2009). Plasmodesmata - bridging the gap between neighboring plant cells. *Trends in Cell Biology*, *19*(10), 495–503. https://doi.org/10.1016/j.tcb.2009.07.003

Ma, Y., Miotk, A., Šutiković, Z., Ermakova, O., Wenzl, C., Medzihradszky, A., Gaillochet, C., Forner, J., Utan, G., Brackmann, K., Galván-Ampudia, C. S., Vernoux, T., Greb, T., & Lohmann, J. U. (2019). WUSCHEL acts as an auxin response rheostat to maintain apical stem cells in Arabidopsis. *Nature Communications*, *10*(5093), 1–11. https://doi.org/10.1038/s41467-019-13074-9

Mandel, T., Moreau, F., Kutsher, Y., Fletcher, J. C., Carles, C. C., & Williams, L. E. (2014). The ERECTA receptor kinase regulates Arabidopsis shoot apical meristem size, phyllotaxy and floral meristem identity. *Development*, *141*(4), 830–841. https://doi.org/10.1242/dev.104687

Matsubayashi, Y. (2014). Posttranslationally Modified Small-Peptide Signals in Plants. *Annual Review of Plant Biology*, *65*(1), 385–413. https://doi.org/10.1146/annurev-arplant-

050312-120122

Mayer, K. F. X., Schoof, H., Haecker, A., Lenhard, M., Jürgens, G., & Laux, T. (1998). Role of WUSCHEL in Regulating Stem Cell Fate in the Arabidopsis Shoot Meristem. *Cell Press*, *95*, 805–815.

McKelvie, A. D. (1962). A list of mutant genes in Arabidopsis thaliana. *Radiation Botany*, *1*, 233–241.

Meyer, M. R., Shah, S., & Rao, A. G. (2013). Insights into molecular interactions between the juxtamembrane and kinase subdomains of the Arabidopsis Crinkly-4 receptor-like kinase. *Archives of Biochemistry and Biophysics*, *535*(2), 101–110. https://doi.org/10.1016/j.abb.2013.03.014

Meyer, M. R., Shah, S., Zhang, J., Rohrs, H., & Rao, A. G. (2015). Evidence for intermolecular interactions between the intracellular domains of the arabidopsis receptor-like kinase ACR4, its homologs and the Wox5 transcription factor. *PLoS ONE*, *10*(3), 1–26. https://doi.org/10.1371/journal.pone.0118861

Miyawaki, K., Tabata, R., & Sawa, S. (2013). Evolutionarily conserved CLE peptide signaling in plant development, symbiosis, and parasitism. *Current Opinion in Plant Biology*, *16*(5), 598–606. https://doi.org/10.1016/j.pbi.2013.08.008

Müller, R., Bleckmann, A., & Simon, R. (2008). The receptor kinase CORYNE of Arabidopsis transmits the stem cell-limiting signal CLAVATA3 independently of CLAVATA1. *Plant Cell*, *20*(4), 934–946. https://doi.org/10.1105/tpc.107.057547

Müller, R., Borghi, L., Kwiatkowska, D., Laufs, P., & Simon, R. (2006). Dynamic and Compensatory Responses of Arabidopsis Shoot and Floral Meristems to CLV3 Signaling. *The Plant Cell*, *18*(5), 1188–1198. https://doi.org/10.1105/tpc.105.040444

Nebenführ, A., Ritzenthaler, C., & Robinson, D. G. (2002). Brefeldin A: Deciphering an enigmatic inhibitor of secretion. *Plant Physiology*, *130*(3), 1102–1108. https://doi.org/10.1104/pp.011569

Ni, J., Guo, Y., Jin, H., Hartsell, J., & Clark, S. E. (2011). Characterization of a CLE processing activity. *Plant Molecular Biology*, *75*(1), 67–75. https://doi.org/10.1007/s11103-010-9708-2

Nimchuk, Z. L. (2017). CLAVATA1 controls distinct signaling outputs that buffer shoot stem cell proliferation through a two-step transcriptional compensation loop. *PLoS Genetics*, *13*(3), 1–19. https://doi.org/10.1371/journal.pgen.1006681

Nimchuk, Z. L., Tarr, P. T., Ohno, C., Qu, X., & Meyerowitz, E. M. (2011). Plant stem cell signaling involves ligand-dependent trafficking of the CLAVATA1 receptor kinase. *Current Biology*, *21*(5), 345–352. https://doi.org/10.1016/j.cub.2011.01.039

Nimchuk, Z. L., Zhou, Y., Tarr, P. T., Peterson, B. a, & Meyerowitz, E. M. (2015). Plant stem cell maintenance by transcriptional cross-regulation of related receptor kinases. *Development*, *142*(6), 1043–1049. https://doi.org/10.1242/dev.119677

Ogawa, M., Shinohara, H., Sakagami, Y., & Matsubayash, Y. (2008). Arabidopsis CLV3 peptide directly binds CLV1 ectodomain. *Science*, *319*(5861), 294. https://doi.org/10.1126/science.1150083

Ohmori, Y., Tanaka, W., Kojima, M., Sakakibara, H., & Hirano, H. Y. (2013). WUSCHEL-RELATED HOMEOBOX4 Is involved in meristem maintenance and is negatively regulated by the CLE gene FCP1 in rice. *The Plant Cell*, *25*(1), 229–241.

https://doi.org/10.1105/tpc.112.103432

Ohyama, K., Shinohara, H., Ogawa-Ohnishi, M., & Matsubayashi, Y. (2009). A glycopeptide regulating stem cell fate in Arabidopsis thaliana. *Nature Chemical Biology*, *5*(8), 578–580. https://doi.org/10.1038/nchembio.182

Olsson, V., Joos, L., Zhu, S., Gevaert, K., Butenko, M. A., & De Smet, I. (2019). Look Closely, the Beautiful May Be Small: Precursor-Derived Peptides in Plants. *Annual Review of Plant Biology*, *70*(1), 153–186. https://doi.org/10.1146/annurev-arplant-042817-040413

Opsahl-Ferstad, H. G., Deunff, E. Le, Dumas, C., & Rogowsky, P. M. (1997). ZmEsr, a novel endosperm-specific gene expressed in a restricted region around the maize embryo. *Plant Journal*, *12*(1), 235–246. https://doi.org/10.1046/j.1365-313X.1997.12010235.x

Pallakies, H., & Simon, R. (2014). The CLE40 and CRN/CLV2 signaling pathways antagonistically control root meristem growth in arabidopsis. *Molecular Plant*, *7*(11), 1619–1636. https://doi.org/10.1093/mp/ssu094

Petersson, S. V., Johansson, A. I., Kowalczyk, M., Makoveychuk, A., Wang, J. Y., Moritz, T., Grebe, M., Benfey, P. N., Sandberg, G., & Ljung, K. (2009). An auxin gradient and maximum in the arabidopsis root apex shown by high-resolution cell-specific analysis of IAA distribution and synthesis. *Plant Cell*, *21*(6), 1659–1668. https://doi.org/10.1105/tpc.109.066480

Pierre-Jerome, E., Moss, B. L., & Nemhauser, J. L. (2013). Tuning the auxin transcriptional response. *Journal of Experimental Botany*, *64*(9), 2557–2563. https://doi.org/10.1093/jxb/ert100

Qian, P., Song, W., Yokoo, T., Minobe, A., Wang, G., Ishida, T., Sawa, S., Chai, J., & Kakimoto, T. (2018). The CLE9/10 secretory peptide regulates stomatal and vascular development through distinct receptors. *Nature Plants*, *4*(12), 1071–1081. https://doi.org/10.1038/s41477-018-0317-4

Reddy, V. G., Heisler, M. G., Ehrhardt, D. W., & Meyerowitz, E. M. (2004). Real-time lineage analysis reveals oriented cell divisions associated with morphogenesis at the shoot apex of Arabidopsis thaliana. *Development*, *131*(17), 4225–4237. https://doi.org/10.1242/dev.01261

Reinhardt, D., Mandel, T., & Kuhlemeier, C. (2000). Auxin regulates the initiation and radial position of plant lateral organs. *Plant Cell*, *12*(4), 507–518. https://doi.org/10.1105/tpc.12.4.507

Reinhardt, D., Pesce, E. R., Stieger, P., Mandel, T., Baltensperger, K., Bennett, M., Traas, J., Friml, J., & Kuhlemeier, C. (2003). Regulation of phyllotaxis by polar auxin transport. *Nature*, *426*(6964), 255–260. https://doi.org/10.1038/nature02081

Rodriguez-Leal, D., Xu, C., Kwon, C. T., Soyars, C., Demesa-Arevalo, E., Man, J., Liu, L., Lemmon, Z. H., Jones, D. S., Van Eck, J., Jackson, D. P., Bartlett, M. E., Nimchuk, Z. L., & Lippman, Z. B. (2019). Evolution of buffering in a genetic circuit controlling plant stem cell proliferation. *Nature Genetics*, *51*(5), 786–792. https://doi.org/10.1038/s41588-019-0389-8

Roeder, A. H. K., Cunha, A., Ohno, C. K., & Meyerowitz, E. M. (2012). Cell cycle regulates cell type in the Arabidopsis sepal. *Journal of Cell Science*, *125*(23), e1–e1. https://doi.org/10.1242/jcs.127902

Sabatini, S., Beis, D., Wolkenfelt, H., Murfett, J., Guilfoyle, T., Malamy, J., Benfey, P., Leyser,

O., Bechtold, N., Weisbeek, P., & Scheres, B. (1999). An auxin-dependent distal organizer of pattern and polarity in the Arabidopsis root. *Cell*, *99*(5), 463–472. https://doi.org/10.1016/S0092-8674(00)81535-4

Samaj, J., Baluska, F., Voigt, B., Schlicht, M., Volkmann, D., & Menzel, D. (2004). Endocytosis, Actin Cytoskeleton, and Signaling. *Plant Physiology*, *135*, 1150–1161. https://doi.org/10.1104/pp.104.040683.1150

Sarkar, A. K., Luijten, M., Miyashima, S., Lenhard, M., Hashimoto, T., Nakajima, K., Scheres, B., Heidstra, R., & Laux, T. (2007). Conserved factors regulate signalling in Arabidopsis thaliana shoot and root stem cell organizers. *Nature*, *446*(7137), 811–814. https://doi.org/10.1038/nature05703

Satina, S., Blakeslee, A. F., & Avery, A. G. (1940). Demonstration of the Three Germ Layers in the Shoot Apex of Datura by Means of Induced Polyploidy in Periclinal Chimeras. *American Journal of Botany*, *27*(10), 895–905.

Satohiro Okuda, Ludwig A. Hothorn, M. H. (2020). Crystal structures of Arabidopsis and Physcomitrella CR4 reveal the molecular architecture of CRINKLY4 receptor kinases. *BioRxiv*, 0–1. https://doi.org/10.1101/2020.08.10.245050

Sauer, M., Balla, J., Luschnig, C., Wiśniewska, J., Reinöhl, V., Friml, J., & Benková, E. (2006). Canalization of auxin flow by Aux/IAA-ARF-dependent feedback regulation of PIN polarity. *Genes and Development*, *20*(20), 2902–2911. https://doi.org/10.1101/gad.390806

Scarpella, E., Marcos, D., Friml, J., & Berleth, T. (2006). Control of leaf vascular patterning by polar auxin transport. *Genes and Development*, *20*(8), 1015–1027. https://doi.org/10.1101/gad.1402406

Schmid, J. B. (2015). On the Role of CLE40 - A Peptide with Antagonistic Functions in Arabidopsis thaliana Shoot Meristem Development. *Dissertation Der Heinrich-Heine-Universität*, *September*.

Schneider, C. A., Rasband, W. S., & Eliceiri, K. W. (2012). NIH Image to ImageJ: 25 years of image analysis. *Nature Methods*, *9*(7), 671–675. https://doi.org/10.1038/nmeth.2089

Schoof, H., Lenhard, M., Haecker, A., Mayer, K. F. X., Jürgens, G., & Laux, T. (2000). The Stem Cell Population of Arabidopsis Shoot Meristems Is Maintained by a Regulatory Loop between the CLAVATA and WUSCHEL Genes. *Cell*, *100*, 635–644.

Scofield, S., & Murray, J. A. H. (2006). KNOX gene function in plant stem cell niches. *Plant Molecular Biology*, *60*(6 SPEC. ISS.), 929–946. https://doi.org/10.1007/s11103-005-4478-y

Shinohara, H., & Matsubayashi, Y. (2015). Reevaluation of the CLV3-receptor interaction in the shoot apical meristem: Dissection of the CLV3 signaling pathway from a direct ligand-binding point of view. *Plant Journal*, *82*(2), 328–336. https://doi.org/10.1111/tpj.12817

Shiu, S. H., & Bleecker, A. B. (2001). Plant receptor-like kinase gene family: diversity, function, and signaling. *Science's STKE : Signal Transduction Knowledge Environment*, *2001*(113), 1–14. https://doi.org/10.1126/scisignal.1132001re22

Shpak, E. D. (2013). Diverse roles of ERECTA family genes in plant development. *Journal of Integrative Plant Biology*, *55*(12), 1238–1250. https://doi.org/10.1111/jipb.12108

Shpak, E. D., Berthiaume, C. T., Hill, E. J., & Torii, K. U. (2004). Synergistic interaction of three ERECTA-family receptor-like kinases controls Arabidopsis organ growth and flower

development by promoting cell proliferation. *Development*, *131*(7), 1491–1501. https://doi.org/10.1242/dev.01028

Stahl, Y., Grabowski, S., Bleckmann, A., Kühnemuth, R., Weidtkamp-Peters, S., Pinto, K. G., Kirschner, G. K., Schmid, J. B., Wink, R. H., Hülsewede, A., Felekyan, S., Seidel, C. A. M., & Simon, R. (2013). Moderation of arabidopsis root stemness by CLAVATA1 and ARABIDOPSIS CRINKLY4 receptor kinase complexes. *Current Biology*, *23*(5), 362–371. https://doi.org/10.1016/j.cub.2013.01.045

Stahl, Y., & Simon, R. (2005). Plant stem cell niches. *International Journal of Developmental Biology*, *49*, 479–489. https://doi.org/10.1387/ijdb.041929ys

Stahl, Y., Wink, R. H., Ingram, G. C., & Simon, R. (2009). A Signaling Module Controlling the Stem Cell Niche in Arabidopsis Root Meristems. *Current Biology*, *19*(11), 909–914. https://doi.org/10.1016/j.cub.2009.03.060

Strabala, T. J., Phillips, L., West, M., & Stanbra, L. (2014). Bioinformatic and phylogenetic analysis of the CLAVATA3/EMBRYO-SURROUNDING REGION (CLE) and the CLE-LIKE signal peptide genes in the Pinophyta. *BMC Plant Biology*, *14*(1), 1–16. https://doi.org/10.1186/1471-2229-14-47

Su, Y. H., Zhou, C., Li, Y. J., Yu, Y., Tang, L. P., Zhang, W. J., Yao, W. J., Huang, R., Laux, T., & Zhang, X. S. (2020). Integration of pluripotency pathways regulates stem cell maintenance in the Arabidopsis shoot meristem. *Proceedings of the National Academy of Sciences*, *117*(36), 202015248. https://doi.org/10.1073/pnas.2015248117

Sun, B., Looi, L. S., Guo, S., He, Z., Gan, E. S., Huang, J., Xu, Y., Wee, W. Y., & Ito, T. (2014). Timing mechanism dependent on cell division is invoked by Polycomb eviction in plant stem cells. *Science*, *343*(6170). https://doi.org/10.1126/science.1248559

Sun, B., Xu, Y., Ng, K. H., & Ito, T. (2009). A timing mechanism for stem cell maintenance and differentiation in the Arabidopsis floral meristem. *Genes and Development*, *23*(15), 1791–1804. https://doi.org/10.1101/gad.1800409

Sun, B., Zhou, Y., Cai, J., Shang, E., Yamaguchi, N., Xiao, J., Looi, L. S., Wee, W. Y., Gao, X., Wagner, D., & Ito, T. (2019). Integration of transcriptional repression and polycomb-mediated silencing of WUSCHEL in floral meristems. *Plant Cell*, *31*(7), 1488–1505. https://doi.org/10.1105/tpc.18.00450

Sundström, J. F., Nakayama, N., Glimelius, K., & Irish, V. F. (2006). Direct regulation of the floral homeotic APETALA1 gene by APETALA3 and PISTILLATA in Arabidopsis. *Plant Journal*, *46*(4), 593–600. https://doi.org/10.1111/j.1365-313X.2006.02720.x

Suzaki, T., Yoshida, A., & Hirano, H. Y. (2008). Functional diversification of CLAVATA3-related CLE proteins in meristem maintenance in rice. *Plant Cell*, *20*(8), 2049–2058. https://doi.org/10.1105/tpc.107.057257

Tanaka, H. (2002). ACR4, a Putative Receptor Kinase Gene of Arabidopsis thaliana, that is Expressed in the Outer Cell Layers of Embryos and Plants, is Involved in Proper Embryogenesis. *Plant and Cell Physiology*, *43*(4), 419–428. https://doi.org/10.1093/pcp/pcf052

Tatsuhiko Kondo, Shinichiro Sawa, Atsuko Kinoshita, Satoko Mizuno, Tatsuo Kakimoto, Hiroo Fukuda, Youji Sakagami, X. (2006). A Plant Peptide Encoded by CLV3 Identified by in Situ MALDI-TOF MS Analysis. *Science*, *313*, 845–848.

Tavormina, P., De Coninck, B., Nikonorova, N., De Smet, I., & Cammuea, B. P. A. (2015). The

plant peptidome: An expanding repertoire of structural features and biological functions. *Plant Cell*, *27*(8), 2095–2118. https://doi.org/10.1105/tpc.15.00440

Torii, K. U., Mitsukawa, N., Oosumi, T., Matsuura, Y., Yokoyama, R., Whittier, R. F., & Komeda, Y. (1996). The Arabidopsis ERECTA Gene Encodes a Putative Receptor Protein Kinase with Extracellular Leucine-Rich Repeats. *The Plant Cell*, *8*(4), 735–746. https://doi.org/10.1105/tpc.8.4.735

Torregrosa, L., Fernandez, L., Bouquet, A., Boursiquot, J.-M., Pelsy, F., & Martínez-Zapater, J. (2010). Origins and Consequences of Somatic Variation in Grapevine. *Genetics, Genomics, and Breeding of Grapes*, 68–92.

Uchida, N., & Tasaka, M. (2013). Regulation of plant vascular stem cells by endodermisderived EPFL-family peptide hormones and phloemexpressed ERECTA-family receptor kinases. *Journal of Experimental Botany*, *64*(17), 5335–5343. https://doi.org/10.1093/jxb/ert196

Ulmasov, T., Murfett, J., Hagen, G., & Guilfoyle, T. J. (1997). Aux/IAA Proteins Repress Expression of Reporter Genes Containing Natural and Highly Active Synthetic Auxin Response Elements. *Society*, *9*(November), 1963–1971. https://doi.org/10.1105/tpc.9.11.1963

Wang, C., Yang, H., Chen, L., Yang, S., Hua, D., & Wang, J. (2018). Truncated BAM receptors interfere the apical meristematic activity in a dominant negative manner when ectopically expressed in Arabidopsis. *Plant Science*, *269*(February), 20–31. https://doi.org/10.1016/j.plantsci.2018.01.003

Wang, H., Inukai, Y., & Yamauchi, A. (2006). Root development and nutrient uptake. *Critical Reviews in Plant Sciences*, *25*(3), 279–301. https://doi.org/10.1080/07352680600709917

Wang, J., Tian, C., Zhang, C., shi, bihai, Cao, X., Zhang, T.-Q., zhao, zhong, Wang, J.-W., & Jiao, Y. (2017). Cytokinin Signaling Activates WUSCHEL Expression during Axillary Meristem Initiation. *The Plant Cell*, tpc.00579.2016. https://doi.org/10.1105/tpc.16.00579

Watanabe, M., Tanaka, H., Watanabe, D., Machida, C., & Machida, Y. (2004). The ACR4 receptor-like kinase is required for surface formation of epidermis-related tissues in Arabidopsis thaliana. *Plant Journal*, *39*(3), 298–308. https://doi.org/10.1111/j.1365-313X.2004.02132.x

Whitewoods, C. D., Cammarata, J., Nemec Venza, Z., Sang, S., Crook, A. D., Aoyama, T., Wang, X. Y., Waller, M., Kamisugi, Y., Cuming, A. C., Szövényi, P., Nimchuk, Z. L., Roeder, A. H. K., Scanlon, M. J., & Harrison, C. J. (2018). CLAVATA Was a Genetic Novelty for the Morphological Innovation of 3D Growth in Land Plants. *Current Biology*, *28*(15), 2365–2376. https://doi.org/10.1016/j.cub.2018.05.068

Wiley, H. S., & Burke, P. M. (2001). Regulation of receptor tyrosine kinase signaling by protein tyrosine phosphatases. *Traffic*, *11*(6), 258–266. https://doi.org/10.1016/S0962-8924(01)01990-0

Williams, R. W., Wilson, J. M., & Meyerowitz, E. M. (1997). A possible role for kinase-associated protein phosphatase in the Arabidopsis CLAVATA1 signaling pathway. *Proceedings of the National Academy of Sciences of the United States of America*, *94*(19), 10467–10472. https://doi.org/10.1073/pnas.94.19.10467

Wink, R. (2013). *On the function of peptide signaling pathways in the root meristem of Arabidopsis thaliana*.

Winter, C. M., Yamaguchi, N., Wu, M. F., & Wagner, D. (2015). Transcriptional programs

regulated by both LEAFY and APETALA1 at the time of flower formation. *Physiologia Plantarum*, *155*(1), 55–73. https://doi.org/10.1111/ppl.12357

Yadav, R. K., Perales, M., Gruel, J., Girke, T., Jönsson, H., & Reddy, V. G. (2011). WUSCHEL protein movement mediates stem cell homeostasis in the Arabidopsis shoot apex. *Genes and Development*, *25*(19), 2025–2030. https://doi.org/10.1101/gad.17258511

Yamaguchi, N., Wu, M. F., Winter, C. M., Berns, M. C., Nole-Wilson, S., Yamaguchi, A., Coupland, G., Krizek, B. A., & Wagner, D. (2013). A Molecular Framework for Auxin-Mediated Initiation of Flower Primordia. *Developmental Cell*, *24*(3), 271–282. https://doi.org/10.1016/j.devcel.2012.12.017

Yamaguchi, Y. L., Ishida, T., Yoshimura, M., Imamura, Y., Shimaoka, C., & Sawa, S. (2017). A Collection of Mutants for CLE-Peptide-Encoding Genes in Arabidopsis Generated by CRISPR/Cas9-Mediated Gene Targeting. *Plant and Cell Physiology*, *58*(11), 1848–1856. https://doi.org/10.1093/pcp/pcx139

Yokoyama, R., Takahashi, T., Kato, A., Torii, K. U., & Komeda, Y. (1998). The Arabidopsis ERECTA gene is expressed in the shoot apical meristem and organ primordia. *Plant Journal*, *15*(3), 301–310. https://doi.org/10.1046/j.1365-313X.1998.00203.x

Zhang, L., DeGennaro, D., Lin, G., Chai, J., & Shpak, E. D. (2021). ERECTA family signaling constrains CLAVATA3 and WUSCHEL to the center of the shoot apical meristem. *Development*, *148*(5), 1–10. https://doi.org/10.1242/dev.189753

Zhou, Y., Liu, X., Engstrom, E. M., Nimchuk, Z. L., Pruneda-Paz, J. L., Tarr, P. T., Yan, A., Kay, S. A., & Meyerowitz, E. M. (2015). Control of plant stem cell function by conserved interacting transcriptional regulators. *Nature*, *517*(7534), 377–380. https://doi.org/10.1038/nature13853

Zhou, Y., Yan, A., Han, H., Li, T., Geng, Y., Liu, X., & Meyerowitz, E. M. (2018). Hairy meristem with wuschel confines clavata3 expression to the outer apical meristem layers. *Science*, *361*(6401), 502–506. https://doi.org/10.1126/science.aar8638

Zimmer, M. (2002). Green fluorescent protein (GFP): Applications, structure, and related photophysical behavior. *Chemical Reviews*, *102*(3), 759–781. https://doi.org/10.1021/cr010142r

Zipfel, C., Kunze, G., Chinchilla, D., Caniard, A., Jones, J. D. G., Boller, T., & Felix, G. (2006). Perception of the Bacterial PAMP EF-Tu by the Receptor EFR Restricts Agrobacterium-Mediated Transformation. *Cell*, *125*(4), 749–760. https://doi.org/10.1016/j.cell.2006.03.037

8. Appendix

8.1 Supplementary Data

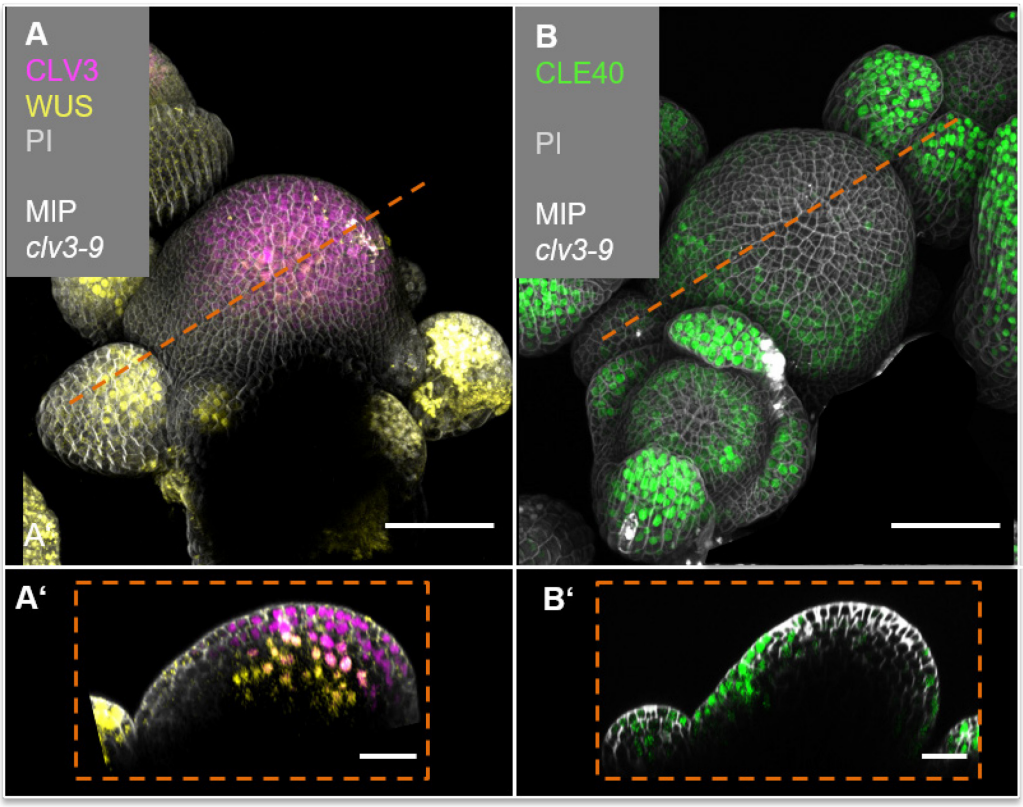

SupplFig. 1: *CLE40* expression is lacking in the CZ and OC.

(A) MIP of *CLV3* and *WUS* expression (*CLV3:NLS-mCherry;WUS:NLS-GFP//clv3-9)* in a *clv3-9* mutant IFM. *CLV3* expression is detected at the tip of the meristem, while *WUS* expression is predominantly found in young primordia surrounding the meristem. **(A')** Optical section through the IFM shows an extended expression domain of *CLV3* in the CZ and *WUS* expressing cells in OC of the IFM. **(B)** MIP of an *clv3-9* mutant IFM expressing *CLE40:Venus-H2B*. *CLE40* is expressed in the PZ of the IFM, in flower primordia and in mature sepal anlagen. **(B')** Optical section through the IFM shows *CLE40* expression in the outer layers of the PZ while it is lacking in the CZ and OC, where *CLV3* and *WUS* are expressed.

Dashed orange line indicates the planes of optical sections; Scale bars: 50 µm (C, D), 10 µm (C', D'), MIP = maximum intensity projection, PI = propidium iodide

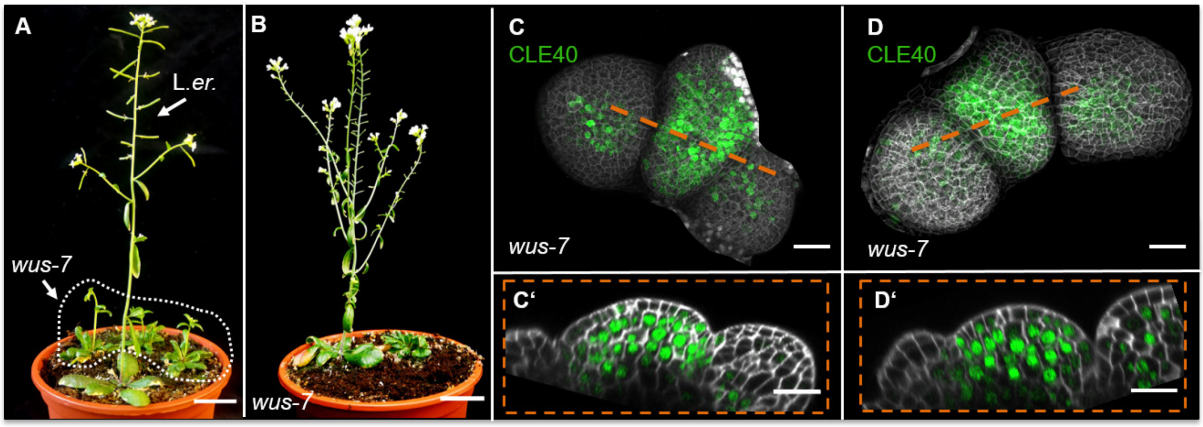

SupplFig. 2: *CLE40* expression is extended in *wus-7* mutants.

(A) L.*er.* wild type plant at 5 WAG shows normal plant growth, while *wus-7* mutants at 5 WAG are delayed in their development (dashed white line). **(B)** *wus-7* mutant at 8 WAG. *wus-7* mutants develop IFMs but give rise to sterile flowers that lack inner organs. **(C and D)** MIP of *wus-7* IFMs at 5 WAG expressing *CLE40:Venus-H2B*. *CLE40* expression is detected through the entire meristem and in the center of primordia. **(D’ and D’)** Optical sections through the meristem show *CLE40* expression in an extended pattern in the PZ and the OC.

Dashed white line in B encloses homozygous *wus-7* mutants, dashed orange line indicates the planes of optical sections; Scale bars: 20 mm (A, B), 20 µm (C-D’)

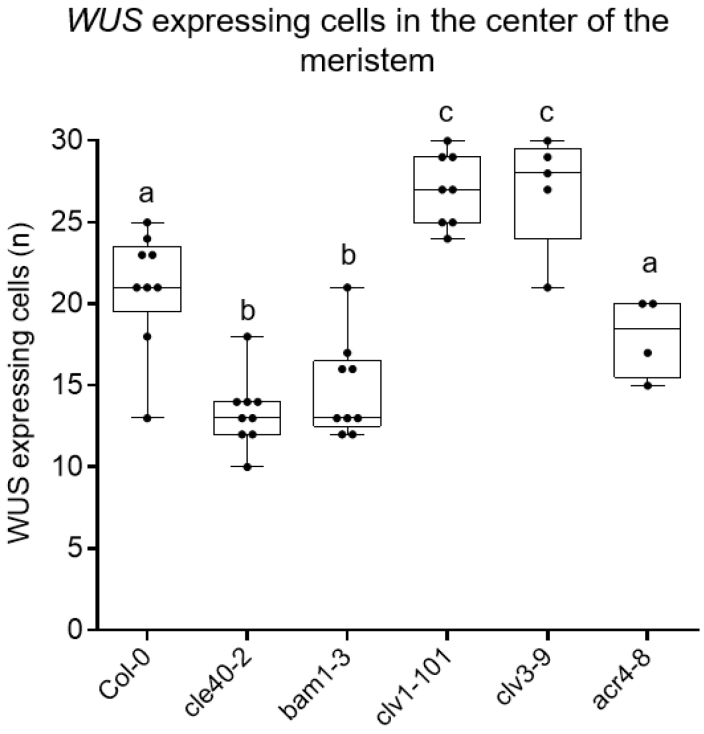

SupplFig. 3: Number of *WUS*-expressing cells in the OC varies in different mutant backgrounds.

Box and whisker plot shows the number of *WUS*-expressing cells in the OC of IFMs of *Col-0*, *cle40-2*, *bam1-3*, *clv1-101*, *clv3-9,* and *acr4-8*. While in wild type plants in average 22 cells show *WUS* activity, only ~13 cells express *WUS* in a *cle40-2* and *bam1-3* mutant background. In *clv1-101* and *clv3-9,* the WUS domain is expanded compared to wild type plants. *clv1-101* and *clv3-9* show in average 26 to 27 *WUS* expressing cells in the CZ. In a*cr4-8* mutants, no change in *WUS*-expressing cells can be detected compared to wild type plants.

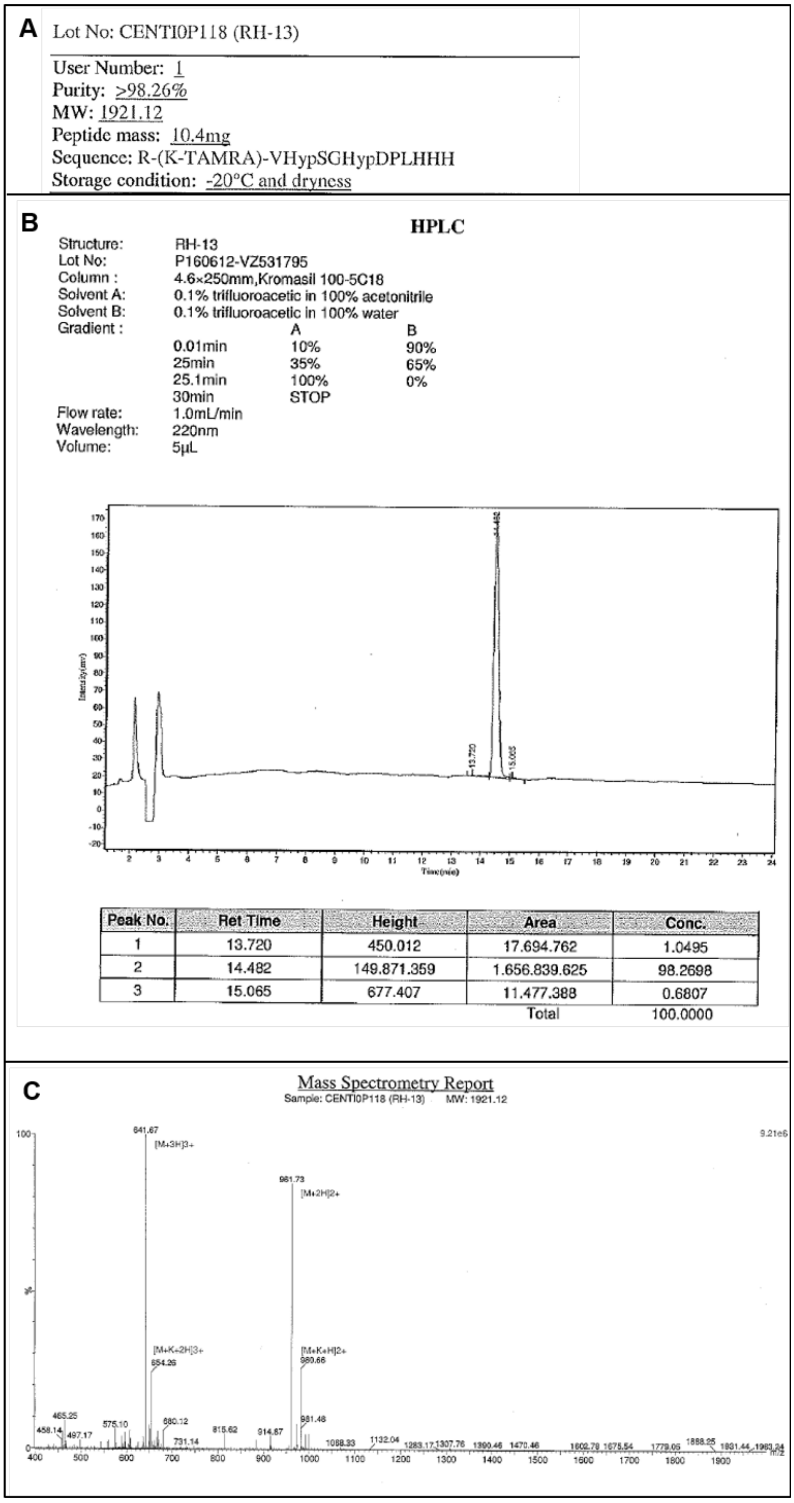

SupplFig. 4: Detailed information of CLV3p-Tamra provided by Centic Biotec®.

(A) Detailed information of CLV3p-Tamra peptide (Purity, molecular weight, peptide mass, sequence and storage conditions.). **(B)** Purification analysis was performed by HPLC method. **(C)** Verification of the CLV3-Tamra molecule by mass spectrometry. All data analysis was provided by Centic Biotec®.

Tab. 9: List of all data/images used in this study.

Figure	staining/ reporter line	plant background	N	comments
Fig. 7	PI	*Col-0*	59	
	PI	*cle40-2*	27	
	PI	*clv3-9*	22	
Fig. 8	PI	*Col-0*	16	
	PI	*cle40-2*	17	
	PI	*cle40-cr1*	24	
	PI	*cle40-cr2*	20	
	PI	*cle40-cr3*	19	
Fig. 9	*CLE40:Venus-H2B*	*Col-0*	25	
	CLE40:Venus-H2B/ CLV3:NLS-3xmCherry	*Col-0*	12	
Fig. 10	*CLE40:Venus-H2B*	*clv3-9*	6	
	CLE40:Venus-H2B vegetative	*Col-0*	5	
	CLE40:Venus-H2B	*CLV3:WUS*	5	
	CLE40:Venus-H2B	*Ler*	8	
	CLE40:Venus-H2B	*wus-7*	12	
Fig. 11	*WUS:NLS-GFP*	*Col-0*	9	
	WUS:NLS-GFP	*cle40-2*	9	
Fig. 12/14/15	*BAM1:BAM1-GFP*	*bam1-3*	15	
	CLV1:CLV1-GFP	*Col-0*	15	
	ACR4:ACR4-GFP	*Col-0*	12	
Fig. 13	PI	*Col-0*	82	same as in Fig.7
	PI	*bam1-3*	54	
	PI	*bam1-4*	17	
Fig.16	*BAM1:BAM1-GFP*	*clv1-20*	9	
	BAM1:BAM1-GFP	*clv3-9*	5	
	BAM1:BAM1-GFP	*cle40-2*	9	
	BAM1:BAM1-GFP	*acr4-8*	5	
Fig.17	PI	*Col-0*	16	
	PI	*bam1-3*	18	
	WUS:BAM1-GFP	*bam1-3*	16	
Fig.18	*WUS:NLS-GFP*	*bam1-3*	9	
Fig.19	PI	*Col-0*	82	same as in Fig.7/13
	PI	*clv1-20*	11	
	PI	*clv1-101*	32	

Fig.20	*CLV1:CLV1-GFP*	*Col-0*	15	
Fig.21	*CLV1:CLV1-GFP*	*bam1-3*	7	
		clv3-9	5	
		cle40-2	9	
		acr4-8	9	
Fig.22	PI	*Col-0*	5	
	PI	*clv1-101*	5	
	WUS:CLV1-mVenus	*clv1-101*	4	
Fig.23	*WUS:NLS-GFP*	*clv1-101*	5	
Fig.24	PI	*Col-0*	82	same as in Fig.7/13/19
	PI	*acr4-2*	15	
	PI	*acr4-8*	39	
Fig.25	*ACR4:ACR4-GFP*	*Col-0*	14	
Fig.26	*ACR4:ACR4-GFP*	*clv1-101*	15	
		bam1-3	11	
		clv3-9	3	
		cle40-2	15	
Fig.27	PI	*Col-0*	9	
	PI	*acr4-8*	8	
	WUS:ACR4-GFP	*acr4-8*	8	
Fig.28	*WUS:NLS-GFP*	*acr4-8*	4	
Fig.31	PI	*Col-0*	82	same as in Fig.7/13/19/24
	PI	*clv3-9*	22	same as in Fig.7
	PI	*cle40-2*	42	same as in Fig.7/13
	PI	*clv1-101*	32	same as in Fig.19
	PI	*bam1-3*	68	same as in Fig.13
	PI	*acr4-8*	39	same as in Fig.24
	PI	*cle40-2;clv1-101*	37	
	PI	*cle40-2;bam1-3*	25	
	PI	*acr4-8;cle40-2*	23	
	PI	*acr4-8;clv1-101*	42	
	PI	*bam1-3;clv1-101*	36	
	PI	*acr4-9;clv1-101;cle40-2*	22	

Fig.32	PI	*Col-0*	48	same as in Fig.7/13/19/24
	PI	*clv3-9*	27	same as in Fig.7/31
	PI	*cle40-2*	36	same as in Fig.7/13/31
	PI	*bam1-3;clv1-101*	40	same as in Fig.31
Fig.33	*CLV1:CLV1-GFP*	*Col-0 + mock*	7	
	CLV1:CLV1-GFP	*Col-0 + CLV3p*	13	
	CLV1:CLV1-GFP	*Col-0 + CLE40p*	6	
	CLV1:CLV1-GFP	*Col-0 + BFA*	5	
Fig.34	*ACR4:ACR4-GFP*	*Col-0 + mock*	2	
	ACR4:ACR4-GFP	*Col-0 + mock*	4	
Fig.35	*ACR4:ACR4-GFP*	*Col-0 + mock (0, 5, 10, 20 min)*	3 to 5	
	ACR4:ACR4-GFP	*Col-0 + CLE40p (0, 5, 10, 20 min)*	3 to 5	
Fig.36	*CLV3p-Tamra*	*Col-0*	6	root
	CLV1:CLV1-GFP + CLV3p-Tamra	*Col-0*	5	root
Fig.38	PI + *CLV3p-Atto488*	*Col-0*	9	root
	PI + *CLV3p-Atto488*	*bam1-3*	5	root
	PI + *CLV3p-Atto488*	*clv1-101*	5	root
	PI + *CLV3p-Atto488*	*bam1-3;clv1-101*	6	root
Fig.39	*DR5rev:GFP*	*Col-0*	8	
	DR5rev:GFP	*cle40-2*	9	
Fig.40	*PIN1:PIN1-GFP*	*Col-0*	6	
	PIN1:PIN1-GFP	*cle40-2*	5	
Fig.41	*CLV3:NLS-mCherry*	*Col-0*	9	
Fig.42	*CLV3:NLS-mCherry*	*clv1-101*	8	
Fig.43	*CLV3:NLS-mCherry*	*clv3-9*	5	
Fig.44	*CLV3:NLS-mCherry*	*cle40-2*	9	
Fig.45	*CLV3:NLS-mCherry*	*bam1-3*	9	

8.2 List of Abbreviations

aa	amino acids
ACR4	ARABIDOPSIS CRINKLY4
AG	AGAMOUS
AHP6	ARABIDOPSIS HISTIDINE PHOSPHOTRANSFER PROTEIN6
ANT	AINTEGUMENTA
AP1	APETALA1
ARF5/MP	AUXIN RESPONSE FACTOR5/MONOPTEROS
ARP	ASYMMETRIC LEAF1/ROUGH SHEATH2/PHANTASTICA
ARR	ARABIDOPSIS RESPONSE REGULATOR
BAM1/2/3	BARELY ANY MERISTEM1/2/3
BFA	Brefeldin A
CC	columella cells
CK	cytokinin
CLE	CLV3/EMBRYO SURROUNDING REGION (ESR)-related
CLV	CLAVATA
CLV1/2/3	CLAVATA1/2/3
CLV3p/CLE40p	CLV3 peptide/ CLE40 peptide
Col-0	Columbia-0
CRN	CORYNE
CSC	columella stem cells
CZ	central zone
DAG	days after germination
DAPI	4′,6-Diamidin-2-phenylindol
DNA	deoxyribonucleic acid

EPFL	EPIDERMAL PATTERNING FACTOR (EPF)-LIKE
ERf	ERECTA family
ERL1/2	ER-LIKE1/2
FM	floral meristem
GFP	green fluorescent protein
HAM1/2/3	HAIRY MERISTEM
IFM	inflorescence meristem
KNOX	KNOTTED-like homeobox
L1/2/3	layer1/2/3
LD	long day
LFY	LEAFY
LRR	leucine-rich-repeat
MAPK	mitogen-activated protein kinase
MS	Murashige & Skoog
MS	Murashige & Skoog
N. benthamiana	Nicotiana benthamiana
NLS	nuclear localization sequence
OC	organizing center
P	primordium
PI	propidium iodide
PIN1	PIN-FORMED1
PLT3	PLETHORA3
PM	plasma membrane
PTM	post-translational modified
PZ	peripheral zone

QC	quiescent center
RAM	root apical meristem
RLK	receptor like kinase
RLP	receptor-like protein
RZ	rip zone
S	sepals
SAM	shoot apical meristem
SDS	Sodium dodecyl sulfate
STM	SHOOT MERISTEMLESS
TA	transit amplifying
TF	transcription factor
TNRF	tumor necrosis factor
TPL	TOPLESS
WAG	weeks after germination
WUS	WUSCHEL

8.3 List of Figures

8. Appendix

8.4 List of Tables

10. Eidesstattliche Erklärung

Eidesstattliche Versicherung zur Dissertation mit dem Titel:

The role of CLE40 in shoot stem cell homeostasis

Ich versichere an Eides Statt, dass die Dissertation von mir selbständig und ohne unzulässige fremde Hilfe unter Beachtung der „Grundsätze zur Sicherung guter wissenschaftlicher Praxis an der Heinrich-Heine-Universität Düsseldorf“ erstellt worden ist.

Außerdem versichere ich, dass ich diese Dissertation nur in diesem und keinem anderen Promotionsverfahren eingereicht habe und dass diesem Promotionsverfahren kein gescheitertes Promotionsverfahren vorausgegangen ist.

Düsseldorf, den 13.10.2021

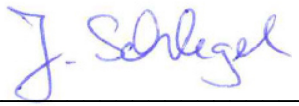

Ort, Datum

Unterschrift

11. Acknowledgment

First of all, I want to thank Rüdiger for giving me the opportunity to do my PhD in his lab, and that I could “waste” as much money as I wanted on countless hours in front of the microscope. Thanks for all the discussions, writing sessions, criticism, words of cheer (at least from time to time ;)) and sharing life stories. Also, thanks for all the fun time we had on lab retreats, lab days out and barbeques. I had a great time!

I also want to thank Matias Zurbriggen for being my co-supervisor, for always supporting my project and for a great collaboration. It was always easy to work with you and your lab. At this point, I want to especially mention Rocio Ochoa-Fernandez, who became a good friend during our collaboration.

Also thanks to Yvonne and the Center for Advanced Imaging (CAi), especially Steffi and Sebastian, for taking such good care of the microscopes and for being there in case something went wrong. Thanks for the support!

However, the greatest and biggest thanks goes to all the people that I worked with during the last 5 years. You made it one of the best times of my life.

The most important people during that time were Karine and Patrick! You are the best! I couldn’t have done it without you and I wouldn’t have had half the fun I had. Thanks for always being there for me, either when I needed advice, motivation, company, a joke or just a beer ;). I know we will stay super good friends for the rest of our lives. Thank you so much! I love you guys!

Next, I also want to mention all the other good friends I made during my time in the lab and who made it an amazing time full of fun and bad jokes. During the last two years, this was especially Isaia and Vivien and nowadays Meik. Thanks for letting me complain all the time, cheering me up with your bad jokes and just for simply hanging out together. Here, I also have to mention Jan, who will always stay in the Simon lab and is always there when you need somebody sober to make fun of you ;).

In the years before I had a great time with Maike, Greg and Barbara who also became my friends. Thanks for everything.

I also want to mention all the other terrific people who made the lab a working place everyone likes: Rebecca, Mehdi, Gwen, Nozomi and now Edgar, Vicky, Neda, Madhu and all the other bachelor and master students over the last years like Abdullah, Anika, Carima, Lillith and Pia. A big thanks goes to Vicky for proof-reading my thesis. Thank you.

11. Acknowledgment

Thanks also to our technicians, Cornelia, Silke and Carin, for all your help with genotyping, all your funny stories and all the “complaints” you had over the years. I always enjoyed talking to you and working with you. Thanks for the support and taking care of the lab.

I also want to thank the Kleins for the nice neighborhood back in the old days. Thanks especially to Thomas and Miri for organizing all the barbeques, breakfasts and public viewing events.

Many thanks to my wonderful sister, Nadine, who was always there for me, in bad and in good times and thanks for the support from her and my parents, Peter and Evelyn, who always supported my “career” and who believed in me. Thanks for being such a loving family.

The last and maybe most important thanks goes to Joe! We only met because of my PhD and I am very thankful for that. Meeting you was the best thing that happened to me. Thanks for giving me so much love, fun, joy and sometimes frustration. You make every day special. I love you to the moon and back!

And last but not least never forget: The only thing that really matters in this world is:

LOVE!

I love you all! Thanks for everything!